Toxicogenomics of precision-cut liver slices for prediction of human liver toxicity

Vatakuti, Suresh

Toxicogenomics of Precision-Cut Liver Slices for Prediction of Human Liver Toxicity

ISBN (ELECTRONIC): 978-90-367-8664-5

ISBN (PRINT): 978-90-367-8665-2

LAYOUT DESIGN: SURESH VATAKUTI

PRINTED BY: IPSKAMP PRINTING

THIS RESEARCH WAS CARRIED OUT IN THE DIVISION OF PHARMACOKINETICS, TOXICOLOGY AND TARGETING, DEPARTMENT OF PHARMACY, FACULTY OF MATHEMATICS AND NATURAL SCIENCES, UNIVERSITY OF GRONINGEN.

THE WORK DESCRIBED IN THIS THESIS WAS FINANCIALLY SUPPORTED BY ZONMW (PROJECT DIERPROEVEN BEGRENSD III, 114011013).

PRINTING OF THE THESIS WAS FINANCIALLY SUPPORTED BY THE UNIVERSITY OF GRONINGEN (RUG), FACULTY OF MATHEMATICS AND NATURAL SCIENCES (FMNS) AND UNIVERSITY LIBRARY.

university of groningen

Toxicogenomics of precision-cut liver slices for prediction of human liver toxicity

PhD thesis

to obtain the degree of PhD at the
University of Groningen
on the authority of the
Rector Magnificus Prof. E. Sterken
and in accordance with
the decision by the College of Deans.

This thesis will be defended in public on

Monday 21 March 2016 at 11.00 hours

by

Suresh Vatakuti

born on 25 December 1985
in Davangere, India

Supervisor
Prof. G.M.M.Groothuis
Prof. P.Olinga

Assessment committee
Prof. B.V.D.Water
Prof. K.N.Faber
Prof. P.Annaert

Dedicated to human liver donors and animals used in the experiments

CONTENTS

1 INTRODUCTION

The liver is the major organ involved in the metabolism and excretion of the majority of drugs and toxins that are introduced into the body. Parent drugs or their metabolites can cause hepatotoxicity, that lead to drug-induced liver injury (DILI). DILI has an estimated annual incidence between 10 and 15 per 10,000 to 100,000 persons exposed to prescription medications [1, 2, 3, 4]. DILI is also the most frequently cited reason for withdrawal of medications from the market [5, 6]. DILI may not be detected in the pre-clinical and clinical studies prior to drug approval, because most new drugs are tested in fewer than 10,000 people prior to drug approval. As a result, DILI with an incidence of 1 in 10,000 may be missed. Apart from the safety issues, drug development is a time consuming process (10-15 years) and huge costs ($2.6 billion) are involved before a new drug is approved on the market [7]. As a consequence, intensive efforts are being made both in academia and industry to develop biomarkers and methodologies to assess hepatotoxic effects as early as possible. The methods include quantitative structure activity relationship assessments, *in vitro* assays, high-content screening assays and omics studies [8, 9]. Currently, hepatotoxicity is evaluated in *in vivo* repeated-dose toxicity tests in animals by analysis of hematological, histopathological and clinical parameters. However, these parameters can generate false negative results due to their insensitivity [10, 11] or due to species differences. In addition the predictive value of these preclinical studies is limited [12]. This emphasizes the need for novel screening methods that facilitate the early assessment of the toxic potential of new molecules []. These new screening methods are preferably applied on *in vitro* test systems to reduce the number of laboratory animals. In addition preferably human derived systems should be used to avoid interspecies extrapolation. To improve the sensitivity of the preclinical parameters, omics-technologies have been developed and in particular the transcriptomics based screenings have already shown promising results for improving the current toxicity tests [8].

The development of predictive models is also hampered by the wide variety of phenotypes of liver injury. DILI is mainly classified into intrinsic (dose-dependent, reproducible) and idiosyncratic (low incidence and largely dose-independent) types. Intrinsic DILI results in different phenotypes of toxic injury based on acute or chronic exposure to drugs such as apoptosis, necrosis, cholestasis, steatosis, fibrosis or cirrhosis. Whereas idiosyncratic drug-induced liver injury (IDILI) is a rare adverse drug reaction of which the mechanism is still poorly understood and which can lead to cholestatic or hepatocellular injury resulting in liver failure, or even death.

1.1 LIVER TOXICITY PHENOTYPES

In this thesis, we focused on four toxic phenotypes: cholestasis, fibrosis, necrosis and idiosyncratic toxicity. Some mechanistic details underlying the studied toxic phenotypes are outlined here.

LIVER NECROSIS Necrosis is caused by acute metabolic perturbation that leads to ATP depletion. Drug-induced cell necrosis results from an intense and massive perturbation of cell homeostasis, with ATP depletion associated with cytoskeletal alterations, cellular swelling and bleb formation and rupture of the lysosomal membrane resulting in release of lysosomal enzymes and irreversible collapse of electrical and ion gradients [13]. The clinical course of acute hepatic necrosis resembles an acute, toxic injury to the liver with sudden and precipitous onset, marked elevations in serum aminotransferase levels, and early signs of hepatic (or other organ) dysfunction or failure despite minimal or no jaundice. Rapid recovery after withdrawal of the causing agent is also typical. Acute hepatic necrosis is typically caused by a direct hepatotoxin and is usually dose dependent and intrinsic, rather than idiosyncratic. In many cases a reactive metabolite is involved that covalently binds to tissue macromolecules.

LIVER CHOLESTASIS Cholestasis is a condition characterized by inhibition of bile flow from the liver to the bile ducts, which may damage the liver. Cholestasis accounts for 40-50 % of all reported DILI cases [14, 15]. The main causative event involved in drug-induced cholestasis is assumed to be BSEP (Bile Salt Export Pump) inhibition by drugs. As a result of this, toxic bile acids accumulate in the hepatocytes or bile canaliculi [16, 17, 18]. These bile salts trigger an adaptive response and a direct deteriorative response. Adaptive response activation counteracts bile accumulation and thus cholestatic liver injury. A complex machinery of transcriptionally coordinated mechanisms mediated by FXR, LXR, CXR and PAR nuclear receptors is activated by bile acids, which collectively decrease the uptake and increase the export of bile acids into and from hepatocytes, respectively. Also, detoxification of bile acids is enhanced, while their synthesis becomes downregulated [19, 16, 17, 18]. Despite the activation of these protective pathways, a deteriorative response occurs, accompanied by mitochondrial impairment, inflammation, the production of reactive oxygen species and ultimately to the onset of cell death by both apoptotic and necrotic mechanisms. Recently, Vinken et al proposed an Adverse Outcome Pathway for cholestasis (fig. 1), which describes the mechanism of cholestasis from the first molecular interaction between the toxin and the cell, via the cellular effects to the effect on the tissue and the final outcome for the organism [16, 17, 18]. Proposed key events are the accumulation of bile acids, the induction of oxidative stress and inflammation, and the activation of nuclear receptors.

LIVER FIBROSIS Liver fibrosis is the scarring process that represents the liver s response to chronic cellular injury and reflects an imbalance between liver repair and scar formation [20]. A central event in liver fibrosis is the activation of hepatic stellate cells to adopt a myofibroblasts like phenotype [21]. Different key events at the cellular and tissue level include hepatocyte injury and cell death, activation of Kupffer cells, expression of transforming growth factor beta 1, activation of hepatic stellate cells, oxidative stress and chronic inflammation, collagen accumulation and changes in hepatic extracellular matrix composition [22]. CCl_4 intoxication, which is a well-known inducer of fibrosis in rat and mouse, is most studied as a model to understand mechanistic events in liver fibrosis [23]. Also for fibrosis an adverse outcome pathway was proposed (fig. 2), clearly indicating the involvement of several liver cell types [22].

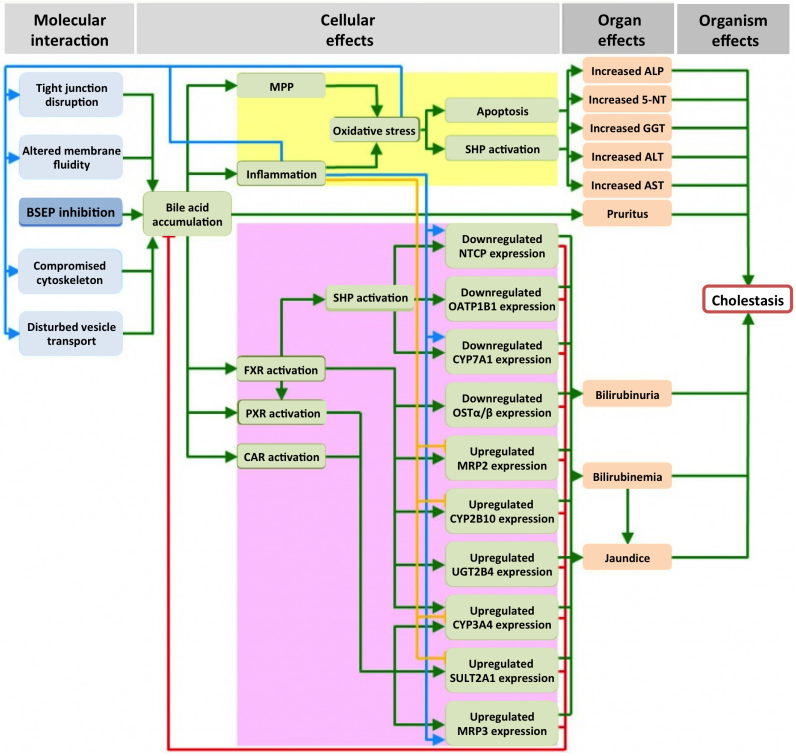

Figure 1: Adverse outcome pathway for cholestasis (reprinted with permission from [18])

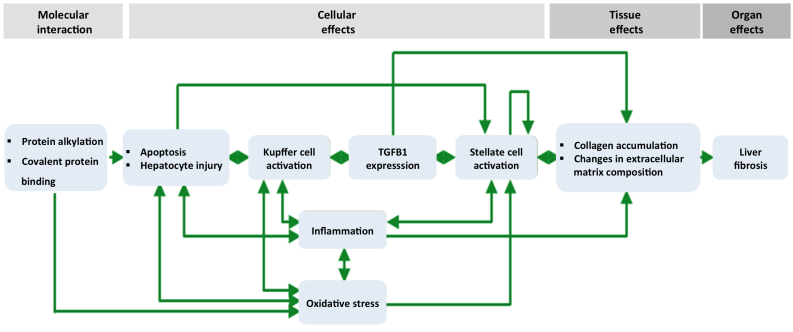

Figure 2: Adverse outcome pathway for fibrosis (reprinted with permission from [22])

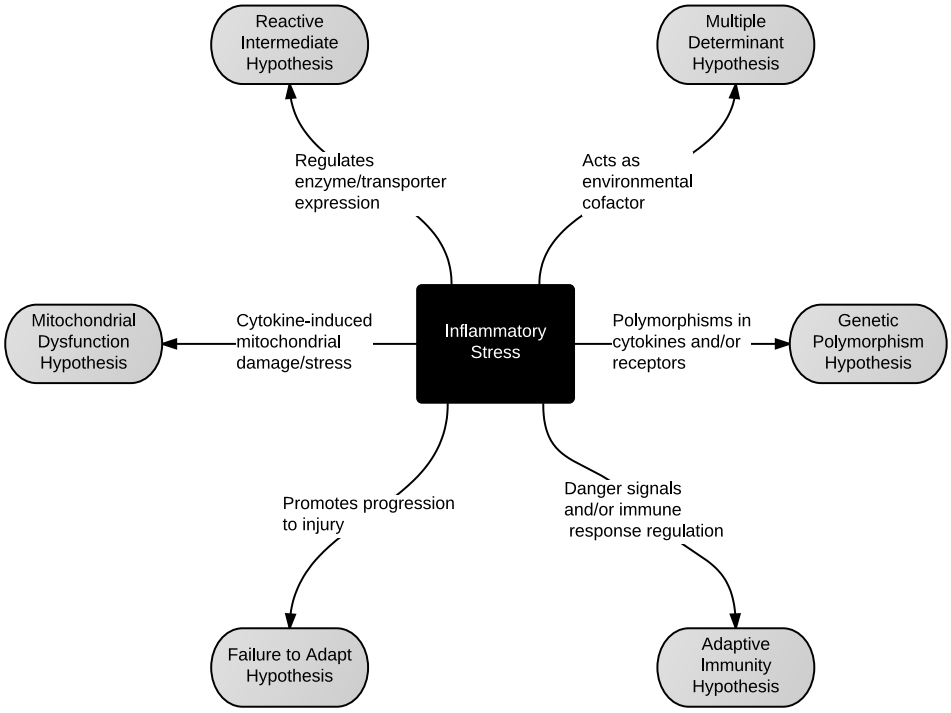

Figure 3: Links between inflammatory stress and other hypotheses for the pathogenesis of IDILI (reprinted with permission from [26])

IDIOSYNCRATIC DILI Idiosyncratic drug-induced liver injury differs from intrinsic toxicity in that IDILI is not directly reproducible in animal models; not strictly dose-dependent (although it occurs mainly with drugs that are dosed at a relatively high dose); variable and often delayed time of onset, variable liver pathology and usually not related to the drug's pharmacologic mechanism of action. To illustrate the latter, clozapine is associated with IDILI whereas olanzapine is not. Although the risk of acute liver failure associated with idiosyncratic hepatotoxins is low (about 1 in ten thousand patients) there are more than 1,000 drugs and herbal products associated with this type of toxic reaction [24, 25].

Several hypothesis are being tested to understand the mechanisms of IDILI drug reactions such as the inflammatory stress hypothesis, hapten hypothesis, failure to adapt hypothesis, danger signal hypothesis, reactive intermediate hypothesis and mitochondrial stress hypothesis (fig. 3) [25, 26, 27]. The inflammatory stress hypothesis is based on the assumption that an acute episode of inflammation has the potential to interact with the concurrent drug therapy to precipitate IDILI. Inflammatory stress models in rodents have suggested the potential role for inflammatory stress in the mechanism of human IDILI. Substantial evidence for interactions between IDILI-causing drugs and inflammation has been reported in these rodent models, which suggests that inflammation plays a role in the idiosyncratic toxicities induced by some well-known IDILI drugs [26]. However, it is also likely that various other mechanisms (fig. 3) alone or in combination, are involved in idiosyncratic toxicities.

1.2 *in vitro* MODEL SYSTEMS TO STUDY DILI

In vivo animal studies are the toxicological gold standard for the assessment of the toxic effect of chemicals. However, this type of study is time consuming, expensive and causes suffering of the animals. Another problem is the increasing number of compounds that have to be tested (among others as a result of the REACH initiative), making the *in vivo* studies not eligible. Although animal studies are an important and useful tool and have to be performed due to guidelines, there are limitations, and a study by Olson et al. showed that half of the drugs that are hepatotoxic in humans did not have the same effect in animals. This study included 221 drugs and the concordance for liver toxicity in humans and experimental animals was 55%, which is only slightly better than tossing a coin, and which is much lower than for other organs, such as the gastrointestinal (85%) and cardiovascular (80%) system [28, 29, 30]. Moreover, in order to reduce the number of animals used in these studies and to increase the possibilities for detailed mechanistic studies, *in vitro* models were developed to evaluate the safety of compounds. *In vitro* models in general are more cost effective and contribute to the replacement, reduction, and refinement of animal testing [31]. For the hepatic metabolism and toxicity evaluation of drugs several *in vitro* models are currently used: the isolated perfused liver (i.e. the intact organ), liver slices, isolated cell preparations (e.g. hepatocytes, or cocultures of hepatocytes with other cell types), cell lines (e.g. HepaRG, HepG2), subcellular fractions (e.g. microsomes), expressed enzymes and in silico models [32]. Stem cell derived hepatocytes are currently under development, which will enable ample availability of differentiated human cells [33].

Drug-induced liver injuries are caused by complex processes, which involve numerous cell types and mediators, making toxicity studies in isolated hepatocytes or liver cell lines incomplete. In contrast, the *ex vivo* model of precision-cut organ slices retains the same multicellular, structural and functional characteristics as the *in vivo* tissue. This model allows a better understanding of cell interactions involved in drug-induced injuries. Precision-cut liver slices (PCLS) retain the organ architecture and compared to primary hepatocytes, they allow the analysis of regional toxicity (e.g. zonal effects across the liver lobule) and the study of the role of all liver cell types in hepatic toxicity [34]. Since the tissue architecture is maintained, the effects of toxicants can be evaluated with morphological techniques (e.g. histological evaluation, immunocytochemistry) in addition to the clinical biochemistry tests [32]. This model can be used for different species and organs (e.g. liver, kidney, lung, brain, small intestine and colon), allowing cross-species and inter-organ comparisons [34]. Although this model has been successfully applied to human liver tissue, like for all *in vitro* models prepared from human tissue, the availability of human tissues limits the throughput of human PCLS. Advantages and disadvantages of the PCLS model in comparison to other *in vitro* systems are summarized in table 1.

Table 1: Summary of commonly used *in vitro* hepatotoxicity model systems

System	Advantages	Disadvantages
Liver slices	- retained organ complexity, cell polarity, intercellular and cell-matrix contacts - similar preparation for all species - several organs from the same donor can be studied and cocultured - histological and biochemical tests - intra-organ regional differences - functional bile canaliculi	- exposure and activity of cells in slices can vary - lifespan limited to 5 days - no cryopreservation available yet - low throughput - development of fibrosis in cultures longer than 2 days
Primary hepatocyte suspensions	- short time maintenance of *in vivo* function - cryopreserved hepatocytes available - medium-high throughput	- *in vitro* lifespan <3 hours - rapid and progressive loss of *in vivo* properties - loss of cell polarity
Hepatocyte monocultures	- polarity partly restored in sandwich cultures - cryopreserved hepatocytes available - medium-high throughput	- limited interactions between cells - absence of other cell types - loss of differentiation and drug metabolism
Co-cultures of hepatocytes and other cells	- better maintenance of differentiation - cryopreserved cells available - specific cell-cell interactions can be studied	- conflicting cell culture requirements for different cells - non-physiological orientation - complex procedures - low throughput
Cell lines	- readily available - relatively reproducible - easy preparation - cryopreserved cell lines available - restored polarity in some cell lines - high throughput	- loss of differentiation - cancer cell properties - lacking many functional characteristics of liver tissue
Stem cell-derived hepatocytes	- once successfully differentiated, ample availability - high throughput - patient-specific cells - cryopreservation possible	- full differentiation not yet achieved - complex preparation
Organoid cultures	- restored cell contacts and polarity - patient-specific cells	- technically complex - low-medium throughput - loss of differentiation
Perfused liver	- biliary excretion functions intact - maintenance of organ complexity, intercellular contacts and cell polarity - intact blood/medium supply through the sinusoids	- short life span (<3h) - difficult to apply to human livers - very low throughput

MODEL COMPOUNDS

For the research studies described in this thesis, prototypical hepatotoxic compounds were selected based on extensive literature search, that are known to induce a specific phenotype of toxicity such as necrosis, cholestasis, fibrosis and IDILI, based on their known *in vivo* toxicity. These well-defined hepatotoxicants served to elucidate the mechanisms underlying the toxic phenotype and classify the hepatotoxicants based on their phenotype of toxicity. The compounds studied in this thesis are briefly described here.

Necrotic compounds

Hepatotoxicants that were described to induce liver necrosis only, with limited or no signs of cholestasis, were selected by literature search and also by using the histopathology data from the TG-GATEs toxicogenomics database (http://toxico.nibiohn.go.jp/).

ACETAMINOPHEN Acetaminophen (paracetamol, APAP) is a widely used over-the-counter drug, used for its analgesic and antipyretic effects. At therapeutic doses, APAP is considered a safe drug, but at higher doses it can produce centrilobular hepatic necrosis, that can be fatal to the patient. APAP hepatotoxicity is by far the most common cause of acute liver failure [35]. The liver injury is attributed to its reactive metabolite (NAPQI), which among others shows mitochondrial toxicity.

BENZIODARONE Benziodarone (BZ) is a vasodilator and a uricosuric agent. It was withdrawn in 1964 due to hepatotoxicity [36]. The compound has a chemical structure similar to benzbromarone, a well-known hepatotoxic agent [37].

CHLORAMPHENICOL Chloramphenicol (CH) is a broad-spectrum antibiotic extracted from the bacterium *Streptomyces venezuelae*. An *in vivo* study in rats showed that CH has necrotic effects on the liver [38]. In humans, acute liver necrosis was reported after CH therapy [39]. Oxidative stress is possibly involved in the CH induced hepatotoxicity [40]. One isolated case of cholestatic jaundice was reported [41].

COLCHICINE Colchicine (CL) is a natural product and secondary metabolite, originally extracted from plants of the genus Colchicum used in treatment of gout. Colchicine is known to cause hepatic necrosis and inhibition of microtubule or spindle formation and mitotic arrest were suggested to be the mechanisms of colchicine hepatotoxicity[42, 43].

N-NITROSODIETHYLAMINE N-nitrosodiethylamine is a carcinogen, and it is used to induce hepatocellular carcinoma in animal experiments [44]. It is also shown to induce hepatic necrosis in mice *in vivo* [45]. Generation of reactive oxygen species (ROS) that results in oxidative stress or cellular injury is the suggested mechanism involved in hepatotoxicity [45].

Cholestatic compounds

Hepatotoxicants, which are known to induce cholestasis by different mechanisms, were chosen from the literature.

1-NAPTHYL ISOTHIOCYANATE (ANIT) ANIT is a model compound which causes cholestasis in experimental animals [46]. ANIT induced cholestasis involves direct injury to bile ducts, called cholangiodestructive cholestasis [47].

CYCLOSPORINE (CS) Cyclosporine is an immunosuppressant drug widely used in organ transplantation to prevent organ rejection. Cyclosporine is known to induce cholestasis in kidney, heart and liver transplant patients [48, 49]. CS is a potent inhibitor of BSEP and BSEP inhibition is the mechanism involved in the CS induced cholestasis [47, 50].

CHLORPROMAZINE (CP) Chlorpromazine is a antipsychotic drug being used to treat schizophrenia. Chlorpromazine treatment was observed to cause hepatocanalicular jaundice in 1% of patients within 1-5 weeks of treatment. Chlorpromazine-induced cholestasis is associated with hypersensitivity or idiosyncratic reaction resulting in cholestatic hepatitis [47]. Other mechanisms have also been suggested, including inhibition of bile flow, inhibition of Na+-K+-ATPase function and an alteration of membrane fluidity.

ETHINYL ESTRADIOL (EE) Ethinyl estradiol is an orally active estrogen used in many formulations of oral contraceptive pills. Pure cholestasis without hepatitis characterized by selective interference with bile excretory mechanisms is observed with ethinyl estradiol [47]. Interference of the glucuronide metabolite of EE with bile excretory transporters (BSEP) is involved in the ET induced cholestasis.

METHYL TESTOSTERONE (MT) Methyl testosterone is used as anabolic steroid. Cholestatic jaundice is observed in a patient with normal or mild elevation of alkaline phosphatase [51]. As like EE, interference with bile excretory mechanisms is involved in the MT induced cholestasis. Pure cholestasis without hepatitis is also observed with methyl testosterone in rats [47, 52].

Idiosyncratic compound

In order to apply toxicogenomics to study the possible mechanisms involved in IDILI, clozapine, which is known to cause drug-induced IDILI in humans was considered.

CLOZAPINE Clozapine is an atypical antipsychotic medication used in the treatment of schizophrenia. Idiosyncratic reactions associated with clozapine include cholestatic liver injury as evidenced by an increase in serum γ-glutamyl transferase (GGT) activity in humans [53]. A non-injurious dose of LPS and nontoxic dose of clozapine in rats resulted in significant increases in serum liver enzymes which did not occur with neither clozapine nor LPS alone [54]. As a non-idiosyncratic pharmacological analogue to clozapine, olanzapine was included in the studies to be able to separate the pharmacological effects from the IDILI. Olanzapine is also an atypical antipsychotic drug and is considered a safe alternative in the treatment of refractory schizophrenia [55].

1.3 TOXICOGENOMICS

Drug induced liver injury is traditionally assessed in preclinical studies using clinical biomarkers. Clinical biomarkers such as alkaline phosphatase, alanine amino-transferase, asparate amino-transferase, gamma glutamyl transferase and bilirubin can give valuable information about liver injury due to drugs but their lack of sensitivity and specificity challenges the identification and differentiation of different liver toxic phenotypes. The current biomarkers for liver injury are reflecting the amplitude of the organ damage rather than the mechanism of action of toxicants. Also, these enzymatic or endogenous markers are released in blood (or medium) as a result of irreversible damage of the cell membrane due to necrosis and mostly reflect a late response to the drug-induced injury. Drug-induced liver injury is the result of alteration of biological processes induced by a drug or its metabolite, resulting in toxic effects. Toxicogenomics deals with the collection and interpretation of information about gene, metabolite and protein expression within a particular cell or tissue in response to toxic substances [56]. It serves to elucidate the molecular mechanisms involved in the toxicity, and to derive molecular expression patterns (i.e. molecular biomarkers) that can predict toxicity [57, 58, 59, 8, 60]. Toxicogenomics combines toxicology with genomics, and uses high throughput molecular profiling technologies such as transcriptomics, proteomics and metabolomics and is being used in the academia and industry for more than a decade to study toxic effects of pharmaceutical drugs or environmental chemicals in various *ex vivo*, *in vitro* and *in vivo* model systems in order to predict the risk to patients or the environment [11, 60].

TRANSCRIPTOMICS Transcriptomics is the study of the transcriptome (the complete set of RNA transcripts) that is produced by the genome, under specific conditions using microarray analysis. Comparison of transcriptomes allows the identification of differentially expressed genes in response to different drug treatments. Toxic drugs can cause alterations in the expression of genes, leading to the interruption of the corresponding biological functions, networks and pathways that are of importance for the normal functioning of the organ [61]. Hence, the alterations in the levels of expression of these genes can reflect underlying toxicity mechanisms [62]. There is also evidence that suggests that the gene expression changes in the target organs present before the appearance of the classical biochemical and histological indicators of toxicity [63, 64], thereby elucidating early events. As such, the determination of changes in gene expression of selective gene markers in the target organs in response to the exposure to toxic drugs helps in the pre-clinical diagnosis of toxic endpoints and in turn helps in the selection of drug candidates. Moreover it may be helpful to design effective intervention strategies for preventing adverse effects. The gene expression data provides insights in the possible mechanisms underlying the toxicity and may also be used to identify biomarkers of early toxicity.

1.4 AIM AND SCOPE OF THE THESIS

The research described in this thesis was focused on the use of precision-cut liver slice (PCLS) as an *ex vivo* model in combination with transcriptomics analysis to predict and understand the possible mechanisms of intrinsic and idiosyncratic DILI. The ultimate goal of this research is to contribute to a better early identification of drugs that cause intrinsic or idiosyncratic toxicity in humans before the drug forward to further preclinical and clinical evaluation, with concurrent reduction in the use of experimental animals.

In Chapter 2, rat PCLS was validated as an *ex vivo* model to identify the fibrotic potential of toxic compounds after short-term exposure using a transcriptomics approach. In rat *in vivo*, both paracetamol (APAP) and carbon tetrachloride (CCl_4) induce liver necrosis, but long-term treatment with CCl_4, in contrast to paracetamol, causes liver fibrosis. The aim of this study was to perform transcriptomic analysis to compare the early changes in mRNA expression profiles induced by APAP and CCl_4 in the rat PCLS and to identify early markers that could predict fibrosis-inducing potential.

In Chapter 3, the human PCLS model was validated as an *ex vivo* model to reflect drug-induced cholestasis and to identify the possible mechanisms of cholestasis-induced toxicity using gene expression profiles. Five hepatotoxicants, which are known to induce cholestasis (alpha-naphthyl isothiocyanate, chlorpromazine, cyclosporine, ethinyl estradiol and methyl testosterone) were tested in the presence of a non-toxic concentration of a physiological bile acid mixture. This non-toxic bile acid mixture (60 μM) was added to the incubation medium in order to create an environment similar to that in the portal vein of human *in vivo*. We aimed to verify whether human PCLS incubated with these cholestatic drugs in the presence of this physiological bile acid mixture, correctly reflect the pathways affected in drug-induced cholestasis in the human liver.

In Chapter 4, we aimed to confirm the hypothesis that hepatotoxicants can be classified according to their phenotype of toxicity using human PCLS *ex vivo*, we tried to classify known hepatotoxicants on their phenotype of toxicity using gene expression profiles. Hepatotoxicants that are known to induce either necrosis (n=5) or cholestasis (n=5) were tested at concentrations inducing low (<30%) and medium (30-50%) toxicity. Random forest (RF) and support vector machine (SVM) algorithms were used to identify classifier genes, which can discriminate hepatotoxicants based on the phenotype of toxicity.

Apart from testing PCLS as a suitable model to study drug induced intrinsic toxic phenotypes such as fibrosis, cholestasis or necrosis, the PCLS model was also used to study drug induced idiosyncratic toxicity. Recently, Hadi et al successfully developed and validated the human PCLS as a model, based on the inflammatory test hypothesis, to discern IDILI-related drugs from non-IDILI-related drugs, using human PCLS co-incubated with IDILI drugs and lipopolysaccharide [65].

In Chapter 5, we carried out a transcriptomic analysis to identify possible biomarkers and pathways responsible for IDILI using clozapine as a well-known IDILI drug and olanzapine as its non-IDILI-associated analogue.

Finally, **Chapter 6** presents a summary and general discussion of the major findings of all studies presented in this thesis and a discussion of the future perspectives of the use of human PCLS as model for the research on drug-induced toxicity in man.

2 ACUTE TOXICITY OF CCL_4 BUT NOT OF PARACETAMOL INDUCES A TRANSCRIPTOMIC SIGNATURE OF FIBROSIS IN PRECISION-CUT LIVER SLICES

Toxicology in Vitro 29 (2015) 1012-1020

Supplementary information available: doi:10.1016/j.tiv.2015.03.015

Suresh Vatakuti[a],
Willem G.E.J. Schoonen[c],
Marieke G.L. Elferink[a],
Geny M. M. Groothuis[a],
Peter Olinga[b]

[a]Division of Pharmacokinetics, Toxicology and Targeting, Department of Pharmacy, Groningen Research Institute for Pharmacy, University of Groningen, Groningen, The Netherlands
[b]Division of Pharmaceutical Technology and Biopharmacy, Department of Pharmacy, Groningen Research Institute for Pharmacy, University of Groningen, Groningen, The Netherlands
[c]Toxicology Consultant, Oss, The Netherlands

ABSTRACT

In rat *in vivo,* both paracetamol (APAP) and carbon tetrachloride (CCl_4) induce liver necrosis, but long-term treatment with CCl_4, in contrast to paracetamol, causes liver fibrosis. The aim of this study was to perform transcriptomic analysis to compare the early changes in mRNA expression profiles induced by APAP and CCl_4 in the rat precision-cut liver slice model (PCLS) and to identify early markers that could predict fibrosis-inducing potential.

Microarray data of rat PCLS exposed to APAP and CCl_4 was generated using a toxic dose based on decrease in ATP levels. Toxicity pathway analysis using a custom made fibrosis-related gene list showed fibrosis as one of the predominant toxic endpoints in CCl_4-treated, but not in APAP-treated PCLS. Moreover, genes which have a role in fibrosis such as alpha-B crystallin, jun proto-oncogene, mitogen-activated protein kinase 6, serpin peptidase inhibitor and also the transcription factor Kruppel-like-factor-6 were up-regulated by CCl_4, but not by APAP. Predicted activation or inhibition of several upstream regulators due to CCl_4 is in accordance with their role in fibrosis.

In conclusion, transcriptomic analysis of PCLS successfully identified the fibrotic potential of CCl_4 as opposed to APAP. The application of PCLS as *ex vivo* model to identify early biomarkers to predict the fibrogenic potential of toxic compounds should be further explored.

2.1 INTRODUCTION

Paracetamol (APAP) and carbon tetrachloride (CCl_4) are two well-known model hepatotoxins. The mechanism of liver toxicity for both compounds is a multicellular phenomenon [66, 67]. Chronic exposure to CCl_4 *in vivo* leads to necrosis and subsequently to fibrosis. In contrast, APAP induces necrosis but no fibrosis [68]. It remains to be established why CCl_4 induces fibrosis and APAP does not. The elucidation of this difference could lead to more insight into the mechanisms of fibrosis and may also be used to find new early biomarkers for fibrosis. If such differences in the mechanism of injury between APAP and CCl_4 could be mimicked *in vitro,* this would enable the study of these processes in man by using human tissue. This would allow prediction of fibrogenic effects in man, thereby circumventing the issue of possible species differences, which arise when using animal models.

The study of fibrosis *in vitro* requires a model with an intact liver architecture that can mimic the multicellular mechanism of this process. One such model is precision-cut liver slices (PCLS), as it has all the different liver cell types in their original architecture. This PCLS model system has been validated extensively for over a decade [69, 70, 71, 72, 73]. Although the process of fibrosis *in vivo* is considered to be the result of chronic exposure, it has been shown that CCl_4 treatment leads to induction of biomarkers for hepatic stellate cell activation in liver slices, as early as after 16 hours of exposure, indicating that the early phase of fibrosis can be detected in this *ex vivo* system [72, 74]. In addition, in PCLS, the other cell types involved in fibrosis, such as hepatocytes, endothelial and Kupffer cells, remain viable and functional during culture and can be activated, as has been shown in studies using endotoxin [75, 76, 77, 78] or bile acids [79, 80]. As the validation of the rat PCLS model is greatly supported by comparison with *in vivo* data, which is largely confined to animal studies and is scarcely available for human liver, we studied the gene expression in rat PCLS after treatment with CCl_4 and APAP. Although we do not make the comparison with *in vivo* data in this paper, we know that in rats *in vivo* CCl_4 induces liver necrosis and fibrosis and that APAP does induce only necrosis. Microarray analysis of rat liver treated with CCl_4 and APAP *in vivo* and in PCLS, using a commercial gene expression *in vivo* database, showed that rat PCLS can predict the toxicity and at least part of the pathology observed *in vivo* [71]. Data of human PCLS are currently being collected and will be analyzed and published in the future.

In the present study we performed further transcriptomic analysis from the data of the above-mentioned experiments with the rat PCLS model to characterise the gene expression profiles induced by APAP and CCl_4 and to elucidate whether a gene expression pattern related to early fibrosis could be detected for CCl_4 but not for APAP. We performed a comparison analysis with respect to the regulated genes, and also analysed upstream regulators, which could possibly be responsible for the observed gene expression changes. If prediction of long-term toxicity appears to be feasible at an early time point using PCLS, this model would contribute greatly to reducing and refining animal experimentation and to reducing costs of toxicity testing.

2.2 MATERIALS AND METHODS

Microarray data of APAP and CCl_4 from our earlier published transcriptomic study using rat PCLS was used [71]. In these experiments rat PCLS were exposed to CCl_4 [72, 74] and APAP [71]. RNA was isolated and the RNA processing and hybridization was performed as described [72, 74, 71]. These methods are described only briefly here; see for details these two references.

RAT LIVER SLICE PREPARATION Rat livers from male Wistar rats (Harlan, Zeist, The Netherlands) were harvested under anesthesia with isoflurane and stored at 4°C in University of Wisconsin organ preservation solution (UW, Dupont Critical Care, Waukegan, IL, USA) until slicing (max 15 min). Precision-cut liver slices (diameter 8 mm, thickness 250 μm) were prepared using a Krumdieck tissue slicer in ice-cold Krebs-Henseleit buffer, pH 7.4, supplemented with glucose to a final concentration of 25mM, saturated with carbogen (95% O_2/5% CO_2). Slices were stored at 4°C in UW until the start of the experiment [71].

RAT LIVER SLICE EXPERIMENTS Slices were pre-incubated individually in 6-well culture plates, each slice in 3.2 ml Williams Medium E with glutamax-1 (Gibco, Invitrogen, Paisley, Scotland) supplemented with 25mM D-glucose and 50 g/ml gentamycin (Gibco, Invitrogen) (WEGG medium) under carbogen atmosphere at 37°C for 1 hour, while gently shaken (90 times/min). After pre-incubation the slices were transferred to fresh WEGG medium. The experiments with APAP were performed in 6-well plates with 3.2 ml medium [71], while CCl_4 slices were incubated in 25 ml Erlenmeyer flasks containing 5 ml medium [72, 74]. The toxic dose was selected at a 60 to 90% decrease in ATP levels with respect to corresponding controls. The PCLS were exposed to 2.5 mM APAP. CCl_4 was spotted in an amount of 5 μl on a filter paper, which was attached to the stopper with a needle and was situated above the liquid phase as described earlier [72, 74]. Since the toxic concentration of CCl_4 at 16 h already showed a relatively large ATP depletion, this 16 h time point was chosen in contrast to 24 h APAP samples. Three different livers were used for each experiment; for RNA isolation 3 slices were pooled and quickly frozen in liquid nitrogen and stored at -80°C.

ISOLATION OF RNA FOR MICROARRAY ANALYSIS Total RNA was isolated from three combined slices from each experiment with the use of Trizol reagent (Invitrogen, Carlsbad, CA, USA). The RNA concentration and quality was determined with use of the NanoDrop (ND-1000 spectrophotometer) and the agilent technology (Agilent 2100 Bioanalyzer with Agilent RNA 6000 Nano kit). Before processing the purity of RNA was determined by measuring E260/E280 and the Agilent RNA Integrity number (RIN) [81]. The E260/E280 values from all samples were >1.8. The RIN values were >8, with one exception: one 16h control for CCl_4 with a RIN value of 7.8. If necessary, RNA was cleaned-up by extraction with phenol/chloroform/isoamylalcohol, followed by a second extraction with chloroform/isoamylalcohol and precipitation with ethanol and lithium chloride.

RNA PROCESSING AND HYBRIDIZATION Double-stranded cDNA was synthesized from 5 μg total RNA using the Custom Superscript ds cDNA synthesis kit (Invitrogen, Carlsbad, CA) and used as a template for the preparation of biotin-labeled cRNA with use of the Bioarray HighYield RNA Transcript Labeling kit (T7) (Enzo Life Sciences, Inc,

Farmingdale, NY). After fragmentation at $1\mu g/\mu l$ according to the manufacturer's protocol, biotin-labeled cRNA (10 g) was hybridized at 45 C for 16-17 hours to the RGU34A array (Affymetrix, Santa Clara, CA). Following hybridization, the arrays were washed, stained with phycoerythrin-streptavidin conjugate (Molecular Probes, Eugene, OR), and the signals were amplified by staining the array with biotin-labeled anti-streptavidin antibody (Vector Laboratories, Burlingame, CA) followed by phycoerythrin-streptavidin. The arrays were laser scanned with a GeneChip Scanner 3000 (Affymetrix, Santa Clara, CA) according to the manufacturer's instructions.

MICROARRAY DATA PRE-PROCESSING AND ANALYSIS Normalization of the microarray data was performed by RMA normalization using MicroarrayRUS v.1.0 software [82]. Control genes are removed from the rest of the analysis. Rank product analysis of the normalized data was performed using MicroarrayRUS v.1.0 software [83]. A list of differentially expressed genes was created using criteria of fold change of 1.5 and multiple hypothesis adjusted p-value 0.05 and used as input for pathway analysis in Ingenuity software.

GENE EXPRESSION DYNAMICS ANALYSIS Gene Expression Dynamics Inspector (GEDI) transforms high-dimensional gene expression data into distinct two-dimensional (2D) color patterns. The graphical output of GEDI gives the visual representation of the samples. The metagene signature of each sample is represented in a grid of 26×25 tiles; each of the tiles contains genes that are highly correlated with each other. The tiles are arranged such that each tile is also correlated with the adjacent tiles. Thus, it allows a global first-level analysis of the data to observe the response due to the effect of a drug. Pattern analysis of the data was performed by GEDI software (default settings) to understand the global transcriptomic changes induced by compounds [84].

PATHWAY AND NETWORK ANALYSIS Ingenuity Pathway Analysis ("http://www.ingenuity.com/products/ipa") was used to determine pathways and networks that could describe the toxicity of APAP and CCl_4. Rat liver tissue specific pathway analysis was performed.

CUSTOM-MADE TOXLIST ANALYSIS Custom-made toxlists were also considered for analysis along with toxlists present in the Ingenuity knowledgebase. Custom fibrosis toxlists were created based on our observation that the toxlist for hepatic fibrosis in IPA does not include all the known genes related to the fibrotic process. Custom-made toxlists for fibrosis were generated by using the information from different sources such as SABioscience fibrosis PCR chip ("http://www.sabiosciences.com/rt_pcr_product/HTML/PARN-120Z.html") and an in-house custom made chip with genes related to collagen synthesis and breakdown [85]. SABioscience provides a custom fibrosis PCR array chip containing genes related to fibrosis. Finally a combined gene list is generated from the genes of IPA fibrosis toxlist, SABioscience and in-house custom array of collagen-metabolism related genes. IPA uses Fisher exact test to calculate statistical significance.

UPSTREAM REGULATOR ANALYSIS Upstream Regulator Analysis was performed to identify the upstream regulators that may be responsible for the observed gene expression

changes. IPA predicts which upstream regulators are likely to be activated or inhibited, which in turn could explain the gene expression changes observed in the dataset. IPA makes predictions on upstream regulators using a z-score algorithm [86]. The z-score value is calculated using the gene expression patterns of the genes downstream of an upstream regulator. P-value of overlap indicates the statistical significance of genes in the dataset that are downstream of the upstream regulator but unlike the z-score, it does not take into consideration up or down-regulation of genes in dataset. Upstream regulators with a z-score greater than 2 or smaller than -2 and p-value of 0.05 were considered significant and their role in fibrosis was studied.

CAUSAL NETWORK ANALYSIS Causal Networks are small hierarchical networks of regulators that control the expression of the regulated genes. This helps to identify novel upstream regulators, because they influence the expression either directly or indirectly via intermediate regulators [86]. Causal networks generated by IPA with an activation z-score greater than 2 or smaller than -2 and p-value of overlap 0.05 were considered significant and their role in fibrosis was studied.

2.3 RESULTS

GENE EXPRESSION DYNAMICS ANALYSIS The expression values of all the replicates of each group were averaged to make a representative self-organizing map of each group using GEDI (Fig. 4). The regions where gene expression patterns are different are indicated in boxes (as in A, B, C, D).

The change in color of the cells in those boxes can be interpreted as change in expression intensity of genes in those cells. The APAP control (A) group at 24h is similar to the CCl_4 control group at 16h (C), although there are slight differences, which may be ascribed to a difference in incubation time. Expression patterns of slices treated with each of the compounds were considerably different from their corresponding controls. Although visually small differences were noticed between the APAP treated (B) and CCl_4 treated (D) group, the gene expression intensity levels were different in those highlighted regions. Since each tile in the GEDI map contains a group of correlated genes, such minor differences could indicate the difference between compounds. Thus, GEDI analysis revealed evidence on the global level that APAP and CCl_4 have induced characteristic expression profiles, which can be explained possibly by the different mechanisms of toxicity of both compounds.

GENE SELECTION BY RANK PRODUCT ANALYSIS The rank product analysis method has been showed to perform well to identify the regulated genes, particularly for datasets that have a low number of samples or a high level of noise [83]. Regulated genes were selected using a criterion of fold change of 1.5 and adjusted p-value of < 0.05 using the MicroarrayRUS program. The Vennplex program [87] was used to observe the commonly up- or down-regulated or contra-regulated genes. Contra-regulated genes are those that are up-regulated in one compound and down-regulated in another compound. In total 174 genes were deregulated in the case of CCl_4 and 116 genes were deregulated in the case of APAP, while 63 genes were similarly regulated in the presence of both compounds, of which 19

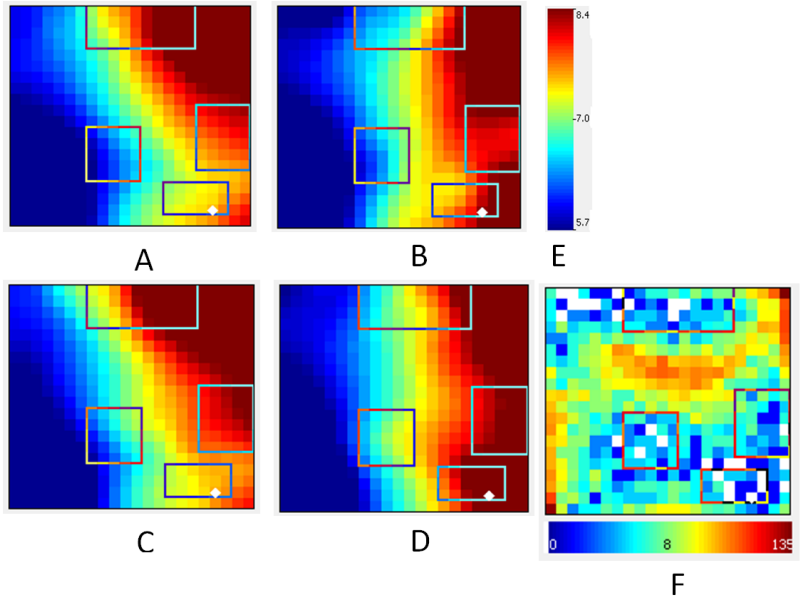

Figure 4: Global Transcriptomic changes induced by APAP and CCl_4
Comparative Gene Expression Dynamics Inspector (GEDI) analysis of averaged values of expression values from biological replicates of APAP control (A) and treated (B), CCl_4 control (C) and treated (D) samples. The Gene density map (E), indicates the number of genes in each cell (white cells indicate the absence of genes in those cells). The expression intensity is indicated in (F). Regions of difference are indicated with squares.

genes were up-regulated and 44 genes were down-regulated. No contra-regulated genes were found as shown in Fig. 5.

The list of genes that are specifically deregulated by either APAP or CCl_4, and also the genes that are regulated in common due to APAP and CCl_4 treatment are shown in Supplementary data S3.

CUSTOM FIBROSIS TOXLIST ANALYSIS Custom fibrosis toxlist analysis was performed using IPA with the toxlists obtained from the different sources described in the materials and methods section. Toxlists regulated with a p-value of < 0.05 were considered significant (corresponds to -log [p value] of 1.3). This analysis indicated that the set of genes in the fibrosis toxlist from SABioscience was significantly regulated by CCl_4 but not by APAP (Fig 6). The other custom toxlists were not found to be significantly regulated as a whole. However, differences between the effects of CCl_4 and APAP were found for some individual genes for the other toxlists as well as for the combined fibrotic toxlist.

Genes such as JUN, LITAF, MAPK6, PLAT and SERPINE1 from the SABioscience fibrotic toxlist were regulated by CCl_4.

In Table 2 the genes from the fibrosis toxlists that are specifically deregulated in CCl_4 are listed. Except for PLAT, all the genes mentioned in Table 2 that are known to play a role in the fibrotic process are specifically deregulated by CCl_4 and not by APAP. Furthermore, the markers specific for hepatic stellate cells such as KLF6 and CRYAB are up-regulated by CCl_4.

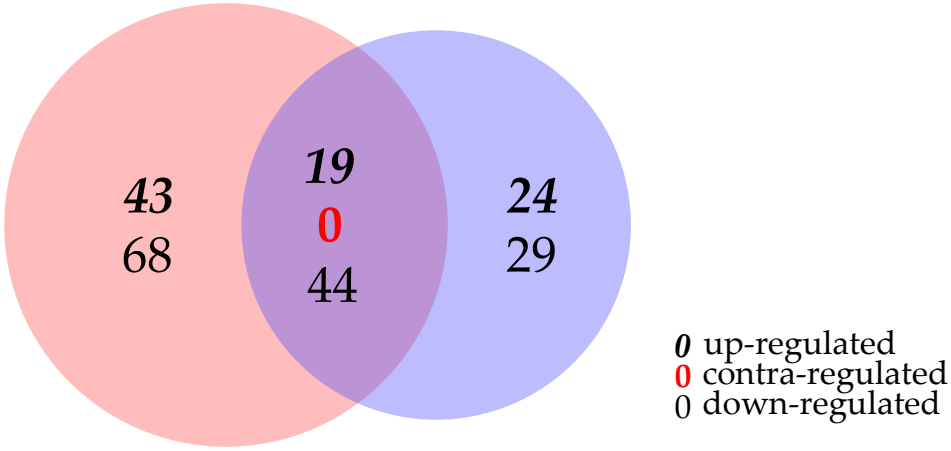

Figure 5: Venn diagram comparison of regulated genes between APAP and CCl_4
Genes regulated with a fold change criterion of 1.5 and multiple hypothesis adjusted p-value of <0.05 were compared. Genes regulated due to CCl_4 and APAP are indicated in yellow and blue circles respectively and the genes regulated in common are indicated in the region of interaction between yellow and blue circles.

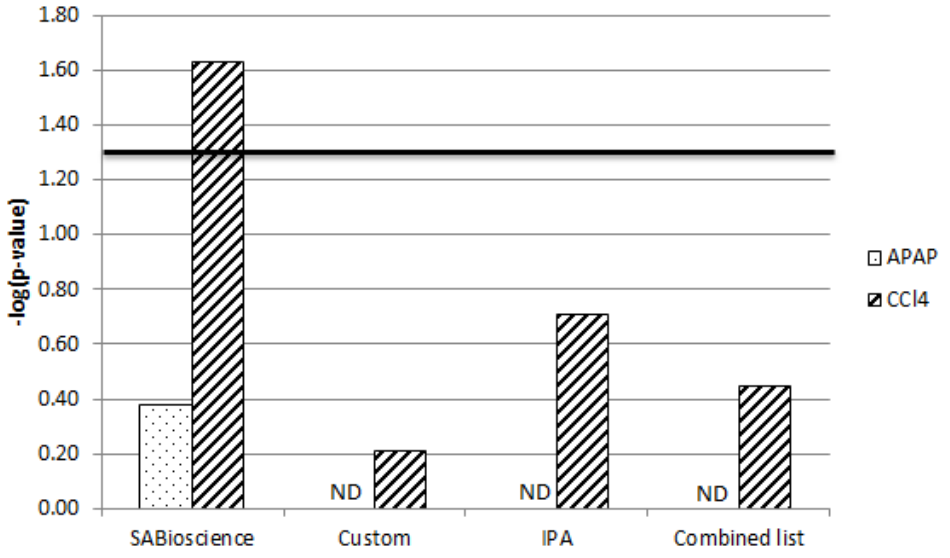

Figure 6: Custom fibrosis toxlist analysis of APAP and CCl_4 regulated genes
Horizontal line indicates the threshold corresponding to p-value of <0.05 and ND means that no regulated genes were found in common with the corresponding toxlist and hence overrepresentation was not assessed.

Table 2: Fibrosis related genes, which are specifically regulated in case of CCl_4

Gene	Description	Fold change	Role in fibrosis
PLAT *	Tissue plasminogen activator	2	PLAT increases extra cellularmatrix (ECM) degradation [88, 89]
SERPINE1	Serpin peptidase inhibitor	3.7	Progression of fibrosis [88]
MAPK6	Mitogen-activated protein kinase 6	2.5	MAPK pathway is known to be involved in the activation of HSC [90]
JUN	Jun proto-oncogene	2.6	JunD is implicated in the regulation of hepatic stellate cell (HSC) activation and liver fibrosis [91, 92]
LITAF	Lipopolysaccharide-induced TNF factor	2.5	Induced in hepatic stellate cells [93]
KLF6	Kruppel-like factor 6	11	Induced in response to early fibrosis [94]
CRYAB	Crystallin, alpha B	10.5	Induced in activated hepatic stellate cells [95]

Genes known to play a role in fibrosis and are specifically regulated in CCl_4 with corresponding fold change and their role in fibrosis. * PLAT is also regulated due to APAP.

Table 3: Upstream regulators predicted to be activated or inhibited due to CCl_4 treatment

Upstream Regulator	Molecule Type	Predicted State	Activation z-score	P-value
EDN1	cytokine	Activated	2.2	4.38E-03
EGF	growth factor	Activated	2.7	1.05E-04
ERN1	kinase	Activated	2.2	1.23E-04
IL1A	cytokine	Activated	2.4	1.67E-02
IL1B	cytokine	Activated	2.2	1.71E-06
NUPR1	transcription regulator	Activated	2.8	2.11E-02
STAT1	transcription regulator	Activated	2	5.33E-02
TGFA	growth factor	Activated	2.4	2.53E-04
TGFB1	growth factor	Activated	3.8	6.40E-04
TNF	cytokine	Activated	3.6	1.00E-09
ACOX1	enzyme	Inhibited	-2.6	1.38E-11
HNF1A	transcription regulator	Inhibited	-2.6	4.55E-10
HNF4A	transcription regulator	Inhibited	-3.0	7.28E-09
PPARA	ligand-dependent nuclear receptor	Inhibited	-2.6	7.66E-22
PPARD	ligand-dependent nuclear receptor	Inhibited	-2.6	1.28E-10
PPARG	ligand-dependent nuclear receptor	Inhibited	-2.4	8.27E-07
RXRA	ligand-dependent nuclear receptor	Inhibited	-2.6	6.74E-09
TFAM	transcription regulator	Inhibited	-2	1.18E-04

Upstream regulators with their corresponding molecular type, predicted activation or inhibition state, activation z-score and p-value of overlap.

UPSTREAM REGULATOR ANALYSIS Upstream Regulator Analysis revealed that several regulators are involved in controlling the expression of the genes regulated by CCl_4 and APAP treatment. These regulators and their target molecules (regulated genes) are shown in Table 3 and Table 4 respectively. ACOX1, HNF4A and HNF1A are predicted to be inhibited and TGFB1 is predicted to be activated due to treatment with both compounds. However PKD1, AKT1, BRCA1, FGF2 and TP53 are unique to APAP treatment and PPARA, NUPR1 IL18, STAT1, TGFA, TNF, PPARD, PPARG, RXRA, TFAM, EDN1, EGF, IL1A and ERN1 are unique to CCl_4 treatment.

TGFB1, a growth factor known to play an important role in hepatic fibrosis during hepatic stellate cell activation, is predicted to be activated due to both APAP and CCl_4. However, 28 genes regulated by CCl_4 treatment are causally linked to activation of TGFB1, whereas only 19 genes are causally linked due to APAP treatment, resulting in a much lower p value for CCl_4 than for APAP. Mechanistic networks for visualizing the causal link between TGFB1 activation and their corresponding target molecules are shown in Fig. 7 and 8.

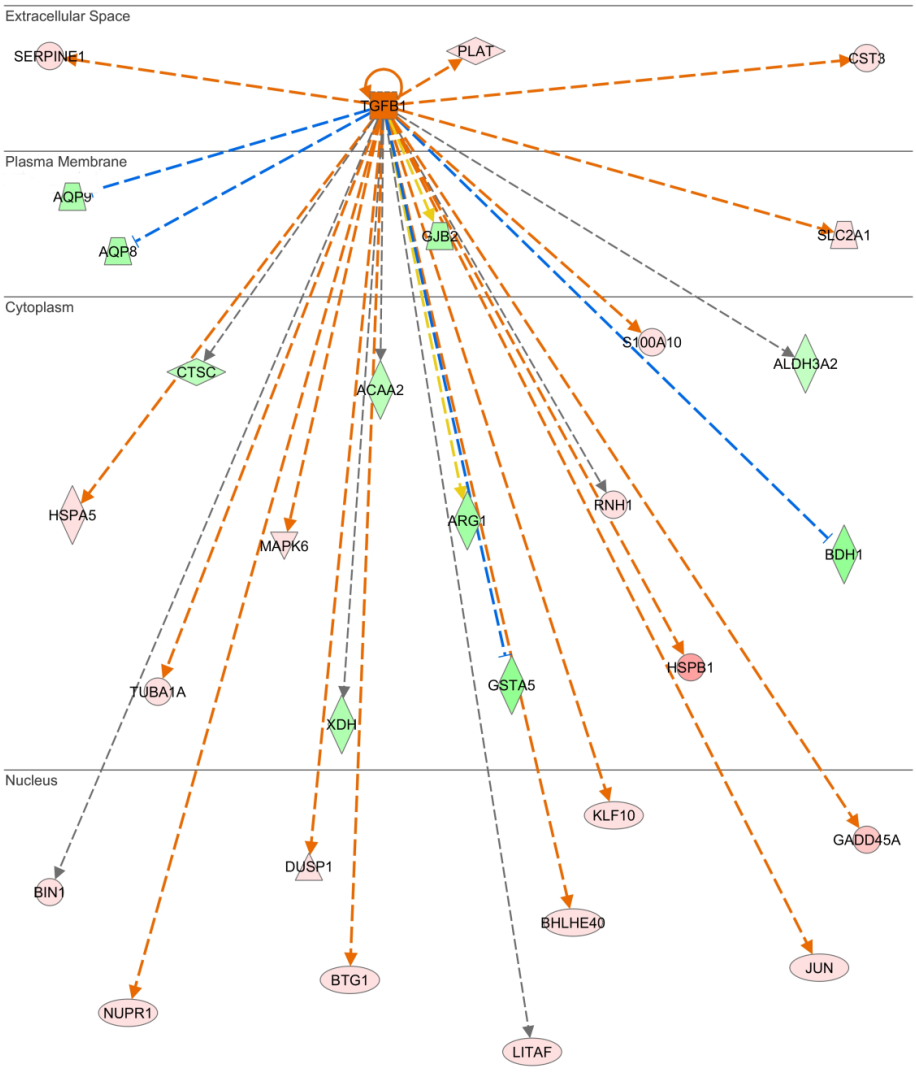

Figure 7: Upstream regulator TGFB1 and corresponding regulated target genes due to CCl_4 treatment TGFB1 is predicted as activated and early fibrotic genes such as JUN, MAPK6, PLAT SERPINE1, are causally linked to TGFB1. Their up-regulation due to CCl_4 is consistent with TGFB1 activation. Regulated genes are highlighted in red or green color, based on up or down-regulation respectively; the intensity of the color increases with degree of fold change. The upstream regulator (TGFB1) is indicated as activated (orange) or inhibited (blue) with the color intensity increasing with the confidence level. Orange lines with arrowheads at the end of interactions indicate activation, while blue lines with bars indicate inhibition. Yellow lines indicate inconsistent findings and grey line indicate effect not predicted.

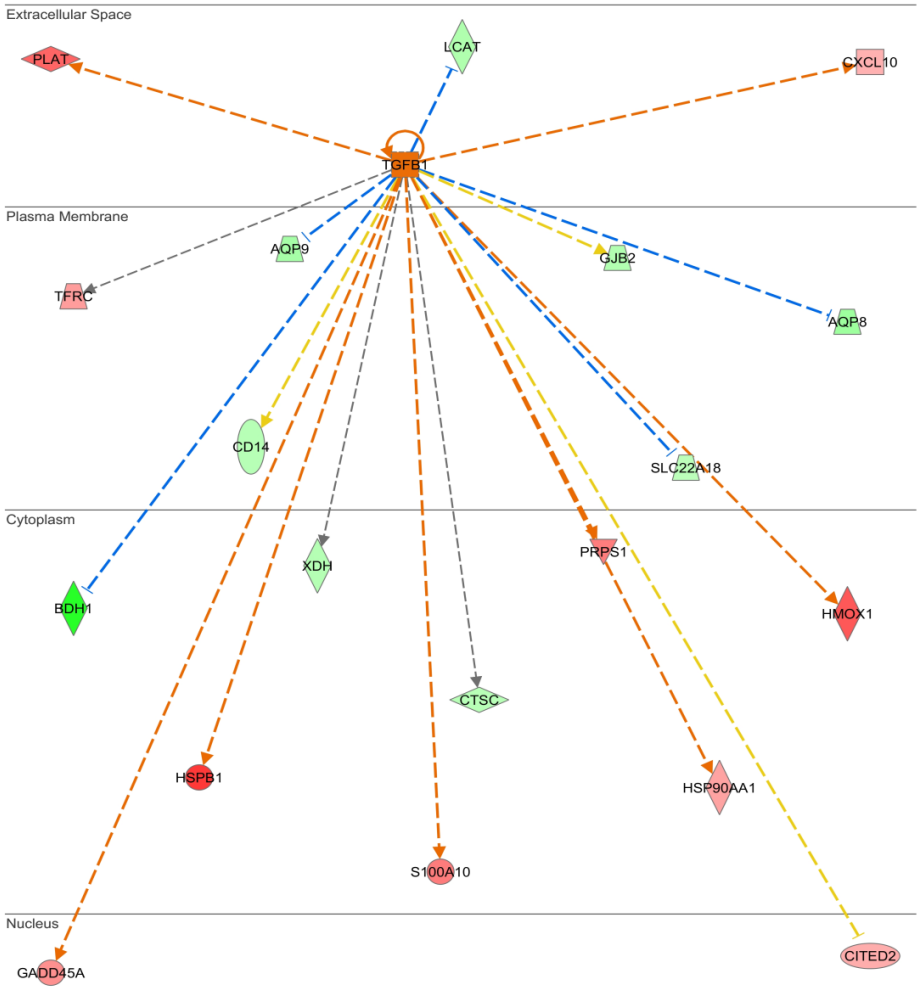

Figure 8: Upstream regulator TGFB1 and corresponding regulated target genes due to APAP treatment

TGFB1 is predicted as activated but none of the fibrosis related genes are causally linked to TGFB1 except for PLAT. Regulated genes are highlighted in red or green color, based on up or down-regulation respectively; the intensity of the color increases with degree of fold change. The upstream regulator (TGFB1) is indicated as activated (orange) or inhibited (blue) with the color intensity increasing with the confidence level. Orange lines with arrowheads at the end of interactions indicate activation, while blue lines with bars indicate inhibition. Yellow lines indicate inconsistent findings and grey line indicate effect not predicted.

Table 4: Upstream regulators predicted to be activated or inhibited due to APAP treatment

Upstream Regulator	Molecule Type	Predicted State	Activation z-score	p-value of overlap
AKT1	kinase	Activated	2.2	4.77E-03
BRCA1	transcription regulator	Activated	2.4	2.67E-04
FGF2	growth factor	Activated	2.2	4.45E-02
TGFB1	growth factor	Activated	2.2	1.27E-03
TP53	transcription regulator	Activated	2.0	1.32E-02
ACOX1	enzyme	Inhibited	-2.6	1.80E-04
HNF1A	transcription regulator	Inhibited	-2.0	2.16E-09
HNF4A	transcription regulator	Inhibited	-2.9	1.33E-04
PKD1	ion channel	Inhibited	-2	2.34E-02

Upstream regulators with their corresponding molecular type, predicted activation or inhibition state, activation z-score and p-value of overlap.

CAUSAL NETWORK ANALYSIS Causal Network Analysis reveals small hierarchical networks of interacting regulators, which explains the gene expression changes observed in the dataset. In the case of treatment with CCl_4, many of these networks involve multiple regulators combined with a master regulator. For example HNF4A interacts with HNF1A and CTNNB1, which in turn have causal relations with 23 genes in the network. All the significant networks which are predicted to be activated or inhibited due to both APAP and CCl_4 are reported in supplementary data S2. There were 24 causal networks predicted as activated or inhibited in case of CCl_4 but only five such significant networks are reported in the case of APAP. Although the overall number of regulated genes affected by exposure to the toxic concentration of APAP or CCl_4 was more or less the same, there were large differences with respect to the resulting causal networks.

2.4 DISCUSSION

In this study, we performed the comparative analysis of the gene expression profiles of rat PCLS induced by APAP and CCl_4, which are known to induce toxicity by different mechanisms. Comparison was performed using gene expression patterns, regulated genes, and pathway and upstream regulator analysis of regulated genes.

Pattern analysis using GEDI revealed characteristic expression patterns due to a toxic concentration of each of the compounds with respect to the corresponding control (Figure 4). The relatively small differences between the APAP and CCl_4 induced expression patterns could be due to the different mechanisms of toxicity, including the onset of fibrosis due to CCl_4. Similarities in the changes in expression patterns may be explained by the fact that both compounds induce necrosis after short-term treatment, which was concluded previously both for CCl_4 after 16 h and for APAP after 24 h by ToxShield prediction [71].

Comparison of the regulated genes showed that there is good overlap among the regulated genes and there is also a significant number of genes uniquely regulated due to either APAP or CCl_4 (Figure 5). Some of those genes uniquely regulated due to CCl_4 treatment include fibrosis related genes (Table 2). With the exception of PLAT, these fibrosis related genes were not found to be regulated by treatment of rat PCLS with the necrosis-inducing compounds iproniazid and bromobenzene either (data not shown).

Bovenkamp et al. showed that in non-treated rat liver slices, the expression of hepatic stellate cell specific markers such as aB-crystallin, KLF6 and heat shock protein 47 remained constant during incubation for 24 h, indicating quiescence of HSC. In contrast, incubation with CCl_4 led to a time- and dose-dependent increase in mRNA expression of these markers. In accordance with these findings, in our microarray analysis, aB-crystallin, KLF6 and HSP47 were also up-regulated [72, 74]. Regulation of these hepatic stellate cell markers indicates initiation of the fibrotic processes in CCl_4 treated slices.

The growth factor TGFB1 plays a key role in fibrosis via hepatic stellate cell activation. When we focused on genes involved in the TGFB1 signaling pathway and their change in expression due to treatment with APAP or CCl_4, we found that more genes involved in the TGFB1 pathway are regulated by CCl_4 than by APAP: 19 target genes in the dataset have an expression direction consistent with activation of TGFB1 due to CCl_4 treatment (Figure 7), in contrast only 13 target genes have an expression direction consistent with activation of TGFB1 due to APAP treatment (Figure 8). This observation gives an indication of early fibrotic processes activated within 16 h due to a toxic concentration of CCl_4. From the TGFB1 network resulting from regulated genes due to APAP or CCl_4 treatment, it can be seen that, in the case of exposure to CCl_4, genes that have a clear role in fibrosis such as JUN, LITAF, MAPK6, PLAT and SERPINE1 are causally linked to TGFB1 and are up-regulated, but in case of exposure to APAP, only PLAT is up-regulated and causal relation to TGFB1 is seen. It has been reported that TGF- induces SERPINE1 expression via pSmad2L/C signaling and promotes extracellular matrix deposition in myofibroblasts, thereby accelerating liver fibrosis [96]. This observation indicates a substantial involvement of TGFB1 in the toxicity process initiated by CCl_4 but not by APAP.

Upstream regulator analysis revealed several regulators that control the expression of regulated genes. Predicted activation or inhibition of those regulators and their relation with hepatic fibrosis is outlined here. While a few upstream regulators were activated or inhibited similarly due to APAP and CCl_4 treatment, some regulators were particularly activated

or inhibited by either APAP or CCl_4. Toxic concentrations of APAP and CCl_4 are known to induce necrosis in short-term treatment; however, transcriptomic analysis in this study revealed significant differences with respect to genes involved in the toxicity process.

ACOX1, a ROS producing enzyme, is down-regulated due to CCl_4 treatment in our study. A mouse study established the role of ACOX1 in fibrosis showing that ACOX1 knockout mice develop fibrosis [97, 98]. ACOX1 is down-regulated due to CCl_4 treatment and also 17 genes which have causal relation to it are regulated. In contrast, in the case of exposure to APAP, ACOX1 expression is not altered. HNF4A and HNF1A transcription factors are predicted to be inhibited due to both APAP and CCl_4 treatment. HNF4A is involved in differentiation of hepatocytes and is known to be down-regulated in fibrosis [99]. Furthermore, HNF1A also plays a role in the differentiation of hepatocytes. Therefore, the predicted inhibition of HNF4A and HNF1A due to both APAP- and CCl_4-induced necrosis is possibly related to their general role in the process of differentiation of hepatocytes after induction of necrosis. Inhibition of PPARG and RXRA activity, which is predicted due to CCl_4 treatment but not to APAP, has been shown to lead to hepatic stellate cell proliferation [100]. PPARD agonistic activity leads to anti-fibrotic effects in a fibrosis mouse model induced with CCl_4 [101]. These results are in accordance with ours, supporting the fibrogenic potential of CCl_4, which is not seen in APAP. PPARA, known to attenuate oxidative stress, one of the most important processes responsible for fibrosis, and to have anti-fibrotic effects in a rat study *in vivo* [102], is predicted to be inhibited by treatment with CCl_4. Thus, the predicted inhibition of PPARA due to CCl_4 also accords with its fibrotic effect. TFAM, a mitochondrial transcription factor, is predicted to be inhibited in the case of CCl_4 treatment in PCLS, whereas it was observed to be activated in maintenance of quiescent hepatic stellate cells [103]. No such predicted inhibition of TFAM was seen due to APAP treatment. PKD1, which is predicted to be inhibited in the case of treatment with APAP but not CCl_4, has not been described as playing a potential role in fibrosis up to now. NUPR1, a transcription factor regulating apoptosis is up-regulated due to CCl_4 and was found to be involved in fibrotic changes due to CCl_4 treatment in mice [104]. ERN1 which is known to play a role in the adaptive response to endoplasmic reticulum (ER) stress is also predicted to be activated due to CCl_4 [105]. In addition, inflammatory cytokines such IL1A, IL1B and TNF are predicted to be activated due to CCl_4. TNF is also known to play a role in HSC proliferation. Overall, transcription factors such as PPARD, PPARA, TFAM, NUPR1, ERN1 and TNF, which are all known to play a role in fibrosis, are predicted to be activated or inhibited only due to CCl_4.

Causal network analysis revealed many causal networks which with either one regulator or with groups of interconnected regulators, may have accounted for the observed gene expression changes. Comparison of the causal networks regulated by APAP and CCl_4 revealed interesting differences since many of the networks were specifically found to be activated or inhibited by CCl_4, whereas in the case of APAP few such networks were observed. For instance, causal network containing NOCR2 transcription factor as master-regulator in connection with other intermediate regulators such as AR, ESR1, HNF4A, NCOR2, NR4A1, PGR, PPARG, RXRA, THRB and VDR could account for the observed expression changes of 35 genes regulated due to treatment with CCl_4. TGFB1 was shown to up-regulate NCOR2 expression [106]. Causal networks helps to identify novel upstream regulators such as NCOR2 with possible role in hepatic fibrosis, which in-turn helps to derive mechanistic hypothesis. Since the aim of this paper was to explore the differences between APAP and CCl_4 in fibrosis, the causal networks were not explored further in detail.

A recent paper reported the characterization of the proteins involved in hepatic stellate cell activation by CCl_4 *in vitro* [107]. When we compared the genes regulated in our transcriptomic analysis with the proteins regulated due to CCl_4 treatment in hepatic stellate cells, 17 genes were found in common with the proteins including CRYAB and SERPINE1. Furthermore, a comparison with genes regulated by APAP treatment and proteins involved in HSC activation revealed that 11 are similarly regulated, but none of them overlap with the fibrosis related genes (Supplementary data S3).

In conclusion, in this study we focused on the changes in gene expression profiles due to treatment of PCLS with APAP or CCl_4 and found that those changes reflect the characteristic difference between these compounds in their ability to induce liver fibrosis after chronic dosing *in vivo*. This study indicates that transcriptomic analysis of PCLS can be used to identify the fibrotic potential of toxic compounds after short-term exposure. Further studies with more fibrotic and non-fibrotic compounds are needed to verify this finding and to identify a set of biomarkers that can be used in drug- induced toxicity screening.

ACKNOWLEDGMENTS

The authors would like to thank Marja van de Bovenkamp, Annelies L. Draaisma and Marjolijn T. Merema for performing the liver slice experiments. Suzanne Bauerschmidt, Jan Polman and Sjeng J.M.J. Horbach from formerly Schering-Plough for performing hybridization of arrays. The authors also would like to thank ZON MW (3170.0047 & 434023) for financial support.

3 VALIDATION OF PRECISION-CUT LIVER SLICES TO STUDY DRUG-INDUCED CHOLESTASIS - A TRANSCRIPTOMICS APPROACH

(Submitted for publication)

Suresh Vatakuti[1],
Peter Olinga[2],
Jeroen L.A. Pennings[3] ,
Geny M. M. Groothuis[1]

[1]Division of Pharmacokinetics, Toxicology and Targeting, Department of Pharmacy, Groningen Research Institute for Pharmacy, University of Groningen, Groningen, The Netherlands
[2]Division of Pharmaceutical Technology and Biopharmacy, Department of Pharmacy, Groningen Research Institute for Pharmacy, University of Groningen, Groningen, The Netherlands
[3]National Institute for Public Health and the Environment, Bilthoven, The Netherlands.

ABSTRACT

Hepatotoxicity is one of the major reasons for withdrawal of drugs from the market. Therefore there is a need to screen new drugs for hepatotoxicity in human at an earlier stage. The aim of this study was to validate human precision-cut liver slices (PCLS) as an *ex vivo* model to predict drug-induced cholestasis and identify the possible mechanisms of cholestasis-induced toxicity using gene expression profiles. Five hepatotoxicants, which are known to induce cholestasis (alpha-naphthyl isothiocyanate, chlorpromazine, cyclosporine, ethinyl estradiol and methyl testosterone) were used at concentrations inducing low (<30%) and medium (30-50%) toxicity, based on ATP content. Human PCLS were incubated with the drugs in the presence of a non-toxic concentration (60 μM) of a bile acid mixture (mimicking the portal vein concentration and composition) as model for bile acid induced cholestasis. Transcriptomics analysis was performed using Illumina bead arrays. A concentration dependent increase in the number of regulated genes was observed for all compounds. Regulated genes include bile acid transporters ABCB11 (BSEP) and ABCB4 (MDR3), and the cholesterol transporters ABCG5 and ABCG8. Pathway analysis revealed that hepatic cholestasis was among the top ten regulated pathways, and signaling pathways such as FXR-, LXR-, PXR- and VDR-mediated responses, which are known to play a role in cholestasis, were significantly affected by all cholestatic compounds. Other significantly affected pathways include unfolded protein response and protein ubiquitination implicating the role of endoplasmic reticulum stress in bile acid induced cholestasis. In addition, NRF2-mediated oxidative stress response was evident. This study shows that human PCLS incubated in the presence of a physiological bile acid mixture correctly reflect the pathways affected in drug-induced cholestasis in the human liver. In the future this human PCLS model can be used to identify cholestatic adverse drug reactions of new chemical entities.

3.1 INTRODUCTION

Drug induced hepatotoxicity (DILI) is one of the major reasons for failure of drugs in the drug development or post marketing phase, leading to withdrawal of drugs from development or from the market respectively. It is of major concern for the consumers, regulatory authorities such as the FDA and the EMA, and pharmaceutical companies. In the drug discovery process, valuable information about possible mechanisms of toxicity is gained by exposing a compound to suitable *ex vivo, in vitro* or *in vivo* models. The possibility to determine early in the drug development process whether a compound causes a particular pathology results in valuable information about the mechanism of action of an as yet uncharacterized compound.

One of the major causes for DILI is cholestasis. Cholestasis is characterized as inhibition of bile flow caused by a variety of mechanisms that can involve elements of the biliary tree, including the bile ducts and ductules, but also the transporters in the basolateral or canalicular membrane, as well as disruption of the tight junctions, of the hepatocytes can be involved. BSEP inhibition is a common cause of cholestasis and the resulting accumulation of bile acids in the hepatocytes triggers a direct cellular response, which is associated with apoptosis, inflammation, oxidative stress, endoplasmic reticulum stress and cell death. It also causes adaptive cellular responses mediated via nuclear receptors [16, 17, 18].

Most of the information has been obtained from *in vivo* models such as bile duct ligation in different animal species, but mechanistic information on human liver *in vivo* is very scarce. In addition, *in vitro* models such as human and rat hepatocytes, HepG2, and HepaRG cells have been investigated as predictive model. Ansede et al., published an *in vitro* assay to assess the transporter-based inhibition of excretion of a tracer concentration of bile acid using sandwich cultured rat hepatocytes [34]**.** But as bile acids are only present at very low concentration, this model may not detect bile-acid dependent toxicity**.** In contrast, Ogimura et al. incubated sandwich cultured rat hepatocytes with cholestatic compounds in the presence of bile acids to develop an experimental model reflecting bile acid dependent cholestatic injury [108]. Both models were developed with rat hepatocytes, and extrapolation of the results to predict human cholestatic injury remains hazardous. Recently, Chatterjee et al., [109, 110] showed that indeed a model with sandwich cultured human hepatocytes in the presence of bile acids predict the cholestatic potential of drugs more accurately in human than rat hepatocytes. However, it is well known that the hepatocytes show dedifferentiation during culture, which is accompanied by a decrease in drug metabolism capacity and unphysiological expression of transporters [111]. Therefore predictions based on sandwich cultures may not always be very precise.

In the present study we aimed to investigate whether human Precision-Cut Liver Slices (PCLS) in the presence of a physiological concentration of bile acids could be used as a predictive model for drug-induced bile acid dependent cholestatic injury. PCLS has been shown to be a viable *ex vivo* tool to study the metabolism and toxicity of xenobiotics for over a decade [34]. Recently mouse PCLS was used as a model to identify the mechanisms of drug induced cholestasis [112, 113], but also this mouse model is prone to problems of species extrapolation and no bile acids were present during the incubation. The possibility to use human tissue for toxicity studies helps to reduce unnecessary animal studies and to identify human specific toxicity. Advantages of this PCLS model include the presence of all cells of the tissue in their natural environment with intact intercellular and cell-matrix

interactions, stable expression of drug metabolizing and detoxification enzymes, the ability to produce bile acids, and most importantly polarized physiological expression of transporters. This model is therefore highly appropriate for studying multicellular drug toxicity processes [72, 74, 71, 114, 73, 115, 116, 85, 117]. Elferink et al., used transcriptomics analysis to show that rat PCLS reflect the proper mechanisms of hepatotoxicity [71]. Moreover they showed that in human PCLS the gene expression profiles of genes related to drug metabolism, transport and toxicity remain fairly constant during 24 h of incubation but that these profiles are affected by paracetamol-induced toxicity. However up to now no transcriptomics data on human PCLS exposed to cholestatic compounds have been reported. Since the primary event involved in the majority of drug induced cholestasis *in vivo* is accumulation of bile acids due to inhibition of export transporters such as BSEP, we hypothesized that to further optimize the PCLS to mimic cholestasis induced by accumulation of the bile acids *in vivo*, the PCLS should be incubated with a non-toxic concentration of a bile acid mix mimicking the portal vein bile acid concentration and composition. Therefore, in this study we exposed human PCLS to drugs or chemicals known to induce cholestasis such as alpha-naphthyl isothiocyanate (ANIT), cyclosporine, chlorpromazine, ethinyl estradiol and methyl testosterone at different concentrations inducing low to moderate toxicity based on either decrease in ATP content in the presence of a physiological bile acid mix. To detect cholestatic injury and the mechanisms involved, the profiles of differentially expressed genes were analyzed using IPA pathway analysis. Moreover they were compared to expression profiles of human *in vivo* late-stage cholestasis caused by biliary atresia and intrahepatic cholestasis.

3.2 METHODS AND MATERIALS

CHEMICALS Alpha-naphthylisothiocyanate (ANIT), chlorpromazine (CP), cyclosporine (CS), ethinyl estradiol (EE) and methyl testosterone (MT) were purchased from Sigma-Aldrich (St.Louis, MO, USA). Stock solutions for all compounds were prepared in DMSO (VWR, Briare, France).

HUMAN LIVER TISSUE Human liver tissue was obtained from the remaining liver tissue after split liver transplantation (TX). The characteristics of the human livers used in the experiments are described in Table 5. The experimental protocols were approved by the Medical Ethical Committee of the University Medical Center Groningen.

PREPARATION AND INCUBATION OF HUMAN PCLS Precision-cut liver slices of 5 mm diameter and 250 μm thickness) were prepared [118]. PCLS were made using the Krumdieck tissue slicer (Alabama R&D, Munford, AL, USA) in ice-cold Krebs buffer at pH 7.42, enriched with glucose to a final concentration of 25 mM, saturated with carbogen (95% O2/5% CO2). Immediately after the slices were made, they were placed in ice-cold University of Wisconsin organ preservation solution (UW, Dupont Critical Care, Waukegan, IL, USA) and stored on ice until the beginning of the experiment. Slices were pre-incubated individually in 12-well plates (Greiner CELLSTAR(R)) in 1.3 ml of Williams Medium E with glutamax-1 (Gibco, Invitrogen, Paisley, Scotland) supplemented with 25 mM D-glucose and 50 μg/ml gentamycin (Gibco, Invitrogen, Paisley, Scotland). In the incubator (Sanyo CO_2/O_2 Incubator, PANASONIC, Secaucus, NJ, USA), the plates were gently shaken (90 times/min) for 1h under 80% O_2 and 5% CO_2 atmosphere at 37 C. This pre-incubation allows the slices to restore their ATP levels. After pre-incubation the slices were moved to different well plates filled with 1.3 ml Williams Medium E with glutamax-1 supplemented with 25 mM D-glucose, 50 μg/ml gentamycin, 60 μM human bile acid mix (table 6) and different concentrations of the compounds ANIT (25 μM, 50 μM and 75 μM), chlorpromazine (9 μM, 18 μM and 27 μM), cyclosporine (9 μM, 12 μM and 15 μM), ethinyl estradiol (25 μM, 50 μM and 75 μM) and methyl testosterone (50 μM, 75 μM and 100 μM) or solvent (DMSO). These concentrations were selected from pilot experiments where a larger concentration range was used to detect concentrations that resulted in low to medium toxicity. The plates were incubated under the same conditions for 24 h. All incubation conditions were carried out in triplicate. Each experiment was performed in slices of 6 different human livers (table 5). Slices were harvested for ATP assay in 100mM Tris buffer with 2 mM EDTA and for RNA isolation in RNAlater.

Table 5: Demographics of donors of human liver tissue used for the experiments

Human liver	Sex	Age
1	Female	58
2	Male	50
3	Female	71
4	Male	24
5	Female	24
6	Male	64

Table 6: Composition of human bile acids mix

Composition of bile acids	Final concentration in the incubation medium (µM)
Cholic acid (CA)	2.65
Chenodeoxy cholic acid (CDCA)	4.51
Deoxycholic acid (DCA)	6.37
Glycochenodeoxycholic acid (GCDCA)	22.69
Glycocholic acid (GCA)	5.44
Glycodeoxycholic acid (GDCA)	5.04
Glycoursodeoxycholic acid (GUDCA)	3.72
Hyodeoxycholic acid (HDCA)	2.79
Lithocholic acid (LCA)	0.40
Taurocholic acid (TCA)	0.64
Taurochenpodeoxycholic acid (TCDCA)	2.79
Taurolithocholic acid (TLCA)	1.15
Taurodeoxycholic acid (TDCA)	0.58
Ursodeoxycholic acid (UDCA)	1.46

The bile acid mix was added to the medium in order to create an environment similar to the physiological concentration in the portal vein. The composition of the serum bile acids was according to Scherer et al., [119]. Pilot experiments were performed to find out the non-toxic concentration of the bile acid mix. A series of concentrations (10-200 μM) of the bile acid mix containing the 14 different bile acids (BA) shown in Table 6 were tested. Concentrations up to 60 μM were found to be non-toxic and hence further experiments were performed using a concentration of 60 μM, which is close to the reported portal vein bile acid concentration [119]. The final concentrations of the bile acids in the incubation medium are presented in Table 6.

VIABILITY ASSAY: ATP AND PROTEIN CONTENT OF PCLS The viability of PCLS was assessed by the content of ATP. The determination of ATP was performed using the ATP Bioluminescence Assay Kit CLS II (Roche, Mannheim, Germany). Three slices were harvested in a 2 mM EDTA solution containing 70% ethanol, pH 10.9, and immediately frozen at -80 C. Slices were homogenized using a mini beat beater and the homogenate was centrifuged for 5 min at 13,000 g. The supernatant was used for the ATP assay and the pellet for the protein analysis. The ATP assay is performed in 96-well plate. 5 μL of sample was diluted 10 times with 100 mM Tris-HCl, 2 mM EDTA buffer pH 7.8. 50 μL of luciferase was added to each sample and the ATP was measured with the Lucy1 luminometer (Anthos, Durham, NC, USA). The protein content of each slice was assessed using the BIO-Rad DC protein assay kit (Bio-Rad, Munich, Germany) as described before [34] and the ATP values are corrected with their corresponding protein content.

RNA ISOLATION RNA was isolated from slices with <10%, <30% and 30-50 % decreased viability. Maxwell(R) 16 LEV Total RNA purification kit (Promega, The Netherlands) with Maxwell(R) 16 LEV Instrument was used to isolated RNA from the samples. Immediately after isolation, the RNA quality was assessed by measuring the 260/280 and 260/230 ratios and the concentration was measured with the ND-1000 spectrophotometer (Fisher Scientific, Landsmeer, The Netherlands). The quality (RIN value) and quantity of the RNA was determined by high throughput Caliper GX LabChip RNA kit (Caliper).

AMPLIFICATION, LABELING, AND HYBRIDIZATION OF RNA SAMPLES Ambion Illumina Total Prep RNA kit was used to transcribe 300 ng RNA to cRNA according to the manufacturer's instructions. A total of 750 ng of cRNA was hybridized at 58°C for 16 hr to the Illumina HumanHT-12 v4 Expression BeadChips. BeadChips were scanned using Iscan software and IDAT files were generated (Illumina, SanDiego, CA).

PREPROCESSING OF GENE EXPRESSION DATA Genome studio software (Illumina) was used to read the IDAT files and generate raw expression values. The ArrayAnalysis webservice (www.arrayanalysis.org/) was used for further preprocessing the data, which uses lumi R package [120]. Raw gene expression data was background corrected (bgAdjust), variance stabilized (VST) and normalized by quantile normalization. After normalization, the data was corrected for batch differences owing to RNA isolation and hybridization using the ComBat method implemented in the swamp package in R [121]. Differentially expressed genes in slices exposed to the cholestatic drugs in the presence of bile acids versus the slices exposed to vehicle (DMSO) in the presence of bile acids were identified using the limma package [122]. Genes that are regulated with a criterion of fold change of 1.5 and FDR corrected p- value 0.05 (Benjamini and Hochberg method) were chosen for pathway analysis. To compare our data with the scarcely available human in vivo data, human *in vivo* late-stage cholestasis data were downloaded from the Gene Expression Omnibus database (GSE46960). These gene expression data were generated in GeneChip human Gene 1.0 ST array (Affymetrix, CA), hybridization experiments using human liver biopsies obtained from 64 infants with biliary atresia, 14 age-matched infants with cholestasis of other origin than biliary atresia, and from 7 deceased healthy children [123]. Affymetrix data normalization and statistical analysis was performed using the ArrayAnalysis website [120] using similar criteria as for the PCLS. A gene is considered as regulated in association with cholestasis in human PCLS if its expression is differentially regulated in the same direction by two or more of the five tested compounds. A gene is considered as regulated *in vivo* in human if its expression is differentially regulated in either biliary atresia or intrahepatic cholestasis.

PATHWAY ANALYSIS Canonical metabolic and signaling pathway analysis was performed using QIAGEN's Ingenuity(r) Pathway Analysis (IPA(r), QIAGEN Redwood City, California, USA). The compound exposures where no or very few genes were regulated (AN 25µM , CP 9µM, CP18µM EE 25µM, EE50µM and MT 25µM) were excluded from the pathway analysis. Comparison pathway analysis feature in IPA was used to compare the canonical pathways affected by the different compounds in human PCLS.

3.3 RESULTS

CONCENTRATION SELECTION FOR TRANSCRIPTOMIC STUDIES Concentration response studies were performed to find out toxic concentrations for the cholestatic compounds. Pilot studies were performed using a range of concentrations (data not shown) and the concentrations which showed a 10-30 % and 30-50% decrease in ATP for each of the tested cholestatic compounds were chosen for the microarray gene expression studies. All five cholestatic compounds showed a concentration dependent decrease in cell viability (Supplementary figure 11). A concentration-dependent increase in the number of regulated genes was observed. From the data on the number of regulated genes (figure 9) it is clear that concentrations that do not result in a substantial reduction of viability do not cause regulation of a significant number of genes. At concentrations causing up to 30% decrease in viability, a relatively limited number of genes were regulated and at higher concentrations, where toxicity amounted to 30-50%, a significant number of genes was regulated. However, despite of a similar decrease in toxicity, the compounds have different effects on gene expression judged on the basis of a different number of regulated genes.

CANONICAL PATHWAY ANALYSIS The Ingenuity knowledgebase contains canonical pathways that are well characterized metabolic and cell signaling pathways. The differentially regulated genes as shown in figure 9 were scored against the canonical pathways and the resulting scaled values for pathway enrichment are shown as a heatmap in figure 10.

Figure 2 shows that many canonical pathways that are related to bile acid homeostasis and cholestasis are regulated in the PCLS treated with the 5 cholestatic compounds in the presence of a portal vein concentration of a physiological bile acid mix. Hepatic cholestasis appeared as one of the top 10 most significantly affected pathways. Moreover, signaling pathways such as FXR, LXR, PXR and VDR, which play a prominent role in cholestasis, are also significantly affected. In addition, endoplasmic reticulum stress (ER stress), unfolded protein response and protein ubiquitination pathways, known to play a role in bile acid induced cholestasis process [124] are significantly affected. Furthermore, the pathways involved in bile acid induced damage such as Nrf2 mediated stress response, coagulation system and complement activation appear affected. The observed patterns of activated genes appeared concentration dependent, nevertheless there was a good overlap of the regulated genes at the different concentrations. Therefore, for the comparison of the genes regulated in these different canonical pathways, the highest concentration for each of the different cholestatic compounds was considered for further analysis. It is interesting to observe that the genes coding for transporters and metabolic enzymes in the hepatic cholestasis pathway are downregulated (table 7). It should be mentioned here that most of the genes involved in the hepatic cholestasis pathway are also part of the signaling pathways mentioned below.

The FXR pathway was the most significantly regulated pathway. The genes regulated in the human PCLS that are involved in FXR mediated response are summarized in table 8. It is apparent that many target genes involved in the FXR pathway such as BSEP, MRP2, MDR3, BACS, BAAT, FGF15 and PXR are downregulated. The LXR pathway was also significantly downregulated in human PCLS exposed to cholestatic compounds and bile acids. The genes regulated in human PCLS that are involved in LXR mediated response are summarized in supplementary table 10. Also the genes involved in the cholesterol biosynthesis pathway were downregulated in human PCLS by the cholestatic compounds

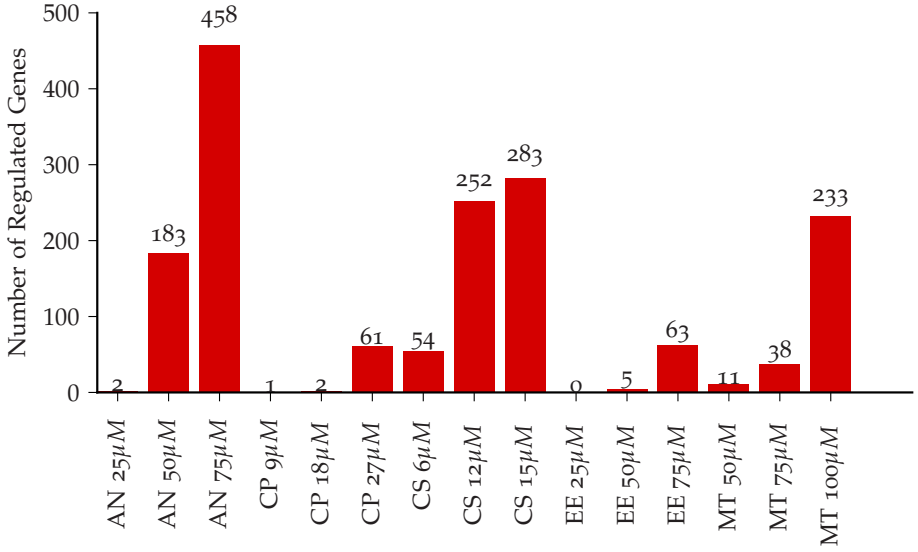

Figure 9: Number of genes differentially regulated with a fold change of 1.5 and multiple hypothesis-adjusted p-value 0.05

Table 7: Genes involved in hepatic cholestasis pathway and their regulation after exposure to cholestatic drugs in human PCLS

		Hepatic cholestasis				
Gene Symbol	**Gene description**	**AN 75μM**	**CP 27μM**	**CS 15μM**	**EE 75μM**	**MT 100μM**
IL1RL1	interleukin 1 receptor-like 1	**2.3**	1.4	1.3	**4.6**	**3.5**
IL1RN	interleukin 1 receptor antagonist	1.3	1.2	-1.2	1.1	**1.9**
IRAK2	interleukin-1 receptor-associated kinase 2	**1.6**	**1.5**	1.4	1.3	1.1
JUN	jun proto-oncogene	1.3	**1.5**	**2.0**	**1.7**	**1.6**
PPRC1	peroxisome proliferator-activated receptor gamma, coactivator-related 1	**1.6**	1.3	1.4	1.4	1.4
ABCB11	ATP-binding cassette, sub-family B (MDR/TAP), member 11	**-1.8**	**-1.5**	-1.3	**-1.6**	**-1.7**
ABCB4	ATP-binding cassette, sub-family B (MDR/TAP), member 4	**-2.1**	**-2.0**	-1.1	**-2.8**	**-3.6**
ABCC3	ATP-binding cassette, sub-family C (CFTR/MRP), member 3	-1.2	-1.1	-1.1	-1.3	**-1.8**
ABCG5	ATP-binding cassette, sub-family G (WHITE), member 5	**-1.5**	-1.4	-1.1	-1.3	**-1.5**
ABCG8	ATP-binding cassette, sub-family G (WHITE), member 8	**-2.3**	**-1.7**	-1.2	**-1.7**	-1.4
CYP27A1	cytochrome P450, family 27, subfamily A, polypeptide 1	-1.3	-1.1	**-1.7**	**-1.7**	**-1.5**
CYP8B1	cytochrome P450, family 8, subfamily B, polypeptide 1	**-3.4**	-2.3	**-2.1**	**-1.7**	1.1
GCGR	glucagon receptor	**-1.9**	-1.7	-1.2	-1.4	1.0
IL1B	interleukin 1, beta	-1.2	-1.1	**-1.5**	-1.1	-1.2
NR0B2	nuclear receptor subfamily 0, group B, member 2	**-1.6**	-1.2	**-1.6**	-1.4	-1.2
NR1H3	nuclear receptor subfamily 1, group H, member 3	**-1.8**	-1.3	-1.3	-1.1	-1.0
NR1H4	nuclear receptor subfamily 1, group H, member 4	**-1.9**	-1.3	-1.4	-1.2	-1.3
RXRA	retinoid X receptor, alpha	**-1.5**	-1.1	-1.3	**-1.6**	**-1.7**
SLC22A7	solute carrier family 22 (organic anion transporter), member 7	**-2.9**	**-2.6**	**-1.9**	**-2.1**	**-1.7**
TNFRSF1B	tumor necrosis factor receptor superfamily, member 1B	**-1.5**	1.0	-1.3	-1.2	1.1

Significantly regulated genes with fold change -1.5 or 1.5 are highlighted in orange and blue color, respectively.

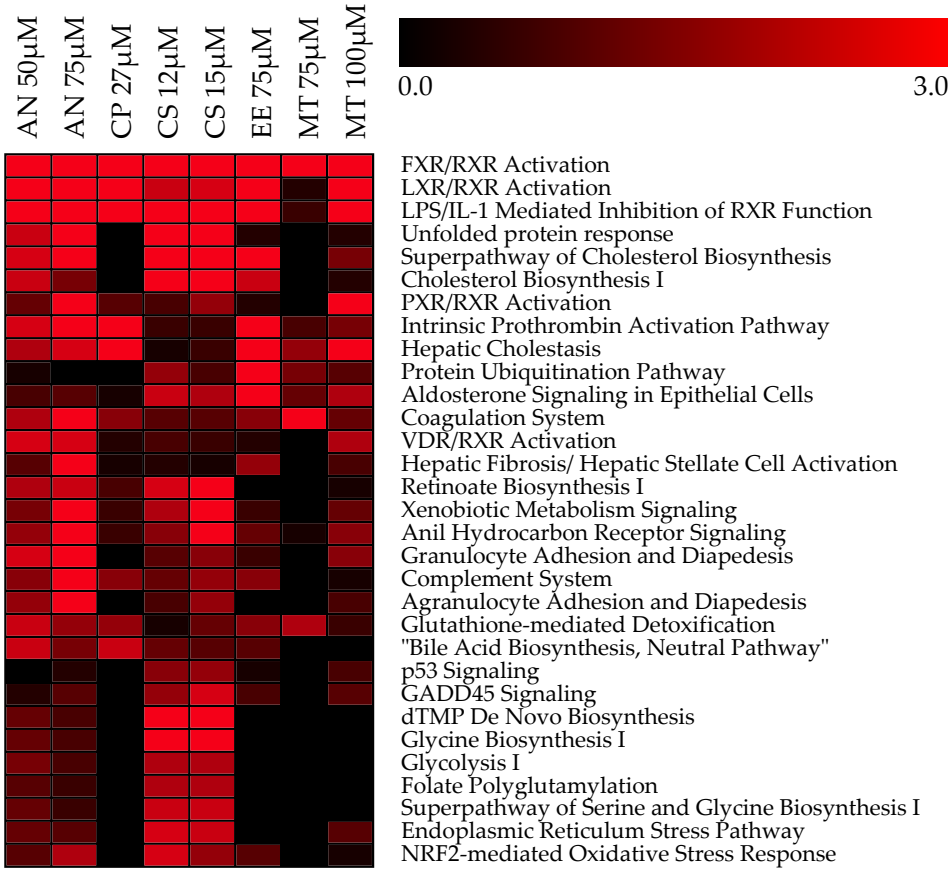

Figure 10: Heatmap of canonical pathway enrichment analysis results
Enrichment values (-log (p-value)) are scaled from 0 to 3 (black to red). Compound exposures where no or very few genes were regulated were excluded.

Table 8: Genes involved in the FXR pathway and their regulation after exposure to cholestatic drugs in human PCLS

FXR signalling pathway						
Gene Symbol	**Gene description**	**AN 75μM**	**CP 27μM**	**CS 15μM**	**EE 75μM**	**MT 100μM**
ABCB11	ATP-binding cassette, sub-family B (MDR/TAP), member 4	**-1.8**	**-1.5**	-1.3	**-1.6**	**-1.7**
ABCB4	ATP-binding cassette, sub-family B (MDR/TAP), member 11	**-2.1**	**-2.0**	-1.1	**-2.8**	**-3.6**
ABCG5	ATP-binding cassette, sub-family G (WHITE), member 5	**-1.5**	-1.4	-1.1	-1.3	**-1.5**
ABCG8	ATP-binding cassette, sub-family G (WHITE), member 8	**-2.3**	**-1.7**	-1.2	**-1.7**	-1.4
APOC2	apolipoprotein C-II	**-1.8**	-1.4	**-1.7**	-1.3	1.0
APOC4	apolipoprotein C-IV	**-1.8**	**-1.8**	**-1.7**	-1.4	-1.1
APOF	apolipoprotein F	**-1.9**	**-1.9**	**-1.9**	-1.5	1.1
BAAT	bile acid CoA:amino acid N-acyltransferase	**-1.7**	-1.3	-1.4	-1.1	1.5
C3	complement component 3	**-1.7**	**-1.5**	-1.5	**-1.8**	**-2.0**
CYP27A1	cytochrome P450, family 27, subfamily A, polypeptide 1	-1.3	-1.1	**-1.7**	**-1.7**	-1.5
CYP8B1	cytochrome P450, family 8, subfamily B, polypeptide 1	**-3.5**	**-2.3**	**-2.1**	-1.7	1.1
FASN	fatty acid synthase	**-2.1**	1.5	**-2.1**	-1.2	1.2
FBP1	fructose-1,6-bisphosphatase 1	**-2.1**	**-1.9**	**-2.0**	-1.4	1.2
FETUB	fetuin B	**-2.0**	**-1.8**	**-1.8**	-1.6	-1.5
FGA	fibrinogen alpha chain	**-2.1**	**-1.7**	-1.6	-1.2	1.9
ITIH4	inter-alpha-trypsin inhibitor heavy chain family, member 4	**-1.5**	-1.2	**-1.6**	-1.4	-1.4
KNG1	kininogen 1	**-2.3**	**-1.8**	-1.3	**-1.9**	**-1.7**
NR0B2 (SHP)	nuclear receptor subfamily 0, group B, member 2	**-1.6**	-1.2	**-1.6**	-1.4	-1.2
NR1H3 (LXR)	nuclear receptor subfamily 1, group H, member 3	**-1.8**	-1.3	-1.3	-1.1	-1.0
NR1H4 (FXR)	nuclear receptor subfamily 1, group H, member 4	**-1.9**	-1.3	-1.4	-1.2	-1.3
PON1	paraoxonase 1	**-2.0**	-1.9	-1.6	-1.4	1.4
RXRA	retinoid X receptor, alpha	**-1.5**	-1.1	-1.3	-1.6	**-1.7**
SCARB1	scavenger receptor class B, member 1	**-2.2**	-1.6	-1.4	**-1.8**	**-1.6**
SDC1	syndecan 1	**-2.4**	-1.4	**-1.9**	**-1.8**	**-1.8**
SERPINF2	serpin peptidase inhibitor, clade F , member 2	**-1.8**	-1.6	**-1.6**	-1.3	1.1
SLC22A7	solute carrier family 22 (organic anion transporter), member 7	**-2.9**	**-2.6**	-1.9	**-2.1**	**-1.7**
SLC51B	solute carrier family 51, beta subunit	**-2.6**	**-1.9**	**-1.7**	**-2.4**	**-2.8**
SULT2A1	sulfotransferase family, cytosolic, 2A, member 1	**-2.1**	-1.9	-1.8	-1.0	1.7

Significantly regulated genes with fold change -1.5 or 1.5 are highlighted in orange and blue, respectively.

Table 9: Genes involved in unfolded protein response (UPR) and their regulation after exposure to cholestatic drugs in human PCLS

Unfolded protein response						
Gene Symbol	**Gene description**	**AN 75μM**	**CP 27μM**	**CS 15μM**	**EE 75μM**	**MT 100μM**
ATF4	activating transcription factor 4	**2.3**	**1.5**	**1.8**	1.3	1.2
DDIT3 (CHOP)	DNA-damage-inducible transcript 3	**2.9**	1.2	**1.8**	1.8	**2.9**
DNAJB9	DnaJ (Hsp40) homolog, subfamily B, member 9	**2.7**	1.0	**3.0**	1.4	1.0
ERN1	endoplasmic reticulum to nucleus signaling 1	**1.6**	1.1	1.1	1.8	**3.0**
HSPA9	heat shock 70kDa protein 9 (mortalin)	**1.9**	1.1	**1.7**	1.4	1.3
HSPH1	heat shock 105kDa/110kDa protein 1	**1.7**	1.4	1.4	**2.8**	1.7
NFE2L2	nuclear factor, erythroid 2-like 2	**1.5**	1.1	**1.2**	1.0	1.1
SYVN1	synovial apoptosis inhibitor 1, synoviolin	**1.5**	1.0	1.8	1.1	-1.1
INSIG1	insulin induced gene 1	**-2.5**	1.3	**-2.0**	-1.7	-1.5

Significantly regulated genes with fold change -1.5 or 1.5 are highlighted in orange and blue respectively.

except for CP (supplementary table 11). The downregulation of the cholesterol biosynthesis genes is well in line with the downregulation of the LXR target genes. As expected, also target genes in the PXR (supplementary table12) and VDR (supplementary table 13) pathways were regulated. Among the PXR target genes some of the Cytochrome P450 isoforms were upregulated *ex vivo* in the slices. In line with the published involvement of ER stress in cholestasis, the unfolded protein response pathway was significantly regulated and most of the genes involved in unfolded protein response (ER stress) were significantly upregulated (table 9).

Complement and coagulation pathways were affected and genes involved in those pathways were mostly downregulated as shown in supplementary table 14 and 15 respectively. NRF2 mediated oxidative stress response was affected and upregulation of genes coding for heat shock proteins and the activation of transcription factors such as ATF4 and NRF2 were apparent (supplementary table 16). In addition, the hepatic fibrosis pathway was affected and some genes involved in the hepatic stellate cell activation were upregulated such as KLF6 (supplementary table 17).

3.4 DISCUSSION

In this study, human PCLS were validated as an *ex vivo* model that reflects the drug-induced cholestasis processes using transcriptomic analysis. Hepatotoxicants that are known to induce cholestasis in humans, such as cyclosporine, chlorpromazine, ethinyl estradiol and methyl testosterone, clearly induced regulation of genes and pathways associated with cholestasis in human PCLS when incubated in the presence of bile acids. In addition, ANIT, a well-known cholestatic compound in rats, was included in the study, and showed a similar cholestatic gene expression pattern in human liver slices. From the data it is clear that concentrations that do not cause a decrease in viability also do not lead to differential expression of a substantial number of genes. Also, the addition of 60 μM of bile acid mix to the incubation medium does not induce major changes in gene expression (data not shown). Pathway analysis clearly showed a gene expression pattern of cholestatic injury, which was concentration dependent for all drugs. The direction of regulation of most genes was similar among the five tested cholestatic drugs, but there were differences with respect to the number of genes that were significantly regulated in each pathway. Importantly, hepatic cholestasis was among the top 5 regulated pathways. The majority of the pathways regulated in the human PCLS are represented in the Adverse Outcome Pathway (AOP) for cholestasis as proposed by Vinken et al, including the primary direct cellular responses and secondary adaptive responses involved in bile acid induced cholestatic injury [16, 17, 18], such as primary toxicity by NRF2 mediated oxidative stress response, inflammation mediated hepatic fibrosis, endoplasmic reticulum stress, and activation of the coagulation and complement system. Moreover signaling pathways such as FXR, LXR, PXR and VDR as well as the related cholesterol biosynthesis pathways were affected. It is generally assumed that the accumulation of bile acids, cholesterol and bilirubin during onset and progression of cholestatic condition induces response processes characterized by the activation of nuclear receptors such as FXR, LXR, PXR and VDR, which triggers cellular adaption to counteract bile acid accumulation and thus cholestatic liver injury [19]. The farsenoid X receptor (FXR) acts as a sensor for intracellular bile acid levels [125] and activation of FXR (NR1H4) induces adaptive gene expression changes in response to accumulation of bile acids in cholestasis such as inhibition of bile acid synthesis, upregulation of phase I bile acid hydroxylation, phase II conjugation enzymes, and induction of the expression of canalicular and basolateral bile acid transporters. In contrast with this expected activation of FXR, in the human PCLS the target genes in the FXR pathway were downregulated. Interestingly a similar trend of downregulation of FXR target genes was observed in mouse PCLS after exposure to cholestatic drugs in the absence of bile acids [112, 113]. Important genes known to play a role in cholestasis such as ABCB4 (MDR3), ABCB11 (BSEP) and NR0B2 (SHP) were downregulated in human PCLS exposed to bile acids and cholestatic drugs. Previously we showed upregulation of SHP and downregulation of BSEP as a response to accumulation of bile acids after incubation of human PCLS with 100 μM CDCA [80]. Either a limited increase in the concentration of the total bile acids and particularly of CDCA in the hepatocytes or the presence of other bile acids such as LCA that can counteract the effect of CDCA [126] may be the cause for this difference. Lew *et al,* showed that FXR controls the gene expression of its target genes in a ligand dependent fashion based on the individual bile acids [127]. However, BSEP down regulation may also indicate a direct effect of the tested cholestatic drugs on the regulation of the BSEP transporter, as potent BSEP inhibitors have been shown to

downregulate BSEP expression in primary human hepatocytes [128]. Moreover the decreased expression of FXR (table 4) can at least partly explain this reduced FXR signalling. This is in line with the finding that both FXR and SHP expression was reduced by 90% or more in cholestatic patients [15]. Thus, based on our findings it can be postulated that exposure to cholestatic compounds could lead to compromised FXR mediated adaptive responses, causing hepatic cholestasis. The Liver X receptor (LXR) is involved in the regulation of metabolism of lipids and cholesterol to bile acid catabolism. Activation of the LXR receptor is shown to prevent toxicity from bile acid accumulation in female mice [129]. We found in human PCLS that the LXR pathway including the genes involved in cholesterol transport such as ABCG5 and ABCG8 was downregulated by the cholestatic drugs, which may indicate a loss of this protective action of LXR. In addition the PXR and VDR pathways are downregulated due to the exposure of PCLS to the cholestatic drugs. The Pregnane X receptor (PXR) is activated by drugs and endogenous molecules and plays a central role in their metabolism by induction of cytochrome P450 enzymes, conjugation enzymes and efflux transporters. PXR activation also regulates bile acid synthesis, their metabolism and transport, cholesterol homeostasis and lipid metabolism. The exposure of the human PCLS to the cholestatic compounds resulted in upregulation of some of the phase I metabolic enzymes such as CYP1A2, CYP2C8 and CYP2C9. However again in contrast to the results obtained after incubation with 100 μM CDCA, there was no change in the expression of CYP7A1 involved in bile acid synthesis in human PCLS. The Vitamin D receptor (VDR) expression is restricted to non-parenchymal cells, such as biliary epithelial cells in the liver [130]. VDR downregulation was not observed in our data but RXR expression is down regulated. Since VDR acts as a heterodimer with RXR, it can be assumed that VDR function is compromised by this lack of RXR expression. Together, the reduced activation of FXR, LXR, PXR and VDR could be responsible for reduced adaptive responses to the effects of the cholestatic drugs and lead to development of cholestasis.Oxidative stress is implicated to play a role in the pathogenesis of drug-induced cholestasis as a result of bile acid accumulation [131, 132, 133]. Oxidative stress was also shown to play a major role as a primary causal event in the early CPZ-induced cholestasis in human HepaRG cells [133]. In addition, the protective role of the NRF2 mediated oxidative stress response was reported in mice in response to ANIT induced cholestasis [131]. This NRF2 mediated oxidative stress response counteracts the cellular oxidative stress by induction of detoxifying and antioxidant enzymes, which also occurred *ex vivo* as ATF4 (activating transcription factor 4) was upregulated in the human PCLS treated with cholestatic drugs. ATF4 is known to increase the activation of phosphorylated NRF2 protein, key regulator of the oxidative stress response. This indicates that detoxifying mechanisms are activated in the PCLS to alleviate the oxidative stress due to accumulating bile acids. Hepatic fibrosis and hepatic stellate cell activation was also observed in human PCLS due to exposure to the cholestatic drugs. Accumulation of bile acids by obstructive cholestasis [134], was shown to lead to an inflammatory response *in vivo* which in turn leads to activation of hepatic stellate cells and liver fibrosis. We showed recently that rat and human PCLS can be a suitable model to identify the early fibrotic changes and fibrosis inducing potential of a compound by transcriptomics [117] or RT-PCR [72, 74, 73, 115, 116, 85] Early fibrotic response genes identified in rat PCLS such as KLF6 and SERPINE1 were upregulated in human PCLS indicating their prominent role in the early onset of fibrosis. A recent study revealed that endoplasmic reticulum stress is involved in the bile acid induced hepatocellular injury [124]. In PCLS, ER stress, UPR and protein

ubiquitination pathways were also among the most affected pathways. The UPR signaling pathway is activated in response to ER stress and promotes cell survival and adaptation. Our results suggest that ER stress, protein ubiquitination and unfolded protein response UPR may be early cellular effects in drug-induced cholestasis.Cholesterol is the starting material for the synthesis of bile acids in liver. Bile acid biosynthesis is the major catabolic pathway for cholestasis. The genes involved in cholesterol biosynthesis were downregulated in human PCLS indicating the adaptive response of hepatocytes to decrease cholesterol synthesis as a response to cholestatic drugs (Supplementary table 11), as was also observed in mouse PCLS [112, 113]. Also genes in the complement system such as C3 and C5 were downregulated in human PCLS indicating possibly the adaptive response to the inflammation leading to fibrosis. The complement system is known to play a critical role in the pathogenesis of chronic liver disease [135] and is regulated by FXR in both human and rodents [136, 137]. The coagulation system is one of the signaling pathways involved in cellular stress and injury. The coagulation system is known to contribute to bile duct ligation induced and ANIT induced liver injury [138, 139] in the rat. Downregulation of genes involved in the coagulation system was observed in human PCLS.

COMPARISON WITH HUMAN *in vivo* CHOLESTASIS The results obtained in PCLS should preferably be validated by comparing with human liver tissue of patients suffering from drug-induced cholestasis. However to the best of our knowledge this data is not available. Therefore we compared our findings with gene expression data obtained from liver samples of patients with cholestasis due to biliary atresia and intrahepatic not drug-induced cholestasis [123]. Despite the fact that these samples represent an end-stage disease situation and were mainly obtained from infants, comparison of the activated pathways between human PCLS and the patient samples revealed that there was good overlap with respect to the processes involved in cholestasis, although more pathways were affected *in vivo* than in the cholestatic PCLS (supplementary figure 12). The FXR pathway was affected both *in vivo* and *ex vivo,* however in human PCLS the genes involved in the FXR pathway were downregulated in contrast to the patient samples, where they were upregulated. The genes involved in the LXR pathway and cholesterol biosynthesis were mostly downregulated in both the human PCLS and the patient livers. Remarkably, among the PXR target genes, some of the Cytochrome P450 isoforms were strongly downregulated in the human cholestatic livers in vivo, but were not regulated or somewhat upregulated in human PCLS. Several genes involved in UPR response were upregulated after exposure to cholestatic drugs in human PCLS, but were downregulated in *in vivo* cholestasis (supplementary figure 13). Genes involved in the complement system were downregulated in both human PCLS and in patient samples. Liver fibrosis or hepatic stellate cell activation is observed both in human PCLS exposed to cholestatic drugs and in *in vivo* cholestasis. Structural alteration of tight junction proteins is observed in the bile duct ligated cholestasis [140]. The tight junction signaling pathway is not activated in slices but significant activation is seen in patient samples (supplementary figure 12). An explanation for the observed differences between in vivo data and the ex vivo data could be due to the different causes of cholestasis or the large difference in time frame.In conclusion, the transcriptomic analysis of human PCLS exposed to cholestatic drugs in the presence of bile acids revealed that this model reflects the primary toxicity processes associated with hepatic cholestasis, and the related processes such as oxidative stress, ER stress and UPR response and therefore seems to be

promising for the future application in drug screening for cholestasis. The results suggest that decreased adaptive responses mediated via nuclear receptors are associated with these cholestatic effects, Our study demonstrates that human PCLS is a suitable model to identify biomarkers and possible mechanisms of toxicity of cholestatic compounds, when incubated in the presence of a physiological concentration of bile acids. Insights from the pathways such as downregulation of cholesterol biosynthesis, ER stress response and NRF2 mediated oxidative stress response could be included in the adverse outcome pathway of cholestasis.

ACKNOWLEDGEMENTS

The authors would like to thank Prof. Dr. Robert Porte and all the surgeons at University Medical Center Groningen for providing human liver tissue. We also thank Marina de Jager, Marjolijn Merema, Miriam Langelaar for their help with preparation and incubation of hPCLS. Roel Bijkerk of Leiden University Medical Center thanked for his assistance with the IPA pathway analysis program.

SUPPLEMENTARY TABLES

Table 10: Genes involved in the LXR pathway and their regulation after exposure to cholestatic drugs in human PCLS

LXR signalling pathway						
Symbol	**Gene description**	**AN 75μM**	**CP 27μM**	**CS 15μM**	**EE 75μM**	**MT 100μM**
IL1RL1	interleukin 1 receptor-like 1	**2.3**	1.4	1.4	4.7	**3.5**
PTGS2	prostaglandin-endoperoxide synthase 2	**3.3**	**2.2**	**1.8**	**2.1**	**2.9**
ABCG5	ATP-binding cassette, sub-family G, member 5	**-1.5**	-1.4	-1.1	-1.3	**-1.5**
ABCG8	ATP-binding cassette, sub-family G, member 8	**-2.3**	**-1.7**	-1.2	**-1.7**	-1.4
APOB	apolipoprotein B	**-1.8**	-1.4	-1.3	-1.3	-1.2
APOC2	apolipoprotein C-II	**-1.8**	-1.4	**-1.7**	-1.3	1.0
APOC4	apolipoprotein C-IV	**-1.8**	-1.8	**-1.7**	-1.4	-1.1
APOF	apolipoprotein F	**-1.9**	-1.9	**-1.9**	**-1.5**	1.1
C3	complement component 3	**-1.7**	-1.5	-1.5	**-1.8**	**-2.0**
C9	complement component 9	-1.7	-1.4	-1.5	-1.3	1.3
FASN	fatty acid synthase	**-2.1**	1.5	-2.1	-1.2	1.2
FDFT1	farnesyl-diphosphate farnesyltransferase 1	**-1.5**	1.6	**-1.6**	**-1.6**	-1.4
FGA	fibrinogen alpha chain	**-2.1**	-1.7	**-1.6**	-1.2	**1.9**
ITIH4	inter-alpha-trypsin inhibitor heavy chain family, member 4	**-1.5**	-1.2	**-1.6**	-1.4	-1.4
KNG1	kininogen 1	**-2.3**	**-1.8**	-1.3	**-1.9**	**-1.7**
NR1H3	nuclear receptor subfamily 1, group H, member 3	**-1.8**	-1.3	-1.3	-1.1	-1.0
NR1H4	nuclear receptor subfamily 1, group H, member 4	**-1.9**	-1.3	-1.4	-1.2	-1.3
PON1	paraoxonase 1	**-2.0**	-1.9	-1.6	-1.4	1.4
RXRA	retinoid X receptor, alpha	**-1.5**	-1.1	-1.3	-1.6	**-1.7**
SCD	stearoyl-CoA desaturase (delta-9-desaturase)	**-1.9**	1.4	**-1.6**	-1.4	**-1.6**
SERPINF2	serpin peptidase inhibitor, clade F, member 2	**-1.8**	-1.6	**-1.6**	-1.3	1.1

Significantly regulated genes with fold change -1.5 or 1.5 are highlighted in orange and blue respectively.

Table 11: Genes involved in cholesterol biosynthesis and their regulation after exposure to cholestatic drugs in human PCLS

Cholesterol biosynthesis						
Gene Symbol	**Gene description**	**AN 75μM**	**CP 27μM**	**CS 15μM**	**EE 75μM**	**MT 100μM**
DHCR24	7-dehydrocholesterol reductase	-1.4	1.1	-1.5	-1.4	-1.2
DHCR7	7-dehydrocholesterol reductase	-2.0	1.4	-1.7	-2.0	-1.5
EBP	emopamil binding protein (sterol isomerase)	-1.9	1.3	-2.0	-1.8	-1.3
FDFT1	farnesyl-diphosphate farnesyltransferase 1	-1.5	1.6	-1.6	-1.6	-1.4
FDPS	farnesyl diphosphate synthase	-1.7	1.6	-1.5	-1.6	-1.6
IDI1	isopentenyl-diphosphate delta isomerase 1	-1.6	1.6	-1.6	-1.8	-1.4
LSS	lanosterol synthase	-1.7	1.4	-1.5	-1.6	-1.6
MSMO1	methylsterol monooxygenase 1	-1.4	1.6	-1.6	-1.7	-1.2
NSDHL	NAD(P) dependent steroid dehydrogenase-like	-1.5	1.5	-1.5	-1.3	-1.1

Significantly regulated genes with fold change -1.5 or 1.5 are highlighted in orange and blue respectively.

Table 12: Genes involved in the PXR pathway and their regulation after exposure to cholestatic drugs in human PCLS

PXR signalling pathway						
Gene Symbol	**Gene description**	**AN 75μM**	**CP 27μM**	**CS 15μM**	**EE 75μM**	**MT 100μM**
IGFBP1	insulin-like growth factor binding protein 1	5.4	1.5	2.0	1.8	**1.9**
CYP1A2	cytochrome P450, family 1, subfamily A, polypeptide 2	**3.9**	**1.7**	-1.2	**1.3**	**2.0**
CYP2C9	cytochrome P450, family 2, subfamily C, polypeptide 9	1.6	1.2	-1.4	1.5	**2.2**
ABCB11	ATP-binding cassette, sub-family B (MDR/TAP), member 11	**-1.8**	**-1.5**	**-1.3**	-1.6	-1.7
ABCC3	ATP-binding cassette, sub-family C (CFTR/MRP), member 3	**-1.2**	**-1.1**	**-1.1**	-1.3	-1.8
ALAS1	5'-aminolevulinate synthase 1	1.1	-1.1	-1.1	1.3	**1.5**
ALDH1A1	aldehyde dehydrogenase 1 family, member A1	**-1.6**	**-1.6**	-1.7	-1.4	-1.4
CES2	carboxylesterase 2	-1.9	-1.5	-2.2	-1.6	**-1.5**
CPT1A	carnitine palmitoyltransferase 1A (liver)	**1.1**	1.0	-1.0	1.1	**1.2**
CYP2C8	cytochrome P450, family 2, subfamily C, polypeptide 8	**-1.1**	-1.4	-1.6	1.5	2.2
GSTA1	glutathione S-transferase alpha 1	**-1.7**	-1.9	-1.9	-1.2	1.4
NR0B2	nuclear receptor subfamily 0, group B, member 2	**-1.6**	-1.2	**-1.6**	-1.4	-1.2
NR1I3	nuclear receptor subfamily 1, group I, member 3	**-1.6**	**-1.7**	**-1.6**	-1.1	1.3
PAPSS2	retinoid X receptor, alpha	-1.2	-1.2	-1.1	-1.0	**-1.6**
PPARGC1A	peroxisome proliferator-activated receptor gamma, coactivator 1 alpha	-1.0	1.0	1.0	1.1	**1.3**
SCD	stearoyl-CoA desaturase (delta-9-desaturase)	**-1.9**	1.4	**-1.6**	-1.4	**-1.6**
SULT2A1	sulfotransferase family, cytosolic, 2A, , member 1	**-2.1**	-1.9	-1.8	-1.0	1.7

Significantly regulated genes with fold change -1.5 or 1.5 are highlighted in orange and blue respectively.

Table 13: Genes involved in the VDR pathway and their regulation after exposure to cholestatic drugs in human PCLS

VDR signalling pathway						
Gene Symbol	**Gene description**	**AN 75μM**	**CP 27μM**	**CS 15μM**	**EE 75μM**	**MT 100μM**
CEBPB	CCAAT/enhancer binding protein (C/EBP), beta	**1.5**	1.3	1.3	1.1	1.0
GADD45A	growth arrest and DNA-damage-inducible, alpha	**2.1**	1.3	1.8	2.5	2.7
IGFBP1	insulin-like growth factor binding protein 1	**5.4**	1.5	**2.0**	1.8	**1.9**
IGFBP3	insulin-like growth factor binding protein 3	**1.8**	1.0	-1.0	1.4	-1.1
IL1RL1	interleukin 1 receptor-like 1	**2.3**	1.4	1.4	4.7	3.5
KLF4	Kruppel-like factor 4 (gut)	**2.0**	1.6	1.8	1.1	-1.1
CXCL10	chemokine (C-X-C motif) ligand 10	**-2.5**	1.0	-1.5	**-1.4**	**-1.6**
HSD17B2	hydroxysteroid (17-beta) dehydrogenase 2	**-1.5**	**-1.6**	**-2.0**	-1.4	-1.6
LRP5	low density lipoprotein receptor-related protein 5	**-1.4**	-1.3	-1.3	-1.4	**-1.6**
PRKCA	protein kinase C, alpha	**-1.4**	**1.0**	-1.1	-1.4	-1.8
RXRA	retinoid X receptor, alpha	**-1.5**	-1.1	-1.3	-1.6	-1.7
SPP1	secreted phosphoprotein 1	-1.9	-1.5	-1.1	-1.2	**1.1**
SULT2A1	sulfotransferase family, cytosolic, 2A, member 1	-2.1	-1.9	-1.8	-1.0	**1.7**

Significantly regulated genes with fold change -1.5 or 1.5 are highlighted in orange and blue respectively.

Table 14: Genes involved in the complement system and their regulation after exposure to cholestatic drugs in human PCLS

Complement system						
Gene Symbol	**Gene description**	**AN 75μM**	**CP 27μM**	**CS 15μM**	**EE 75μM**	**MT 100μM**
CD55	CD55 molecule, decay accelerating factor for complement	**1.8**	1.4	**1.7**	**1.6**	1.3
C6	complement component 6	-1.4	**-1.5**	-1.3	-1.2	1.4
C1QB	complement component 1, q subcomponent, B chain	**-2.1**	-1.1	**-1.9**	-1.5	-1.3
C3	complement component 3	**-1.7**	-1.5	-1.5	**-1.8**	**-2.0**
C4BPB	complement component 4 binding protein, beta	**-1.5**	-1.4	-1.4	-1.5	-1.4
C5	complement component 5	**-1.5**	-1.5	-1.0	-1.3	-1.0
C9	complement component 9	**-1.7**	-1.4	-1.5	-1.3	1.3
CFH	complement factor H	**-2.1**	**-1.7**	**-1.6**	**-1.9**	-1.4
ITGB2	integrin, beta 2	**-1.7**	-1.1	-1.4	**-1.5**	-1.3
MBL2	mannose-binding lectin (protein C) 2, soluble	**-1.8**	**-1.9**	**-2.2**	-1.4	1.2

Significantly regulated genes with fold change -1.5 or 1.5 are highlighted in orange and blue respectively.

Table 15: Genes involved in the coagulation system and their regulation after exposure to cholestatic drugs in human PCLS

Coagulation system						
Gene Symbol	**Gene description**	**AN 75μM**	**CP 27μM**	**CS 15μM**	**EE 75μM**	**MT 100μM**
SERPINE1	serpin peptidase inhibitor, clade E , member 1	**1.8**	1.4	1.3	-1.1	-1.0
A2M	alpha-2-macroglobulin	**-1.9**	-1.3	-1.5	**-1.5**	-1.4
F5	coagulation factor V (proaccelerin, labile factor)	**-1.5**	-1.4	-1.3	-1.3	1.1
F9	coagulation factor IX (proaccelerin, labile factor)	-1.2	-1.2	-1.1	1.0	1.7
FGA	fibrinogen alpha chain	**-2.1**	**-1.7**	**-1.6**	-1.2	**1.9**
KLKB1	kallikrein B, plasma (Fletcher factor) 1	**-1.9**	**-2.0**	-1.4	-1.4	-1.2
KNG1	kininogen 1	**-2.3**	**-1.8**	-1.3	**-1.9**	**-1.7**
PROS1	protein S (alpha)	**-1.8**	-1.4	**-1.9**	**-1.6**	-1.1
SERPINA5	serpin peptidase inhibitor, clade A, member 5	**-1.6**	**-1.6**	-1.5	-1.4	-1.0
SERPIND1	serpin peptidase inhibitor, clade D, member 1	-1.4	-1.3	**-1.8**	**-1.7**	**-1.7**
SERPINF2	serpin peptidase inhibitor, clade F, member 2	**-1.8**	**-1.6**	**-1.6**	-1.3	1.1

Significantly regulated genes with fold change -1.5 or 1.5 are highlighted in orange and blue respectively.

Table 16: NRF2 mediated oxidative stress response genes and their regulation after exposure to cholestatic drugs in human PCLS

NRF2 mediated oxidative stress response						
Gene Symbol	**Gene description**	**AN 75μM**	**CP 27μM**	**CS 15μM**	**EE 75μM**	**MT 100μM**
TXNRD1	thioredoxin reductase 1	**3.0**	**1.5**	**1.5**	**1.5**	1.0
ATF4	activating transcription factor 4	**2.3**	**1.5**	**1.8**	1.3	1.2
ATM	ATM serine/threonine kinase	-1.1	-1.0	1.2	-1.1	-1.2
DNAJB1	DnaJ (Hsp40) homolog, subfamily B, member 1	**1.8**	1.4	1.5	**3.3**	1.7
DNAJB11	DnaJ (Hsp40) homolog, subfamily B, member 11	1.4	1.1	**1.7**	1.1	-1.3
DNAJB9	DnaJ (Hsp40) homolog, subfamily B, member 9	**2.7**	1.0	**3.0**	1.4	1.0
DNAJC1	DnaJ (Hsp40) homolog, subfamily C, member 1	1.2	1.1	**1.5**	1.1	-1.0
DNAJC10	DnaJ (Hsp40) homolog, subfamily C, member 10	1.2	1.0	**1.6**	-1.1	-1.1
FTH1	ferritin, heavy polypeptide 1	**1.6**	**1.6**	1.3	1.3	1.1
GCLM	glutamate-cysteine ligase, modifier subunit	**1.9**	1.2	1.1	1.2	-1.2
HERPUD1	homocysteine-inducible, endoplasmic reticulum stress-inducible, ubiquitin-like domain member 1	**1.6**	1.2	**1.7**	1.1	1.0
JUN	jun proto-oncogene	1.3	**1.5**	**2.0**	**1.7**	1.6
MAFF	v-maf avian musculoaponeurotic fibrosarcoma oncogene homolog F	**2.3**	1.3	**1.6**	**1.7**	2.1
MAP2K1	mitogen-activated protein kinase kinase 1	1.3	1.2	1.3	1.1	1.1
NFE2L2	nuclear factor, erythroid 2-like 2	**1.5**	1.1	1.2	1.0	1.1
RRAS2	related RAS viral (r-ras) oncogene homolog 2	**1.7**	1.2	1.1	1.2	-1.0
STIP1	stress-induced phosphoprotein 1	1.2	1.3	1.1	**1.6**	1.2
CAT	catalase	**-1.6**	**-1.5**	**-1.8**	-1.2	1.4
GSTA1	glutathione S-transferase alpha 1	**-1.7**	**-1.9**	**-1.9**	-1.2	1.4
GSTK1	glutathione S-transferase kappa 1	**-1.7**	-1.4	-1.3	-1.3	-1.1
MGST2	microsomal glutathione S-transferase 2	**-1.7**	-1.2	-1.4	-1.4	-1.3
SCARB1	scavenger receptor class B, member 1	**-2.2**	**-1.6**	-1.4	**-1.8**	**-1.6**

Significantly regulated genes with fold change -1.5 or 1.5 are highlighted in orange and blue respectively.

Table 17: Genes involved in hepatic fibrosis/ hepatic stellate activation and their regulation after exposure to cholestatic drugs in human PCLS

Hepatic fibrosis						
Gene Symbol	**Gene description**	**AN 75μM**	**CP 27μM**	**CS 15μM**	**EE 75μM**	**MT 100μM**
CTGF	angiotensinogen (serpin peptidase inhibitor, clade A, member 8)	1.3	1.2	**1.7**	**1.5**	**1.7**
CYP2E1	cytochrome P450, family 2, subfamily E, polypeptide 1	1.2	-1.1	1.0	1.1	**1.5**
EDNRB	endothelin receptor type B	1.0	1.1	1.1	**1.6**	1.4
FGF2	fibroblast growth factor 2 (basic)	**1.5**	**1.5**	**1.5**	1.1	1.2
IGFBP3	insulin-like growth factor binding protein 3	**1.8**	1.0	-1.0	1.4	-1.1
IL1RL1	interleukin 1 receptor-like 1	**2.3**	1.4	1.4	4.7	3.5
KLF6	Kruppel-like factor 6	**1.9**	**1.7**	**1.5**	**1.7**	**1.8**
SERPINE1	serpin peptidase inhibitor, clade E, member 1	**1.8**	1.4	1.3	-1.1	-1.0
MET	MET proto-oncogene, receptor tyrosine kinase	1.2	1.1	1.1	1.2	**-1.5**
AGT	angiotensinogen (serpin peptidase inhibitor, clade A, member 8)	-1.3	-1.4	**-1.5**	-1.2	1.2
AGTR1	angiotensin II receptor, type 1	**-1.5**	-1.3	**-1.6**	-1.2	-1.2
COL18A1	collagen, type XVIII, alpha 1	**-2.1**	**-1.5**	-1.3	**-1.7**	**-1.5**
COL3A1	collagen, type III, alpha 1	**-2.1**	-1.4	-1.6	-1.6	**-1.5**
COL4A1	collagen, type IV, alpha 1	**-2.0**	1.1	-1.4	-1.2	1.1
IL1B	interleukin 1, beta	-1.2	-1.1	**-1.5**	-1.1	-1.2
MMP9	matrix metallopeptidase 9 (type IV collagenase)	**-1.6**	-1.0	-1.4	-1.3	-1.1
PDGFRB	platelet-derived growth factor receptor, beta polypeptide	**-1.7**	-1.0	-1.2	**-1.5**	-1.2
STAT1	signal transducer and activator of transcription 1, 91kDa	**-1.6**	-1.1	-1.1	-1.1	-1.4
TIMP2	TIMP metallopeptidase inhibitor 2	**-1.7**	-1.0	**-1.5**	-1.3	-1.1
TNFRSF1B	tumor necrosis factor receptor superfamily, member 1B	**-1.6**	1.0	-1.3	-1.2	1.1
TNFSF10	tumor necrosis factor (ligand) superfamily, member 10	**-2.3**	-1.2	-1.3	-1.3	**-1.9**
VCAM1	vascular cell adhesion molecule 1	**-2.3**	-1.4	-1.3	-1.4	**-1.7**

Significantly regulated genes with fold change -1.5 or 1.5 are highlighted in orange and blue respectively.

SUPPLEMENTARY FIGURES

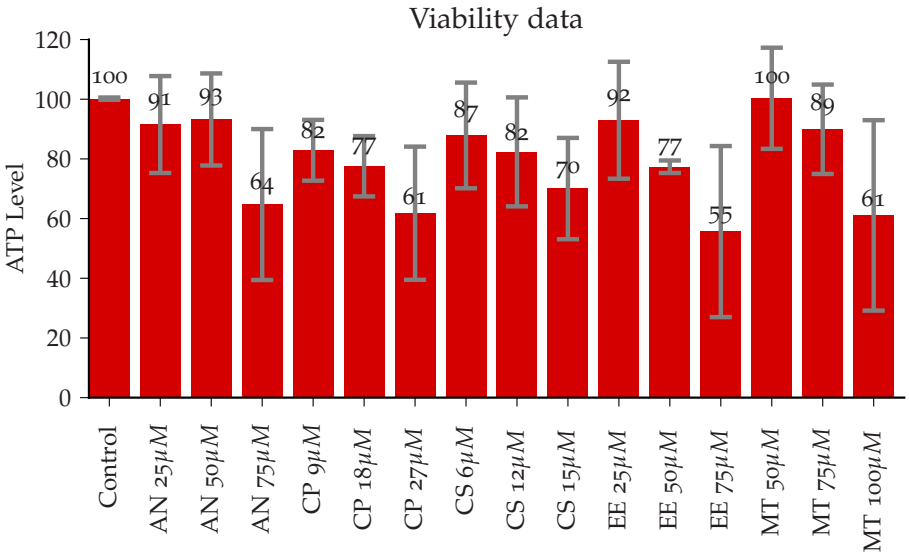

Figure 11: Viability of human PCLS indicated by the ATP content after 24hr incubation with various cholestatic drugs. ATP content ($pmol/\mu g$) is expressed as relative values to the control values (error bar represent the standard deviation)
Data represent the average values from 3-5 experiments, using three PCLS per experiment.

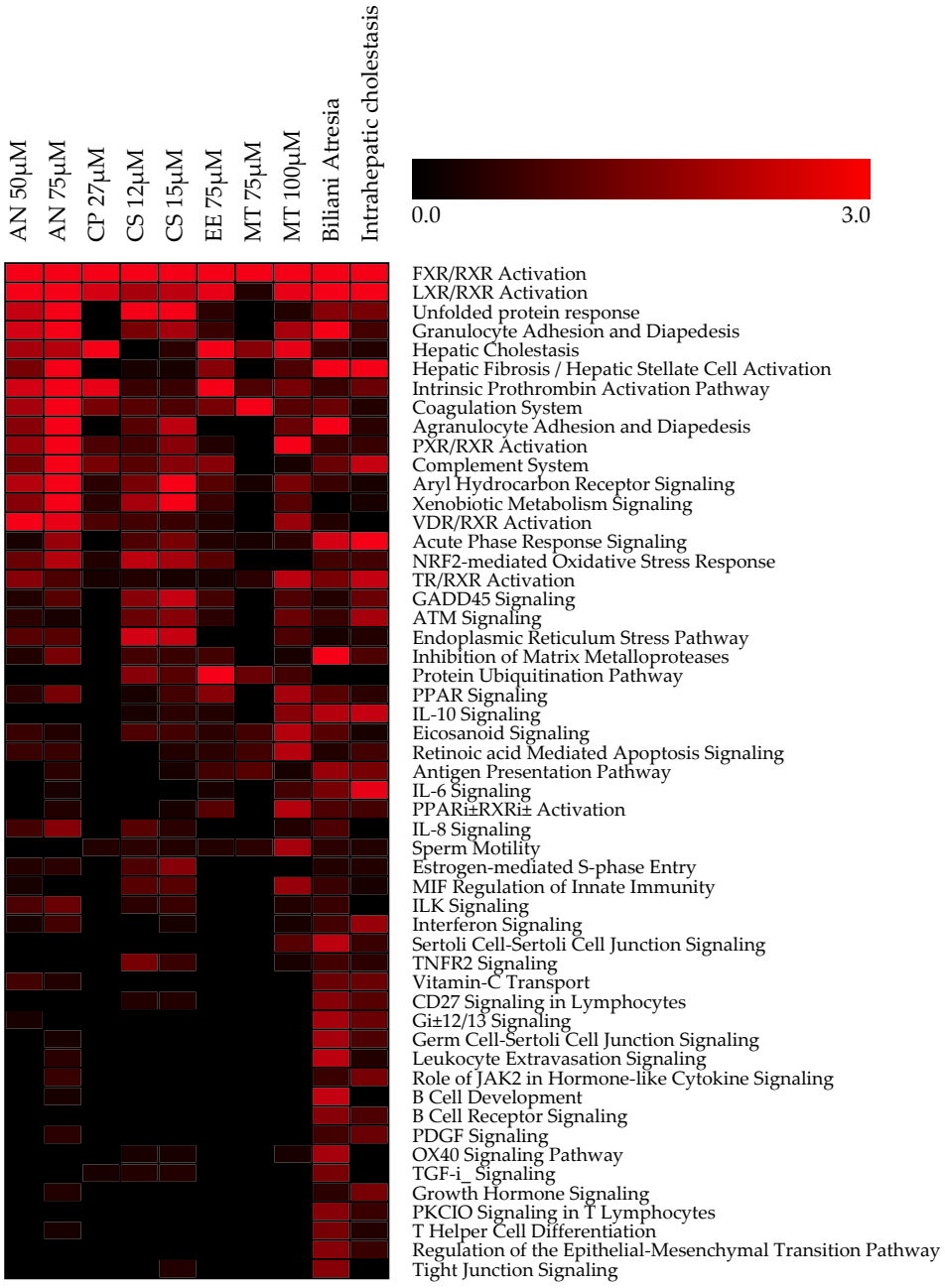

Figure 12: Heatmap of canonical pathway enrichment analysis results
Results from hPCLS were compared with in vivo cholestasis represented by biliary atresia and intrahepatic cholestasis. Enrichment values (-log (p-value)) are scaled from 0 to 3 (black to red).

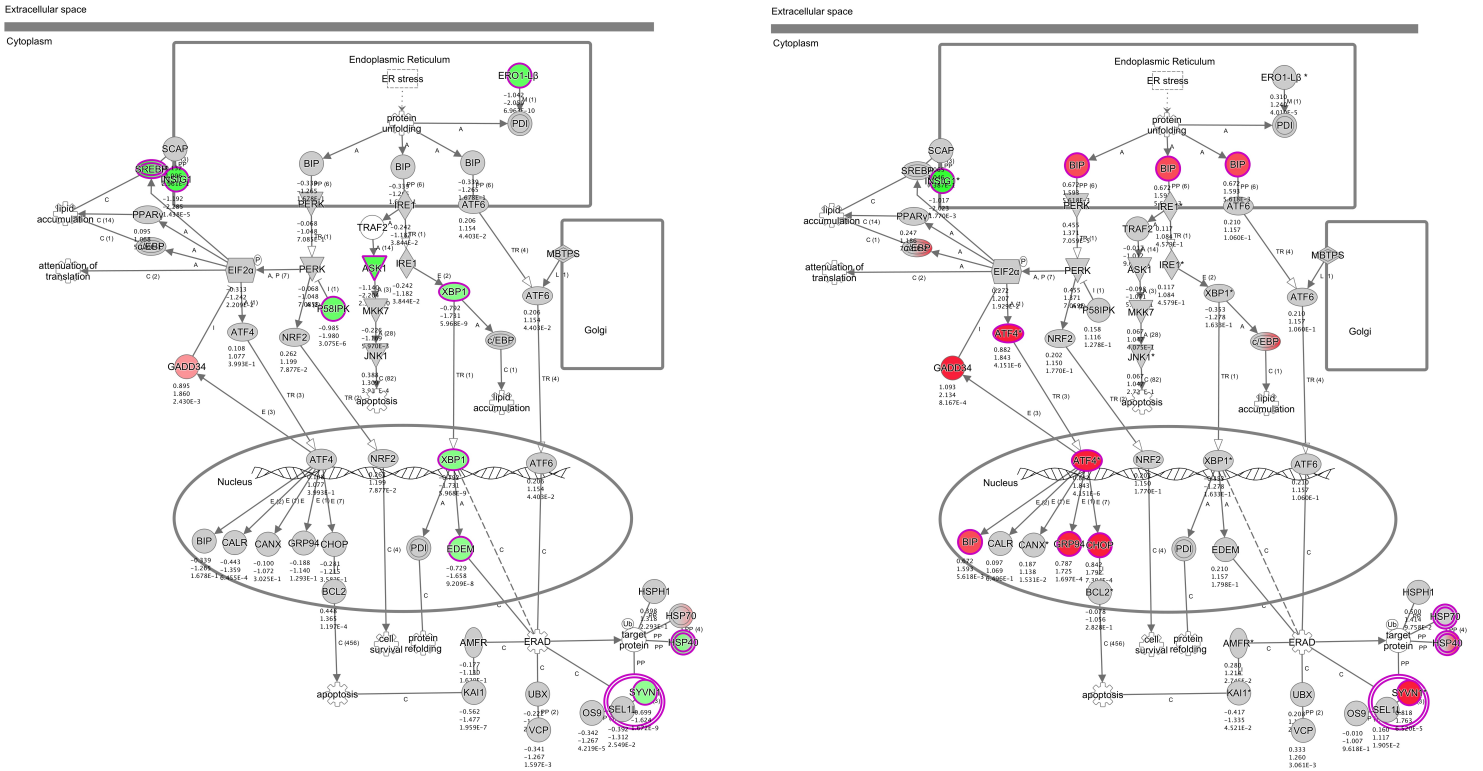

Figure 13: Unfolded protein response genes regulated due to biliary atresia (A) and cyclosporine 15 μM concentration in human PCLS (B)

4 CLASSIFICATION OF CHOLESTATIC AND NECROTIC HEPATOTOXICANTS USING TRANSCRIPTOMICS ON HUMAN PRECISION-CUT LIVER SLICES

(Chem. Res. Toxicol., Accepted Manuscript)

DOI: 10.1021/acs.chemrestox.5b00491

Supplementary information available: DOI: 10.1021/acs.chemres-tox.5b00491

Suresh Vatakuti[1],
Jeroen L.A. Pennings[3],
Emilia Gore[2],
Peter Olinga[2] ,
Geny M. M. Groothuis[1]

[1]Division of Pharmacokinetics, Toxicology and Targeting, Department of Pharmacy, Groningen Research Institute for Pharmacy, University of Groningen, Groningen, The Netherlands
[2]Division of Pharmaceutical Technology and Biopharmacy, Department of Pharmacy, Groningen Research Institute for Pharmacy, University of Groningen, Groningen, The Netherlands
[3]National Institute for Public Health and the Environment, Bilthoven, The Netherlands.

ABSTRACT

Human toxicity screening is an important stage in the development of safe drug candidates. Hepatotoxicity is one of the major reasons for withdrawal of drugs from the market because the liver is the major organ involved in drug metabolism and it can generate toxic metabolites. There is a need to screen molecules for drug-induced hepatotoxicity in humans at an earlier stage. Transcriptomics is a technique widely used to screen molecules for toxicity and to unravel toxicity mechanisms. To date the majority of such studies were performed using animals or animal cells, with concomitant difficulty in interpretation due to species differences, or in human hepatoma cell lines or cultured hepatocytes, suffering from the lack of physiological expression of enzymes and transporters and lack of non-parenchymal cells. The aim of this study was to classify known hepatotoxicants on their phenotype of toxicity in man using gene expression profiles *ex vivo* in human precision-cut liver slices (PCLS). Hepatotoxicants known to induce either necrosis (n=5) or cholestasis (n=5) were used at concentrations inducing low (<30%) and medium (30-50%) cytotoxicity, based on ATP content. Random Forest and Support Vector Machine algorithms were used to classify hepatotoxicants using a leave-one-compound-out cross-validation method. Optimized biomarkers sets were compared to derive a consensus list of markers. Classification correctly predicted the toxicity phenotype with an accuracy of 70-80%. The classification is slightly better for the low than for the medium cytotoxicity. The consensus list of markers includes endoplasmic reticulum stress genes such as C2ORF30, DNAJB9, DNAJC12, SRP72, TMED7 and UBA5, and a sodium/bile acid cotransporter (SLC10A7). This study shows that human PCLS are a useful model to predict the phenotype of drug-induced hepatotoxicity. Additional compounds should be included to confirm the consensus list of markers, which could then be used to develop a biomarker PCR-array for hepatotoxicity screening.

4.1 INTRODUCTION

Drug induced hepatotoxicity is one of the major reasons for withdrawal of drugs in the drug development or post marketing phase. It is of major concern for consumers, regulatory authorities such as the FDA, and pharmaceutical companies. In the drug discovery process, valuable information about possible mechanisms of toxicity may be gained by exposing liver cells to a compound, which in turn gives insights about how a potential therapeutic drug affects the liver. The ability to quickly determine whether a compound causes a particular pathology is valuable information in assessing the mechanism of action of an uncharacterized compound. It would be valuable to have a classification model that is able to accurately predict or classify compounds based on the possible mechanism of toxicity or pathological changes.

Acute exposure to a drug may result in different types of cell injury such as cholestasis, necrosis and steatosis, whereas chronic exposure results in cholestasis, cirrhosis or carcinogenesis[141]. Cholestasis is characterized as inhibition of bile flow caused by a wide variety of mechanisms. Several mechanisms have been postulated to account for impaired bile secretion such as inhibition of BSEP, impaired function of the microfilaments, intracellular calcium homeostasis alteration, alteration of canalicular carriers, and ductular obstruction [142, 143, 144]. Severe cholestasis is accompanied by cell death, both apoptosis and necrosis. Necrosis is characterized by loss of cell membrane integrity, intracellular swelling, cytoplasmic breakdown of nuclear DNA, and localized inflammation as a result of release of cellular constituents. As necrosis can be the result of a primary toxic effect of a chemical or be secondary to cholestasis, a method to classify a drug as inducing cholestasis or necrosis would be very useful for prediction of drug-induced injury.

Several studies are reported in the literature using assay methods or omics based classification models, which can discriminate hepatotoxicants based on their phenotype of toxicity. One such study used cell based assay methods using hepatocyte cultures combined with imaging technologies to identify hepatotoxicity of a compound as well as the pathology involved in hepatotoxicity[145]. Hrach *et al.*, reported a gene set of 724 genes, capable of discriminating hepatotoxic from non-hepatotoxic compounds in primary rat hepatocytes after repeated dosing for 9 days[146]. However, these data are obtained in rats and primary hepatocytes cultured for 9 days loose some liver-specific characteristics, which makes the use of this gene set for human predictions uncertain. A transcriptomics approach also has been applied in several studies to derive cholestasis specific gene expression signatures. In a rat *in vivo* study, a cholestasis gene expression signature was identified using a set of cholestatic compounds[147]. The cholestasis signature identified is comprised of molecules associated with apoptosis, cell signaling, acute phase responses, biotransformation of epoxides and peroxides. In another rat *in vivo* study, classifier or predictive genes specific to bile duct hyperplasia (BDH), inflammation and necrosis were reported. BDH is one of the morphological features of cholestatic livers[148]. BDH classifier genes are mainly associated with p53 and ERBB2 pathways. Inflammation signature genes are involved in the NFkB inflammatory pathway and the necrosis signature genes are involved in NFkB complex and cell death[29, 30]. Hirode et al, derived a cholestasis signature (59 genes) using compounds inducing elevation of bilirubin in rat *in vivo*, which is often associated with cholestasis. The identified genes were related to lipid metabolism, transport, ubiquitin-proteasome related factors, and mitochondrial components[52]. HEPG2, a human

liver carcinoma cell line, was also used to identify markers, which can discriminate cholestatic compounds from non-hepatoxicants. Of the 12 classifier genes selected, 6 were related to endoplasmic reticulum stress and the unfolded protein response [149]. However, the unphysiological expression of transporter proteins and biotransformation enzymes in these cells, as well as their cancer characteristics induce uncertainty with respect to the predictive value for the human liver. Also, different hepatotoxicants were classified based on their mechanism or phenotype of toxicity using rat *in vivo* transcriptomics data[150]. Moreover, a proteomics approach has been used to identify protein expression patterns, which can classify hepatotoxicants in primary human hepatocytes.

In order to find a more relevant model for human, that retains the normal liver characteristics during the experiment and which reflects the complex liver cellular composition better, we started a study using human precision-cut liver slices (PCLS).

PCLS are viable ex *vivo* for at least 48 hours and have been used for over a decade to study the metabolism and toxicity of xenobiotics[34]. Advantages of the PCLS model include the presence of all cells of the tissue in their natural environment with intact intercellular and cell-matrix interactions, stable expression of drug metabolizing and detoxification enzymes up to at least 24 hours and the ability to produce bile acids[114]. The presence of all cell types in this model is important for toxicological studies as the involvement of Kupffer cells, endothelial cells, hepatic stellate cells and bile duct epithelial cells in for instance inflammation, necrosis, fibrosis and cholestasis is evident. PCLS are therefore highly appropriate for studying multicellular acute drug toxicity processes[71, 114, 117]. The ability to use human tissue for toxicity studies also helps to reduce unnecessary animal studies and to identify human specific toxicity, thereby avoiding erroneous inter-species extrapolation.

Recently we reported on the use of human PCLS to study drug-induced cholestatic injury (DICI) using microarray analysis [151]. To optimize the PCLS to mimic cholestasis induced by accumulation of the bile acids *in vivo*, the PCLS model was incubated with a non-toxic concentration of a bile acid mix, which is important as the toxicity of the increased bile acid accumulation is thought to play an important role in DICI. Pathway analysis resulted in interesting insight in the mechanisms involved in DICI, including regulation of FXR, LXR and cholesterol metabolism pathways as well as endoplasmic reticulum (ER) stress [151].

In this study, we report on the results of toxicogenomics analysis of experiments where precision-cut liver slices were exposed to drugs or chemicals known to induce necrosis at different toxic concentration levels. The data of PCLS exposed to the cholestatic compounds [117] were now used together with the data of PCLS exposed to the necrotic compounds to develop classifiers for the identification of the type of injury based on the random forest (RF) and support vector machine (SVM) algorithms. The prediction performance of classifiers was determined by leave-one-chemical-out cross-validation. Pathway analysis of the classifier genes was performed to understand the role of the classifier genes.

4.2 METHODS AND MATERIALS

CHEMICALS Acetaminophen (APAP), alpha-naphthylisothiocyanate (ANIT), chloramphenicol (CH), chlorpromazine (CP), colchicine (CL), cyclosporine (CS), ethinyl estradiol (EE), methyl testosterone (MT), and nitroso diethylamine (ND) were purchased from Sigma-Aldrich (St.Louis, MO, USA). Benziodarone (BD) was purchased from Kemprotec Limited (Middlesbrough, United Kingdom). Stock solutions were prepared for all the compounds in DMSO (VWR, Briare, France) except for APAP. For APAP stock solutions were prepared using WME medium. RNA*later*(R) reagent was purchased from Sigma-Aldrich (St.Louis, MO, USA).

HUMAN LIVER TISSUE Human tissue was obtained from the remaining liver tissue after split liver transplantation from six donors (TX). The characteristics of the human livers used in the experiments are described in Table 18. The experimental protocols were approved by the Medical Ethical Committee of the University Medical Center Groningen.

PREPARATION AND INCUBATION OF HUMAN PCLS (HPCLS) Precision-cut liver slices (PCLS - diameter 5 mm, thickness 250 μM) were prepared following the methods described earlier[34]. PCLS were made using the Krumdieck tissue slicer (TSE, Bad Homburg, Germany). The slices were prepared in ice-cold Krebs buffer at pH 7.42, enriched with glucose to a final concentration of 25 mM, saturated with carbogen (5% CO_2/95% O_2). Immediately after the slices were made, they were moved to ice-cold University of Wisconsin organ preservation solution (UW, Dupont Critical Care, Waukegan, IL, USA) and stored on ice until the beginning of the experiment. Slices were pre-incubated individually in 12-well plates in 1.3 ml of Williams Medium E with glutamax-1 (Gibco, Invitrogen, Paisley, Scotland) supplemented with 25 mM D-glucose and 50μg/ml gentamycin (Gibco, Invitrogen, Paisley, Scotland). In the incubator (Sanyo CO_2/O_2 Incubator, PANASONIC, Secaucus, NJ, USA), the plates were under 5%/ CO_2 and 80 % O_2 atmosphere at 37^0C for 1 h, while gently shaken (90 times/min). Pre-incubation allows the slices to restore the ATP levels[34]. After pre-incubation, the slices were moved to different well plates filled with 1.3 ml Williams Medium E with glutamax-1 supplemented with 25 mM D-glucose, 50 μg/ml gentamycin, 60 μM human bile acid mix and different concentrations of the tested compounds. It is important to note that PCLS of each liver were exposed to all 10 compounds, as well as controls, in order to limit the influence of nonbiological experimental variation. This experimental design helps to limit inter-individual variation between compound classes, as

Table 18: Demographics of donors of human liver tissue used for the experiments

Human liver	Sex	Age
1	Female	58
2	Male	50
3	Female	71
4	Male	24
5	Female	24
6	Male	64

Table 19: Composition of human bile acids mix

Composition of bile acids	Final concentration in the incubation medium (µM)
Cholic acid (CA)	2.65
Chenodeoxy cholic acid (CDCA)	4.51
Deoxycholic acid (DCA)	6.37
Glycochenodeoxycholic acid (GCDCA)	22.69
Glycocholic acid (GCA)	5.44
Glycodeoxycholic acid (GDCA)	5.04
Glycoursodeoxycholic acid (GUDCA)	3.72
Hyodeoxycholic acid (HDCA)	2.79
Lithocholic acid (LCA)	0.40
Taurocholic acid (TCA)	0.64
Taurochenpodeoxycholic acid (TCDCA)	2.79
Taurolithocholic acid (TLCA)	1.15
Taurodeoxycholic acid (TDCA)	0.58
Ursodeoxycholic acid (UDCA)	1.46

well as between compounds and controls, in the data set. We tried to limit this unwanted variation as humans have more inter-individual variation than cell lines or animals. The plates were incubated in the same conditions for 24 h. The bile acid mix was added in order to create an environment similar to the physiological plasma concentration in the portal vein. [119]. Pilot experiments were performed to find out the non-toxic concentration of the bile acid mix. The human bile acid mix was made as presented in Table 19. A series of concentrations of bile acid mix were tested (10 μM, 30 μM, 60 μM, 200 μM and 600 μM) and concentrations up to 60 μM were found to be non-toxic and hence further experiments were performed using 60 μM concentration. Three slices were used for each experimental condition.

VIABILITY ASSAY: ATP AND PROTEIN CONTENT OF PCLS After 24 h of incubation, the viability of PCLS was assessed in three individual slices for each experimental condition by measuring the content of ATP using the ATP Bioluminescence Assay Kit CLS II (Roche, Mannheim, Germany) as described before (Vatakuti et al.). In brief, the slices were homogenized in in a buffer containing 70% ethanol, 100mM Tris-HCl and 2 mM EDTA and after centrifugation, the supernatants were diluted 10 times with 100 mMTris-HCl, 2 mM EDTA buffer. 5 μL of each sample was added to 50 μL of luciferase and the ATP was measured with the Lucy1 luminometer (Anthos, Durham, NC, USA). The protein content of each slice was assessed using the BIO-Rad DC protein assay kit (Bio-Rad, Munich, Germany), as described before [117] and the ATP values of the slices were corrected for their corresponding protein content.

RNA ISOLATION After the incubation, the three slices of each incubation condition were combined in 1 ml RNA*later*(R) and stored at -20^{o}C. After thawing, the Maxwell(R) 16 LEV Total RNA purification kit was used to isolate RNA from the samples. Immediately after isolation, the RNA concentrations were measured and the RNA quality was assessed by measuring the 260/280 and 260/230 ratios with the ND-1000 spectrophotometer (Fisher Scientific, Landsmeer, The Netherlands). The quality (RIN value) and quantity of the RNA was determined by high throughput Caliper GX LabChip RNA kit (Caliper).

AMPLIFICATION, LABELING, AND HYBRIDIZATION OF RNA SAMPLES The Ambion Illumina Total Prep RNA kit was used to transcribe 300 ng RNA to cRNA according to the manufacturer's instructions. A total of 750 ng of cRNA was hybridized at 58^{o}C for 16 hr to the Illumina HumanHT-12 v4 Expression BeadChips. BeadChips were scanned using Iscan Software (Illumina, SanDiego, CA).

PREPROCESSING OF GENE EXPRESSION DATA. Genome studio software (Illumina) was used to read the IDAT files and generate raw expression values. The raw expression values were background corrected and normalized by the neqc method[152, 153]. Probes were re-annotated using the illuminaHumanv4.db annotation package of Bioconductor [154, 155]. Probe filtering was performed to remove non-responding probes and probes with a high expression level caused by non-specific hybridization. After normalization and filtering, the probe set expression value of each sample was corrected with time-matched controls. To assess the effect of inter-individual variation on the prediction results, gene expression analysis was performed both unpaired and paired. For paired analysis, gene expression data from each treatment sample of each human liver were corrected using the corresponding control sample. For unpaired analysis, expression data were corrected for the average of all control samples. Subsequently, classification was performed on the corrected data.

CLASS PREDICTION. SVM and RF algorithms were used for class prediction. SVM is based on hyperplane separation, whereas RF is based on a decision tree network. Both algorithms were employed to check the robustness of the obtained classifier genes. SVM was applied using a radial kernel on scaled data for classification of the complete set of chemicals. The training set data comprised the data for all-but-one chemical; the test set contained the data for the remaining chemical. This type of cross-validation, called leave-one-chemical-out cross-validation, keeps replicate samples of each compound together. For the training set, features (probe sets or genes) were selected by applying a Student's t-test using the two classes, where different numbers of top-ranking features were tested for use in the classifier. For RF, different numbers of top-ranking features were tested with the ranking based on the importance measure as determined by the RF algorithm. After prediction, the prediction accuracy for the left out compound samples was determined. The percentage of correct classifications was calculated as the average of all 10 predictions. For each training set, a set of biomarkers was optimized to get the maximum prediction accuracy, thus yielding 10 sets of biomarkers. The genes that are present in 6 or more of these were selected as consensus classifier genes.

PATHWAY ANALYSIS IPA ingenuity knowledgebase (QIAGEN's Ingenuity(R) Pathway Analysis tool (IPA(R), QIAGEN Redwood City)), was used to retrieve the annotations of the classifier genes and their role in toxic responses. A literature search was also performed.

4.3 RESULTS

TOXIC CONCENTRATION SELECTION Compounds that are known to induce cholestasis or necrosis were incubated with PCLS in presence of bile acid mixture (60 μM) to identify low (concentration that causes less than 30 % decrease in ATP (TC<30) in comparison to controls) and medium concentration (concentration that causes 30-50% decrease in ATP (TC30-TC50) in comparison to controls). The concentrations that were finally chosen for the gene expression studies are shown in table 20. Viability data represented by the decrease in ATP content due to exposure of hPCLS to the low and medium concentration are provided as supplementary data (supplementary figures 17 and 18).

CLASSIFICATION MODEL DEVELOPMENT SVM and RF machine learning algorithms were used to develop classifiers and to identify classifier genes. Using multiple algorithms to develop classifiers also helps to check the robustness of the predictions as well as the classifier genes selected. Using a combination of two algorithms (SVM and RF) and two concentrations (low and medium), four models were developed namely, SVM low concentration model (SVMlow), SVM medium concentration model (SVMmedium), RF low concentration model (RFlow), RF medium concentration model (RFmedium). Prediction accuracy for necrosis and cholestasis based on all combined data per compound (figure 14A) and for each of the samples (figure 14B) using low and medium concentration is summarized in figure 14. Both SVM and RF algorithms using both low and medium concentration gene expression data correctly predicted the mechanism of the toxicity for each compound with 60-100% prediction accuracy. Cholestasis compound prediction accuracy was greater than 80%, while the necrotic compound prediction accuracy was only 60% by the four models. It was also evident that the prediction accuracy is higher for the individual cholestatic samples than for the necrotic samples. All four models showed prediction accuracy greater than 80% for the cholestatic samples, with the SVMlow model being the best model in classifying the cholestatic samples with a prediction accuracy of 87%. It is worthwhile to mention here that the SVM algorithm using low and medium concentration gave a comparable accuracy in predicting the correct class of samples but noticeable differences were found in the accuracy by the RF algorithm (figure 14).

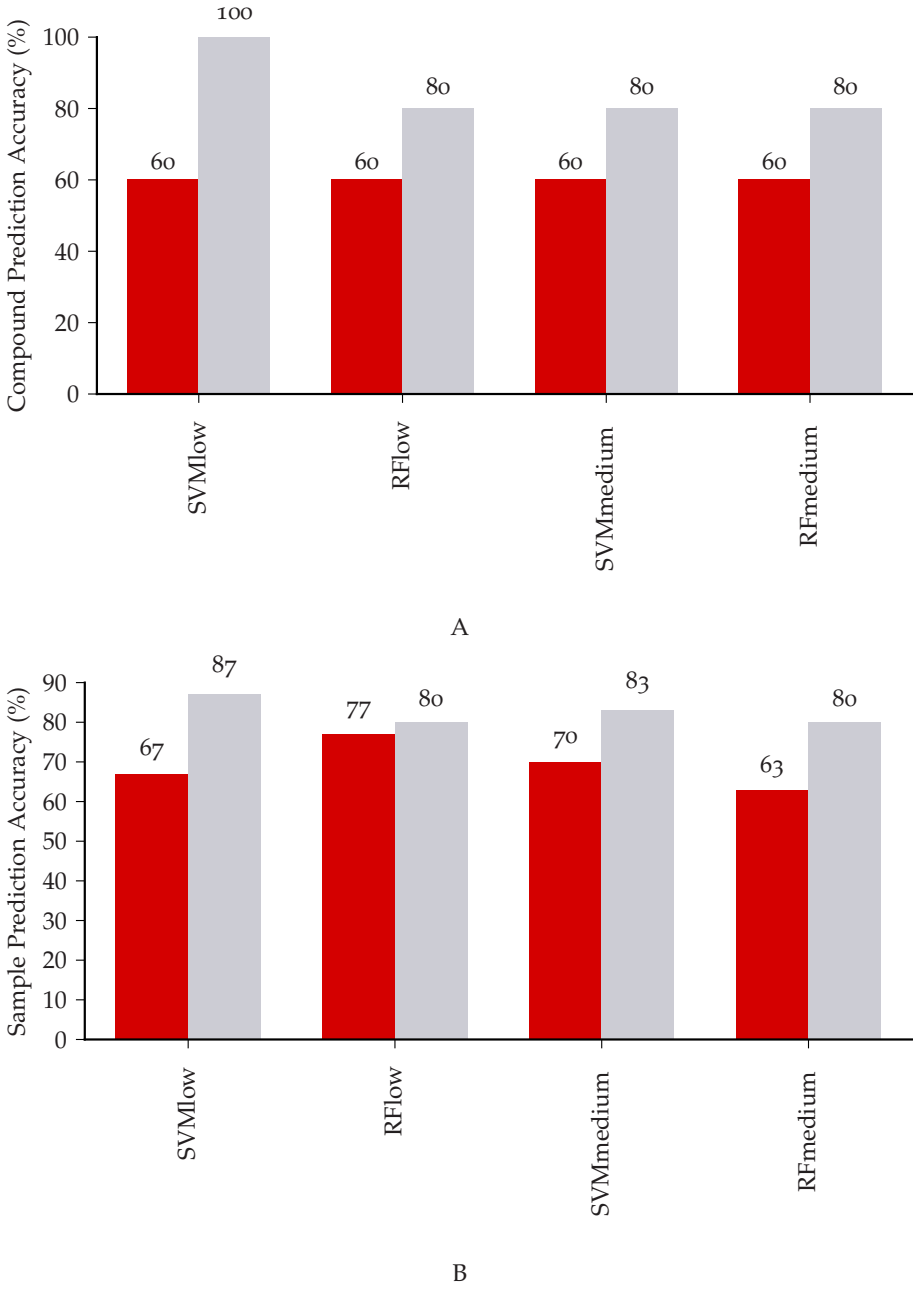

Figure 14: Prediction accuracy (%) of the compounds (A) and separate samples of the compounds (B) of SVM and RF models using low and medium concentration

Table 20: Concentrations selected for hepatotoxicants based on low (TC<30) and medium (TC30-TC50) toxicity

Necrosis Class

Compound	Low	Medium
Acetaminophen (AP)	2.5 mM	5 mM
Benziodarone (BD)	5 µM	7.5 µM
Chloramphenicol (CH)	0.5 mM	1 mM
Colchicine (CL)	2.5 mM	5 mM
Nitroso diethylamine (ND)	8 mM	15 mM

Cholestasis Class

Compound	Low	Medium
1-naphthyl isothiocyanate (AN)	50 µM	75 µM
Chlorpromazine (CP)	18 µM	27 µM
Cyclosporine (CS)	12 µM	15 µM
Ethinyl estradiol (EE)	50 µM	75 µM
Methyl testosterone (MT)	75 µM	100 µM

COMPARISON OF CLASSIFICATION ACCURACY Predictions for the individual samples of each compound by the four prediction models are shown in Table 21. Of the cholestasis inducing drugs ANIT, chlorpromazine, cyclosporine and ethinyl estradiol were correctly predicted by all the models. However, methyl testosterone was only correctly predicted as cholestatic by the SVMlow model. Acetaminophen, colchicine and nitroso-diethylamine were correctly predicted as necrotic drugs by all the four models. However, benziodarone and chloramphenicol were not correctly predicted by all the four models. In case of benziodarone, out of the 6 individual livers, 2 to 3 samples were correctly classified but for chloramphenicol the majority of the predictions were not correct. Overall, if the models are compared based on how they would classify drugs rather than individual samples, their performances are comparable. This indicates that the results are not too dependent on a particular algorithm or concentration. The SVMlow model gives the best overall performance.

CORRECTION FOR INTER-INDIVIDUAL DIFFERENCES Genetic variability in drug metabolizing enzyme levels of each individual human liver could lead to variability in response to drug induced injury[156]. It can be hypothesized that inter-individual differences in response to drug treatments could affect the prediction results. To assess this we also carried out a paired analysis to account for the inter-individual differences. The corresponding predictions are summarized in Table 22. It is apparent from the predictions that there is no further improvement with the paired analysis.

COMPARISON OF CLASSIFIER GENES SELECTED BY LOW AND MEDIUM CONCENTRATION For each of the classifier models, a consensus set of classifier genes was obtained. The consistency of the selected classifier genes was assessed across low and medium concentration as well as across SVM and RF algorithms. It is evident from the

Table 21: Summary table indicating the predictions from the unpaired analysis for each of the samples of 10 compounds (6 samples each) by the SVM and RF algorithms using low and medium concentration

			SVM low prediction		RF low prediction		SVM medium prediction		RF medium prediction	
No.	Compound	Real class	N	C	N	C	N	C	N	C
1	Acetaminophen	N	6	0	6	0	6	0	6	0
2	Benziodarone	N	2	4	3	3	3	3	2	4
3	Chloramphenicol	N	1	5	3	3	0	6	0	6
4	Colchicine	N	5	1	5	1	6	0	5	1
5	Nitrosodiethylamine	N	6	0	6	0	6	0	6	0
6	1-Naphthyl isothiocyanate	C	1	5	0	6	0	6	0	6
7	Chlorpromazine	C	1	5	2	4	0	6	1	5
8	Cyclosporine	C	0	6	1	5	0	6	0	6
9	Ethinyl estradiol	C	0	6	0	6	1	5	1	5
10	Methyl testosterone	C	2	4	3	3	4	2	4	2

N refers to the necrosis class and C refers to the cholestasis class. The numbers reflect the identity number of the individual livers. For any compound if at least 4 out of 6 samples were predicted correctly, then the predictions for that compound were considered successful (indicated with green color).

Table 22: Summary table indicating the predictions from the paired analysis for each of the samples of 10 compounds (6 samples each) by the SVM and RF algorithms using low and medium concentration

			SVM low prediction		RF low prediction		SVM medium prediction		RF medium prediction	
No.	Compound	Real class	N	C	N	C	N	C	N	C
1	Acetaminophen	N	6	0	5	1	5	1	4	2
2	Benziodarone	N	0	6	3	3	3	3	5	1
3	Chloramphenicol	N	1	5	1	5	0	6	0	6
4	Colchicine	N	6	0	5	1	6	0	6	0
5	Nitrosodiethylamine	N	6	0	6	0	6	0	6	0
6	1-Naphthyl isothiocyanate	C	0	6	0	6	0	6	0	6
7	Chlorpromazine	C	1	5	1	5	0	6	2	4
8	Cyclosporine	C	1	5	0	6	0	6	0	6
9	Ethinyl estradiol	C	0	6	1	5	1	5	1	5
10	Methyl testosterone	C	3	3	3	3	4	2	4	2

N refers to the necrosis class and C refers to the cholestasis class. The numbers reflect the identity number of the individual livers. For any compound if at least 4 out of 6 samples were predicted correctly, then the predictions for that compound were considered successful (indicated with green color).

Venn diagram comparison, that there is good overlap between the classifier genes selected by the low and medium concentration gene expression profiles (figure 15aA and B). Classifier genes based on SVM are somewhat more consistent across concentrations than the classifiers based on the RF algorithm. Among the 14 classifier genes selected by the SVMlow model, 12 classifier genes were found in common with classifier genes selected by the SVMmedium model, which include C2ORF30, CADPS2, DNAJB9, DNAJC12, NFXL1, PAN2, REEP5, SLC10A7, SORL1, SRP72, TMED7 and UBA5. In contrast, 6 of the 10 classifier genes selected by the RFlow model were in overlap with classifier genes selected by the RFmedium model, which include C2ORF30, C7ORF54, DNAJB9, FILIP1L, SRP72 and TMED7.

COMPARISON OF CLASSIFIER GENES SELECTED BY RF AND SVM ALGORITHMS To check the consistency of the selected classifier genes by the two different algorithms RF and SVM, the classifier genes selected by both SVM and RF algorithms using low and medium concentration were compared. There was also good overlap with classifier genes selected by SVM and RF (figure 15aC and D). Among the 14 classifier genes selected by the SVMlow model, 5 classifier genes were found in common with classifier genes selected by the RFmedium model, which includes DNAJB9, ERLEC1, SRP72, TMED7 and UBA5. Similarly 49 of the 52 classifier genes selected by the RFmedium model were in overlap with classifier genes selected by the SVMmedium model (supplementary information 2). To summarize, a considerable number of class-predictive genes were selected by different algorithms as well as at different concentrations. Further comparison of the classifier genes selected in paired and unpaired analysis using SVM and RF algorithms revealed that 8 classifier genes were consistently selected across the low and medium concentration in paired and unpaired analysis using SVM algorithm. Those genes include C2ORF30, DNAJB9, DNAJC12, SLC10A7, SRP72, PAN2, TMED7 and UBA5; in contrast only one classifier gene (C2ORF30) was found in common using the RF algorithm. Thus, correction for intra-individual differences does not further improve classification accuracy, but does seem to negatively affect the consistency of biomarker selection.

SVMlow markers and their expression levels in necrotic and cholestatic samples are shown in figure 16. Classifier genes have high expression levels in cholestasis samples in comparison to necrotic samples (figure 16A). Also the PCA plot shows clear separation of necrotic samples from cholestatic samples on the first principal component axis (figure 16B). The 14 classifier genes selected by the SVMlow model were further studied for their role in the mechanism of toxicity. Interestingly most of the classifier genes are related to the cellular toxicity processes ER stress, oxidative stress and unfolded protein response.

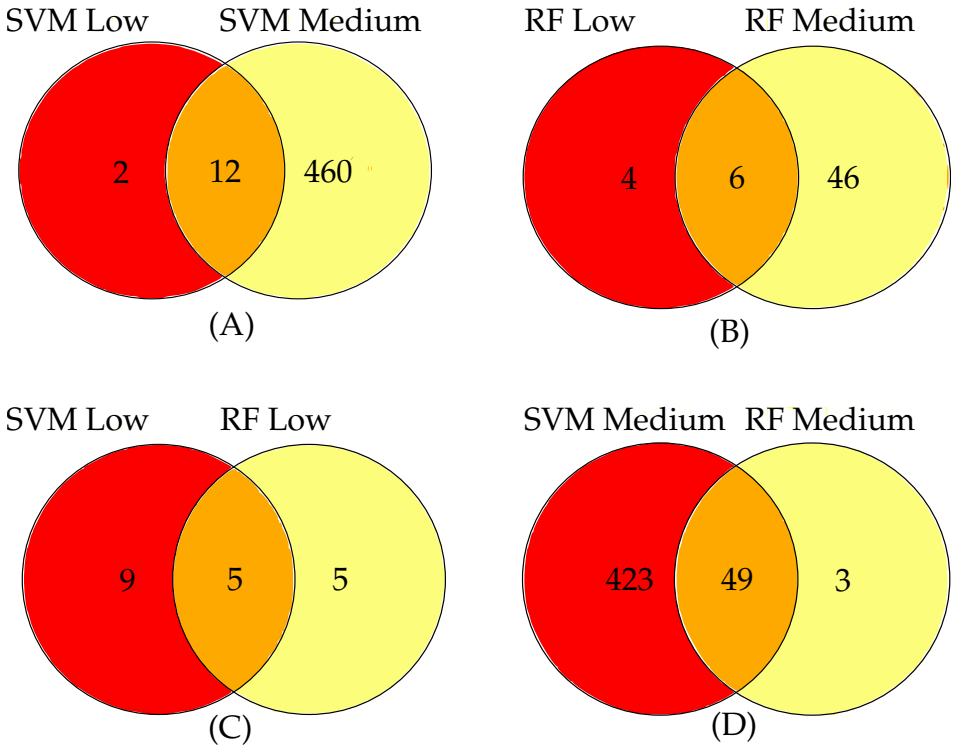

(a) Venn diagram comparison of classifier genes selected using low and medium concentration by the SVM (A) and RF (B) algorithms; classifier genes selected by the SVM and RF algorithms using low (C) and medium (D) concentration

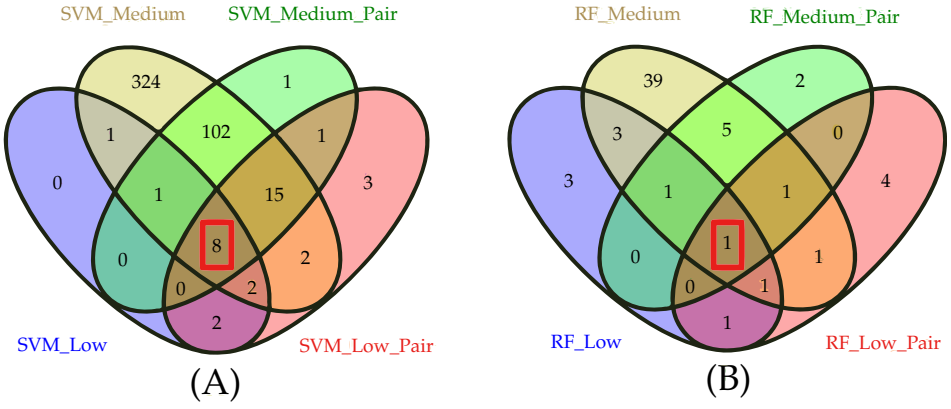

(b) Venn diagram comparison of classifier genes selected in paired and unpaired analysis using SVM (A) and RF algorithm (B).RF_Medium_Pair - RF with paired analysis for the medium concentration; RF_Low_Pair - RF with paired analysis for the low concentration; SVM_Medium_Pair - SVM with paired analysis for the medium concentration; SVM_Low_Pair - SVM with paired analysis for the medium concentration

Figure 15: Venn Diagram comparisons of classifier genes

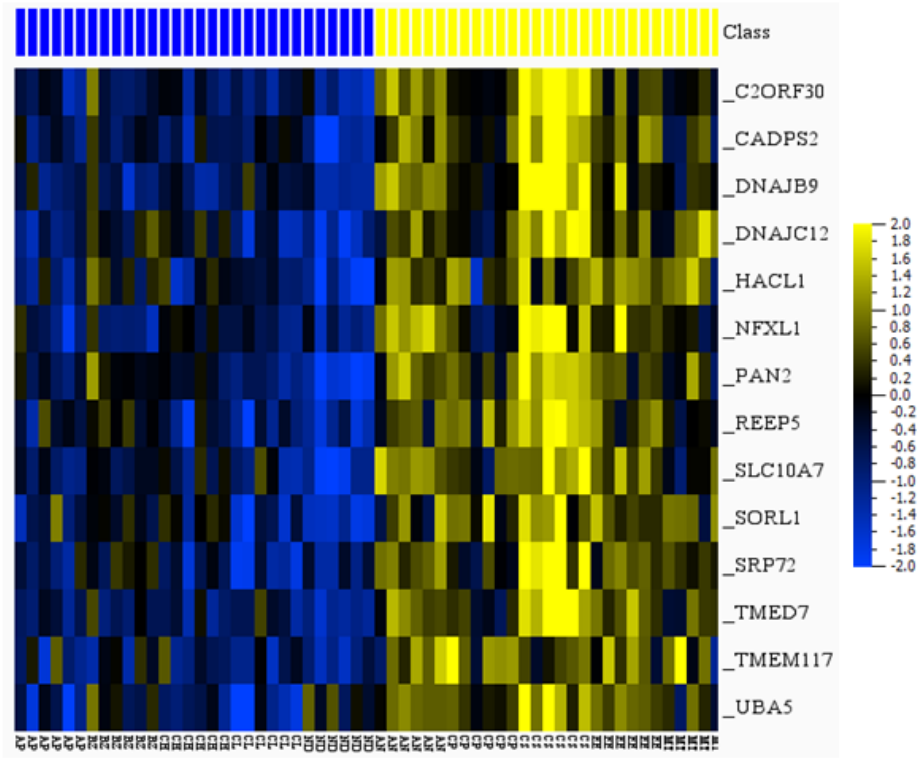

4A

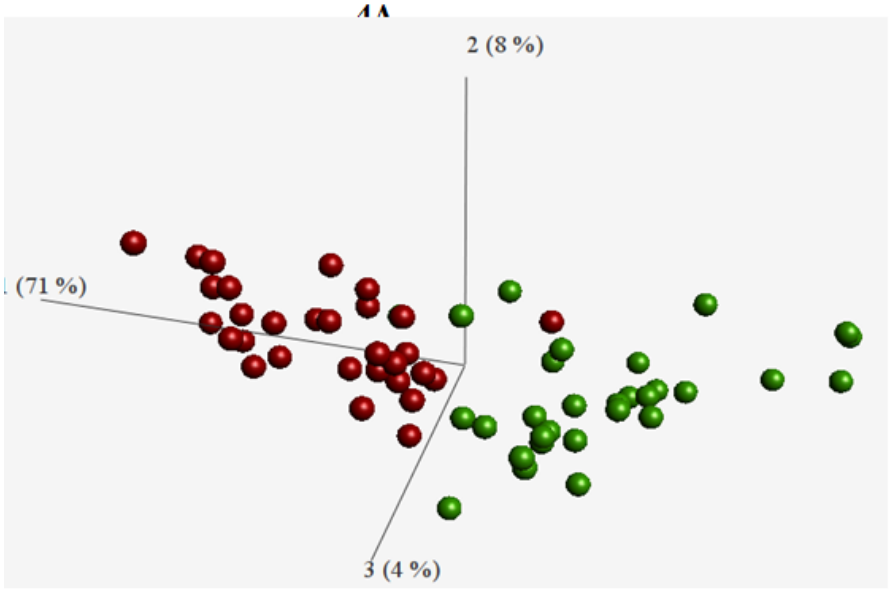

4B

Figure 16: A: Heatmap of the gene expression levels of the 14 classifier genes that discriminated the cholestatic compounds (yellow color) from the necrotic compounds (blue color) using the SVMlow model
B: PCA plot showing the separation of compounds using the 14 classifier genes (red circles refer to necrosis samples and green circles refer to cholestasis samples)

4.4 DISCUSSION

In this study, we aimed to classify hepatotoxicants according to their phenotype of toxicity based on the gene expression profiles after exposure of human precision-cut liver slices (hPCLS). The hPCLS were exposed to ten hepatotoxicants with a well-characterized mechanism of toxicity: acetaminophen, benziodarone, chloramphenicol, colchicine, and nitroso-diethylamine are known to induce hepatic necrosis; ANIT, chlorpromazine, cyclosporine, ethinyl estradiol and methyl testosterone are known to cause hepatic cholestasis. Machine learning on gene expression data of PCLS exposed to these five cholestatic and five necrotic compounds resulted in four classification models based on two different algorithms (SVM and RF algorithm) and two different tested concentrations (low and medium), which were 70-80% accurate in predicting the phenotype of hepatotoxicants. Cholestatic compounds such as ANIT, chlorpromazine, cyclosporine and ethinyl estradiol were classified correctly. Similarly, three of the necrotic compounds (acetaminophen, colchicine, and nitrosodiethylamine) were correctly classified, but two others, benziodarone and chloramphenicol, were not. Although the compounds were chosen based on their reported phenotype of liver injury, it is well known that some compounds can cause a mixed type of toxicity. For instance, among the cholestatic compounds considered in this study, cyclosporine, ethinyl estradiol and methyl testosterone can cause cholestasis without hepatitis but chlorpromazine causes cholestasis with hepatitis and is associated with bile duct injury[141]. Moreover cholestasis often presents as mixed cholestatic and hepatocellular injury[141]. Chloramphenicol is generally considered a direct acting necrotic compound; however a few older reports indicated that it can also cause cholestasis with hepatitis[157]. This possibly explains the fairly consistent classification of chloramphenicol as cholestasis inducing drug by all the models (table 21 and table 22). If chloramphenicol would be considered as cholestatic, then the compound prediction accuracy improved. Many studies about the mechanisms of cholestatic liver injury indicated bile acid-induced apoptosis as the mechanism involved in cholestatic liver injury[158, 159]. However, recent evidence suggests that inflammatory cell-mediated necrosis might also accompany cholestasis[160]. This overlap of mechanisms involved in the toxicity of necrotic and cholestatic compounds further complicates the classification of hepatotoxicants into the correct phenotype of toxicity[150]. There is no evidence in the literature about the mechanism of toxicity of benziodarone apart from being necrotic, but based on the results presented here, it may be worthwhile to investigate whether the hepatotoxicity of benziodarone is accompanied by cholestasis. Despite the complexity owing to overlap of mechanisms in toxicity for the classification of necrosis and cholestasis, the classification models developed in this study were able to classify the hepatotixicants with relatively good accuracy. Low concentration gene expression profiles gave a better prediction accuracy than the medium concentration, which may be due to the accompanying necrosis at higher concentrations. The SVM low concentration model shows the highest prediction accuracy in correctly classifying all 5 cholestatic compounds, including methyl testosterone (Table 21). In addition, the SVM classifier genes are more consistent across the approaches used such as different concentrations (Figure 15a) or considering inter-individual variation (Figure 16). Although the RFlow model gives a better accuracy than the SVMlow model for predicting the necrotic compounds, the classifier genes were less consistent across the concentrations or considering inter-individual variation. In conclusion, all models give a reasonably comparable overall performance in compound class prediction

accuracy. However, the accuracy of the SVMlow model is highest and this model gives biomarkers that are consistent across concentrations and not too sensitive for inter-individual variation, which would give this model greater applicability in future settings. Further analysis of the function of the classifier genes identified by the SVMlow model showed that they are involved in ER stress, oxidative stress and unfolded protein response (UPR), and lipid and cholesterol metabolism. Nine of the classifiers are related to ER stress. The SRP 72 gene encodes the 72-kDa component of the signal recognition particle, a ribonucleoprotein complex that mediates the targeting of secretory proteins to the endoplasmic reticulum (ER). Caspase cleavage of SRP 72 is thought to shut down or alter the translation of secretory proteins[161]. UBA5, a homodimer member of the E1 enzyme family is known to activate Ubiquitin-fold modifier 1 (UFM1) and their interaction is proposed to play an important role in the endoplasmic reticulum (ER) stress response[162]. Also DNAJC12, which belongs to the Heat shock protein 40 (HSP40) family, is known to be upregulated in response to ER stress[163]. HSP40 family proteins are known to bind to HSP70 through their J-domain and regulate the function of HSP70 by stimulating its adenosine triphosphatase activity. The endoplasmic reticulum localized DNAJ homologue ERDJ4 (DNAJB9) is up-regulated by ER stress and is implicated in ER-associated degradation (ERAD) of multiple unfolded secretory proteins[164]. C2ORF30, also known as CIM or ERLEC1 (endoplasmic reticulum lectin 1), is known to be involved in ER-associated degradation via its interaction with the membrane-associated ubiquitin ligase complex. It binds selectively to improperly folded luminal proteins and functions in endoplasmic reticulum quality control and ERAD of both non-glycosylated proteins and glycoproteins[165]. C2ORF30 is also involved in UPR through its interaction with the key ER stress protein BiP, influencing cell proliferation under ER stress conditions. REEP5 (Receptor expression enhancing protein 5), is a membrane protein involved in the structural development of ER by shaping the tubular form of the endoplasmic reticulum[166].In addition to these ER stress related proteins, SLC10A7 (Sodium/Bile Acid Cotransporter 7) appeared as classifier, which belongs to the solute carrier family 10 (SLC10) comprising influx transporters for molecules such as bile acids and steroidal hormones, but the substrate specificity of SLC10A7 is not defined so far in the literature[167]. In addition, its expression is shown to be upregulated in response to treatment with ER stress inducers such as tunicamycin and thapsigargin[168]. NFXL1 (nuclear transcription factor, X-box binding-like) is a transcription factor, which is shown to be upregulated along with other NRF2 dependent genes in response to tunicamycin induced ER stress in mouse liver[169]. TMEM-117 (Transmembrane protein 117) is an integral membrane component of the endoplasmic reticulum. Two of the classifiers, TMED7 and CADPS2, are related to oxidative stress. TMED7 (transmembrane p24 trafficking protein 7) is involved in trafficking of TLR4 (Toll like receptor 4) from the ER to the plasma membrane. TLR4 participates in the activation of many downstream intracellular pathways such as the NFkB pathway in response to cellular stress[170]. Knockdown of CADPS2 (Calcium-dependent activator protein for secretion 2) was shown to play a cell protective role under oxidative stress in human iPSCs[171]. Two classifiers, SORL1 and HACL1, are related to cholesterol and lipid metabolism. SORL1 (Sortilin-Related Receptor 1), is involved in cholesterol metabolism and HACL1 (2-Hydroxyacyl-CoA Lyase 1) is involved in lipid metabolism. Both cholesterol and lipid metabolism are affected in cholestasis as shown in the pathway analysis of these hPCLS [117]. Finally, PAN2 (Poly (A) Specific Ribonuclease Subunit) is involved in ubiquitin proteasome dependent proteolysis. The involvement of ER stress in cholestasis

has been described before. Hepatocytes are enriched with endoplasmic reticulum, which is highly involved in protein synthesis, and it is generally assumed that endoplasmic stress might play an important role in liver toxicity[172, 173, 174, 175]. A recent in vitro study in human HEPG2 cells[176, 177, 149] showed that cholestatic compounds were classified from non-hepatotixicants with good accuracy and 5 out of the 12 classifier genes were related to endoplasmic reticulum stress and unfolded protein response, in accordance with our findings. Adachi et al. elucidated the role of endoplasmic reticulum stress in bile acid mediated hepatocellular injury. Bile acids were shown to elevate intracellular Ca^{2+} and reactive oxygen species (ROS), leading to induced ER stress mediated apoptosis, which correlated with the hydrophobicity of the bile acids[124]. Toxicogenomics studies using in vitro models also revealed the involvement of ER stress in cyclosporine-mediated DICI [178, 149, 179]. Additional studies would be necessary to further elucidate the exact role of ER stress in cholestasis. When the classifier genes identified in our human PCLS model were compared with cholestasis-specific classifier genes reported in different rat *in vivo* studies[150, 147, 52, 29, 30], no overlap among the classifiers genes between rat *in vivo* and human *ex vivo* were found. This can at least partly be explained by species differences and underlines the importance of the use of human cells or tissues. Surprisingly, there was also little or no overlap among the classifier genes found between the different rat *in vivo* studies (supplementary information). This lack of concordance further questions the applicability of the identified markers and could be partly due to overfitting of the data. Liu et al. reported a novel algorithm to find classifier genes with functional relevance to the phenotype with a reduced risk of overfitting in classification. Drugs inducing biliary duct hyperplasia (BDH) were compared to drugs inducing necrosis or inflammation; and the accuracy of the classification was determined. Classifier genes for each phenotype were identified and validated, however the authors assigned some of the compounds to more than one phenotype, complicating the interpretation of the classifier genes. In conclusion, gene expression profiling after *ex vivo* exposure of precision-cut human liver slices to hepatotoxicants known to induce either cholestasis or necrosis resulted in a classification model that was 70-80% accurate in distinguishing cholestasis from necrosis. This is the first *ex vivo* study with human tissue to test the possibility of discriminating hepatotoxicants based on the phenotype of toxicity. It supports the importance of incubating hPCLS with a bile acid mixture to create an environment similar to the physiological concentration in the portal vein *in vivo* to be able to mimic the toxic mechanisms underlying the cholestasis phenotype. Apart from being predictive, the identified classifiers were mechanistically involved in endoplasmic reticulum stress, unfolded protein response and other stress response pathways, phenomena shown to play a role in cholestasis. They appeared consistent across different concentration levels, different predictive algorithms and inter-individual variation in response. A limitation of our study is the low sample size and further validation of the identified classifiers by incorporating additional compounds in the model building process will be necessary. Moreover different time points should be considered. Despite the limitation of the low sample size and a single time point (24 h), the developed models were able to classify the hepatotoxicants based on their phenotype or mechanism of toxicity with a good accuracy and the identified classifier genes are associated with the phenotype of toxicity. Hence, the human PCLS model is a useful model to study the mechanisms of drug-induced toxicity and to classify toxins based on their mechanism of toxicity and to identify and validate classifiers responsible for drug-induced liver toxicity in humans.

ACKNOWLEDGEMENTS

The authors would like to thank Prof. Dr. Robert Porte and all the surgeons at University Medical Center Groningen for providing human liver tissue. We also thank Marina de Jager, Marjolijn Merema, Miriam Langelaar for their help with preparation and incubation of hPCLS.

SUPPLEMENTARY FIGURES

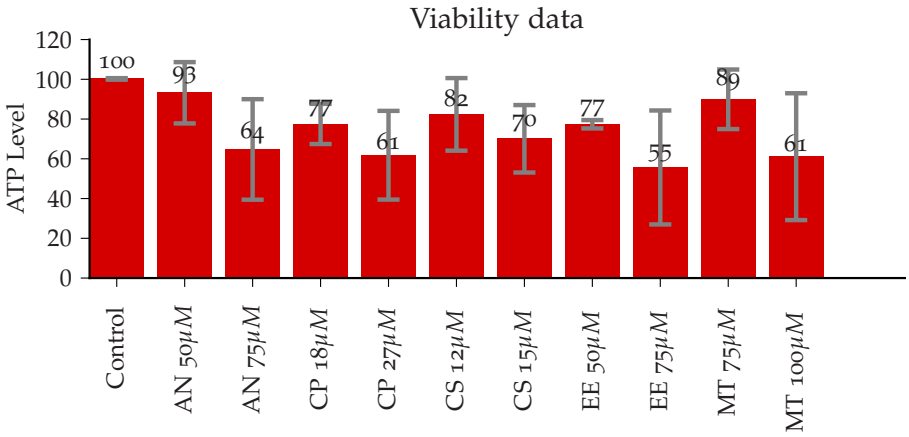

Figure 17: Viability of human PCLS indicated by the ATP content (pmol/μg) after 24hr incubation with various cholestatic compounds

ATP content is expressed as relative values to the control values. Data represent the average values from 3-5 experiments, using three PCLS per experiment (error bars represent the standard deviation)

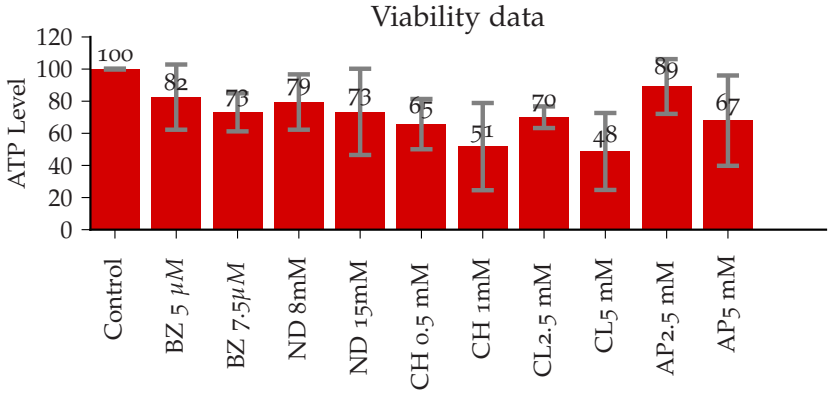

Figure 18: Viability of human PCLS indicated by the ATP content (pmol/μg) after 24hr incubation with various necrotic compounds

ATP content is expressed as relative values to the control values. Data represent the average values from 3-5 experiments, using three PCLS per experiment.

5 TRANSCRIPTOMICS ANALYSIS OF HUMAN PRECISION-CUT LIVER SLICES REVEALS PATHWAYS INVOLVED IN IDIOSYNCRATIC DRUG-INDUCED LIVER INJURY

(Submitted for publication)

Suresh Vatakuti[a*],
Mackenzie Hadi[a*],
Peter Olinga[b],
Geny M.M. Groothuis[a]

* equal contribution

[a] Division of Pharmacokinetics, Toxicology and Targeting, Department of Pharmacy, Groningen Research Institute for Pharmacy, University of Groningen, Groningen, The Netherlands

[b] Division of Pharmaceutical Technology and Biopharmacy, Department of Pharmacy, Groningen Research Institute for Pharmacy, University of Groningen, Groningen, The Netherlands

ABSTRACT

Idiosyncratic drug-induced liver injury (IDILI) is a major concern leading to drug withdrawal or post market restrictions. Low incidence in patients and low concordance of animal and human data necessitate the need of robust screening methods to predict IDILI early in the drug development process. Several possible hypotheses are being tested using *in vitro* or *in vivo* models to understand the possible mechanisms underlying IDILI. One such hypothesis is the inflammatory stress hypothesis. Recently, we have successfully developed and validated a model using human precision-cut liver slices model (hPCLS) based on this hypothesis to screen IDILI-related drugs from non-IDILI-related drugs, using hPCLS co-incubated with drugs and lipopolysaccharide (LPS). As a follow-up to this work, we carried out a transcriptomic analysis to identify possible biomarkers and pathways responsible for IDILI using clozapine as a well-known IDILI drug and olanzapine as its non-IDILI-associated analogue. Gene expression pattern analysis revealed that LPS+clozapine-treated samples were clearly separated from samples treated with LPS alone or clozapine alone in contrast to LPS+olanzapine-treated samples, confirming synergistic toxicity caused by LPS and clozapine. Gene expression analysis revealed that the activation of HMGB1, p38 MAPK, NFkB and NRF2 signaling pathways is involved in the LPS+clozapine-induced IDILI. A significant number of genes were uniquely expressed in LPS+clozapine-treated hPCLS compared to LPS+olanzapine, LPS, clozapine or olanzapine alone. Pathway analysis of the uniquely regulated genes due to LPS+clozapine revealed oxidative phosphorylation as the predominantly affected pathway implicating the role of mitochondrial dysfunction in IDILI. Furthermore, IFN-gamma, IL1A, IL1B, MAPKAPK2, NFkB and PAI-1 were up regulated uniquely or to a greater degree in LPS+clozapine-treated hPCLS compared to LPS or LPS+olanzapine and need to be further validated as biomarkers for IDILI. In conclusion, our study reveals the possible involvement of inflammation and mitochondrial dysfunction signalling pathways in IDILI in the human liver.

5.1 INTRODUCTION

Idiosyncratic drug-induced liver injury (IDILI) occurs in a small fraction of the exposed patients, but is the cause of severe morbidity and mortality. It is not predicted by preclinical animal studies and in clinical patient studies, since these adverse reactions occur at very low frequency both in animals and in patients. The low incidence of IDILI combined with the insufficient predictive power of the existing in vitro models used in regular toxicity screening makes it difficult to detect IDILI in the drug development process.

The mechanisms underlying IDILI are poorly understood for the vast majority of drugs although it is generally recognized that it is not related to the pharmacological activity of the drugs. There are numerous proposed mechanisms of action of IDILI in the literature. In many, but not all, cases reactive metabolites and/or induction of specific immunological responses play a prominent role [180, 181]. In addition, the presence of hepatic inflammation may lead to cytokine release, which in turn reduces the threshold for drug toxicity thereby eliciting an individual susceptible to IDILI. This is the basis of the inflammatory stress hypothesis. Furthermore, there is increasing evidence that mitochondrial dysfunction is involved in IDILI [182, 183, 184].

Several animal models have been developed on the basis of this inflammatory stress hypothesis with the aim of mimicking IDILI, where IDILI related drugs were rendered more toxic in rats or mice in vivo due to an inflammation caused by co-treatment with lipopolysaccharide (LPS) [185, 186, 187, 188, 189, 190, 191]. The insights provided by these animal models of IDILI were instrumental for the development of human IDILI-predictive models to be used during preclinical studies with the aim to detect and eliminate new drug candidates that have the potential to cause human IDILI.

Recently, we have developed the human and mouse PCLS model to test the inflammatory stress hypothesis. PCLS represent an *ex vivo* system that retains the normal tissue architecture of an intact liver with all its cell types in their natural arrangement and are metabolically fully competent with active phase I and II drug metabolism enzymes during 24 h incubation [114]. The gene expression profile of rat PCLS was shown to have a higher degree of similarity to intact liver compared to primary hepatocytes and cell lines [192]. Transcriptomics analysis using rat PCLS showed that they could mimic the toxicity as observed in vivo and discriminate between different mechanisms of hepatotoxicity [71, 117]. It has also been shown that LPS treatment induces an inflammatory response by activation of Kupffer cells in PCLS, leading to the production of nitric oxide (NO) and inflammatory cytokines, such as tumor necrosis factor- (TNF), interleukin 6 and interferon gamma [75, 76, 77, 193, 78, 194, 65].

We tested several IDILI-inducing drugs and their non-IDILI-associated analogues and found that synergistic toxicity was observed when human precision-cut liver slices (hPCLS) were co-incubated with LPS and the IDILI drugs [195]. Concentration-response studies were performed to select a slightly toxic concentration and subsequently it was tested whether the selected concentration could become significantly more toxic under inflammatory stress conditions. For instance, hPCLS treated with the combination of LPS+clozapine showed extensive necrotic areas and decreased ATP content, while incubation with LPS alone or the drug alone showed only minor toxicity. However, treatment with olanzapine did not show any appreciable difference in damage in the absence or presence of LPS. In addition, the release of inflammatory mediators into the medium of hPCLS was analyzed.

Marked elevation of inflammatory mediators was observed in the case of LPS+clozapine in comparison with LPS+olanzapine [195].

In this study, we used a transcriptomic approach in order to identify biomarkers and possible mechanisms of the synergistic toxicity by comparing the gene expression profiles induced by clozapine and olanzapine in the absence and presence of LPS in hPCLS. Comparison of these hepatic gene expression profiles might help to identify gene expression changes critical for LPS+clozapine induced liver injury and possibly also for clozapine induced idiosyncrasy. We tested the hypothesis that co-treatment with LPS and clozapine triggers not only a unique profile of gene expression in comparison to clozapine or LPS alone, but also augments changes in gene expression caused by LPS itself, which does not occur in olanzapine and LPS co-treatment. The objectives of this study were to determine possible pathways responsible for the IDILI using hPCLS and a transcriptomics approach.

5.2 MATERIALS AND METHODS

Chemicals

Clozapine and LPS derived from Escherichia coli serotype B55:O55 (Lot 050M4014, 600,000 EU/mg) were purchased from Sigma-Aldrich (St. Louis, MO). Olanzapine was a kind gift from MSD (Oss, The Netherlands). All other drugs and chemicals were purchased from Sigma-Aldrich unless stated otherwise. Stock solutions of each drug were prepared using dimethyl sulfoxide (VWR, Briare, France) as solvent.

Human Liver Tissue

Pieces of human liver tissue were obtained from patients undergoing partial hepatectomy for the removal of carcinoma (PH) or from liver tissue remaining as surgical waste after split liver transplantation (TX), as described previously [195]. Six different livers were used. The experimental protocols were approved by the Medical Ethical Committee of the University Medical Center Groningen.

Table 23: Human liver donor characteristics used in this study (n = 6)

Human liver	Type	Sex	Age	ATP at 24h (nmol/mg protein)
1	TX	Female	10	9.3
2	TX	Male	7	10.7
3	PH	Male	58	7.3
4	TX	Female	67	6.7
5	TX	Male	55	5.6
6	PH	Male	59	7

PH is liver tissue after partial hepatectomy; TX is liver tissue remaining from donor liver after transplantation.

PREPARATION OF THE HUMAN PCLS Human PCLS were made as described previously [34]. Pieces of human liver were perfused with a cold University of Wisconsin (UW) organ preservation solution (DuPont Critical Care, Waukegan, IL) either in situ in case of surgical waste of donor livers, or in case of tissue obtained after partial hepatectomy, immediately after removal from the body. Cores with a diameter of 5 mm were punched out of the tissue, and these cores were sliced with a Krumdieck tissue slicer (Alabama R&D, Munford, AL) in ice-cold Krebs-Henseleit buffer saturated with carbogen (95% O_2 and 5% CO_2). The hPCLS (5 mm diameter, 200-300μm thick, and 4.5-5.5 mg wet weight) were stored in an ice-cold UW solution until they were incubated.

INCUBATION OF THE HUMAN PCLS The hPCLS were pre-incubated at 37 C for 1 h individually in a well containing 1.3 mL of Williams' medium E with glutamax-1 (Gibco, Paisley, U.K.), supplemented with 25 mM D-glucose and 50μg/mL gentamicin (Gibco) (WEGG medium) in a 12-well plate with shaking (90 times/min) under a saturated carbogen atmosphere. After preincubation, the hPCLS were transferred to fresh WEGG medium in the presence or absence of LPS (24000 EU/mL) and in combination with clozapine (60μM) or its analogue olanzapine (60μM) or the vehicle (the final concentration of DMSO during incubation was always 0.5%) and incubated for an additional 24 h without any further change in medium. The concentrations of drugs used in this study were selected from initial concentration-response relationship studies, where the highest concentration that elicits no or minimal drug-only hepatotoxicity was selected. This concentration was used to test whether a nontoxic concentration would become toxic under inflammatory conditions. Preliminary concentration-response studies were also performed for LPS, with the objective of identifying a concentration of LPS that generated significant inflammatory responses based on the measurements of pro-inflammatory cytokines while causing minimal toxicity. LPS and the drug were administered simultaneously.

VIABILITY OF HPCLS The viability of the hPCLS after incubation for 24 h with various treatments was determined by measuring the ATP content and morphology as described [195].

RNA ISOLATION AND HYBRIDIZATION The triplicate slices of the each treatment or control group were pooled and snap frozen and the total RNA was isolated using the RNeasy mini kit (Qiagen, Venlo, Netherlands). The quality control, RNA labeling, hybridization and data extraction were performed at ServiceXS B.V. (Leiden, The Netherlands). RNA concentration was measured using the Nanodrop ND-1000 spectrophotometer (Nanodrop Technologies, Wilmington, DE, and U.S.A). The RNA quality and integrity was determined using Lab-on-Chip analysis on the Agilent 2100 Bioanalyzer (Agilent Technologies, Inc., SantaClara, CA, U.S.A.) Biotinylated cRNA was prepared using the Affymetrix 3' IVT Express Kit (Affymetrix, Santa Clara, CA, USA) according to the manufacturer's specifications with an input of 100 ng total RNA. The quality of the cRNA was assessed using the Shimadzu MultiNA in order to confirm if the average fragment size was according to Affymetrix' specifications. Per sample, 7.5μg cRNA of the obtained biotinylated cRNA samples was fragmented and hybridized in a final concentration of 0.0375μg/μl on the Affymetrix HT Human Genome U133+ PM array plate (Affymetrix, Santa Clara, CA, USA). After an automated process of washing and staining by the GeneTitan machine (Affymetrix,

Santa Clara, CA, USA) using the Affymetrix HWS Kit for GeneTitan (part nr. 901530), absolute values of expression were calculated from the scanned array using the Affymetrix Command Console v3.2 software.

MICROARRAY PREPROCESSING AND ANALYSIS ArrayAnalysis webservice [120] was used for preprocessing the data. Microarray data was normalized using the robust multichip average RMA algorithm. After normalization the data was corrected for batch differences using the ComBat method implemented in the swamp package in R [121]. Significantly regulated genes with a fold change of 1.5 and multiple hypothesis corrected p-value of 0.05 were identified using Limma R package. The oposSOM package was used to visualize the microarray data and perform gene set enrichment analysis [196]. The SOM-algorithm distributes the genes over a 20 x 20 two-dimensional grid such that each gene profile is associated with the most similar grid point using the Euclidian distance as criterion. Gene profile refers to the changes in expression level of any gene with exposure to different treatment groups. The resulting two-dimensional map of meta-profiles optimally covers all gene profiles observed experimentally. Moreover, the map becomes self-organized, which means that genes with similar profiles of expression changes are clustered together, whereas genes with distinct profiles of expression changes localize in different regions of the map. The training thus translates the data given as N x M matrix (N = 19000: number of genes, M= 36 number of samples) into a K x M matrix (K = 400: number of meta genes). Metagene refers to the set of genes, whose expression changes similarly with exposure to different treatment groups. Each sample is visualized by color-coding the meta-genes in the two-dimensional grid according to their abundance values from red to blue for high to low abundance values, respectively. Neighboring meta-genes tend to be colored similarly owing to their similar profiles. oposSOM also performs second-level SOM analysis, which enables to visualize the differences between different treatment groups. The second level SOM analysis visualizes the similarity between individual first level SOM portraits. In short, it maps all samples together into a two-dimensional mosaic pattern to visualize the degree of similarity between their metagene expression profiles as described above. The mutual distances between the samples in the map are related to the degree of similarity of their SOM expression pattern. Also hierarchical clustering of the different treatment groups was performed using the 35 most regulated metagene profiles.

PATHWAY ANALYSIS Canonical metabolic and signaling pathway analysis was performed using QIAGEN's Ingenuity(R) Pathway Analysis (IPA(R), QIAGEN Redwood City). More specifically, significantly regulated genes from each of the different treatment groups were scored against the canonical signalling pathways involved in immune mediated reactions. Comparison pathway analysis feature in IPA was used to compare the canonical pathways affected by the different treatment groups in human PCLS. Pathways with an activation z-score of 1.3 or -1.3 due to any one of the treatment groups were considered for visualization in a heatmap.

5.3 RESULTS

VIABILITY OF HUMAN PCLS Hadi *et al.* studied the effect of LPS and drugs on the viability of hPCLS by comparing the ATP content after 24 h incubation. The drug concentrations were selected to cause a minimal decrease in ATP content; the selected concentration of 60μM clozapine and 60μM olanzapine significantly decreased the ATP content in the hPCLS of the liver by 18% and 19% respectively after a 24 h incubation without LPS. LPS itself caused slight but significant toxicity in hPCLS incubated for 24 h (13% loss of ATP content). However, synergistic toxicity was observed when the hPCLS were incubated with LPS and clozapine compared to LPS or clozapine alone. LPS and clozapine co-incubation resulted in a decrease in ATP levels to 46 % of the value of the control hPCLS [195]. This synergistic toxicity was substantial considering that treatment with clozapine or LPS alone caused only a slight ATP decrease. In contrast, the incubation of the non-IDILI-associated olanzapine with LPS did not exhibit this phenomenon (22% decrease in ATP). The effect of LPS on the toxicity of the drugs was also assessed by histomorphology. The histomorphology data also confirmed the findings made using the ATP viability data. hPCLS co-incubated with the combination of LPS and clozapine showed extensive necrotic areas, while incubation with LPS alone or the drug alone showed only minor toxicity. Similar to the ATP results, 24 h treatment with olanzapine did not show any appreciable difference in morphological damage in the absence or presence of LPS [195].

SELF-ORGANIZING MAP (SOM) ANALYSIS From the self-organizing maps, it is evident that the expression patterns induced by clozapine are different from those induced by olanzapine and a larger separation of clozapine treated samples from the control group is observed compared to olanzapine treated samples (Figure 19). In addition, LPS treatment induced clear changes in gene expression patterns. An LPS/drug-induced synergistic effect is also evident as the profiles of the LPS+clozapine-treated samples are clearly separated from those of the LPS treated samples in contrast to LPS+olanzapine-treated samples.

Hierarchical clustering analysis was performed for all samples and the 35 most regulated metagene profiles to identify the similarity in gene expression patterns between the samples. It can be seen that a similar trend is observed as seen in the SOM analysis (Figure 20). The control samples and olanzapine samples show similar patterns, indicating little effect of olanzapine. Similarly LPS alone and LPS+olanzapine show similar patterns, indicating that the gene expression pattern of LPS+olanzapine is mainly determined by the LPS treatment. However, the pattern of clozapine+LPS is clearly different from both clozapine alone and LPS alone, indicating specific additional effects.

VENN COMPARISON OF REGULATED GENES Comparison of significantly regulated genes by LPS, olanzapine or clozapine shows that many genes were uniquely regulated in LPS (925 out of 1787) and clozapine (682 out of 1581) indicating compound-dependent gene expression changes and thus different mechanisms of toxicity (Figure 21A). In contrast, in olanzapine treated hPCLS only 17 out of 210 genes were uniquely regulated; the 172 overlapping genes by olanzapine and clozapine possibly indicate class-specific effects, which may not be related to IDILI. Comparison of the genes regulated by LPS alone with those regulated by LPS in combination with clozapine or olanzapine indicates that many genes are uniquely regulated in case of LPS+clozapine (Figure 21B). To identify which genes are

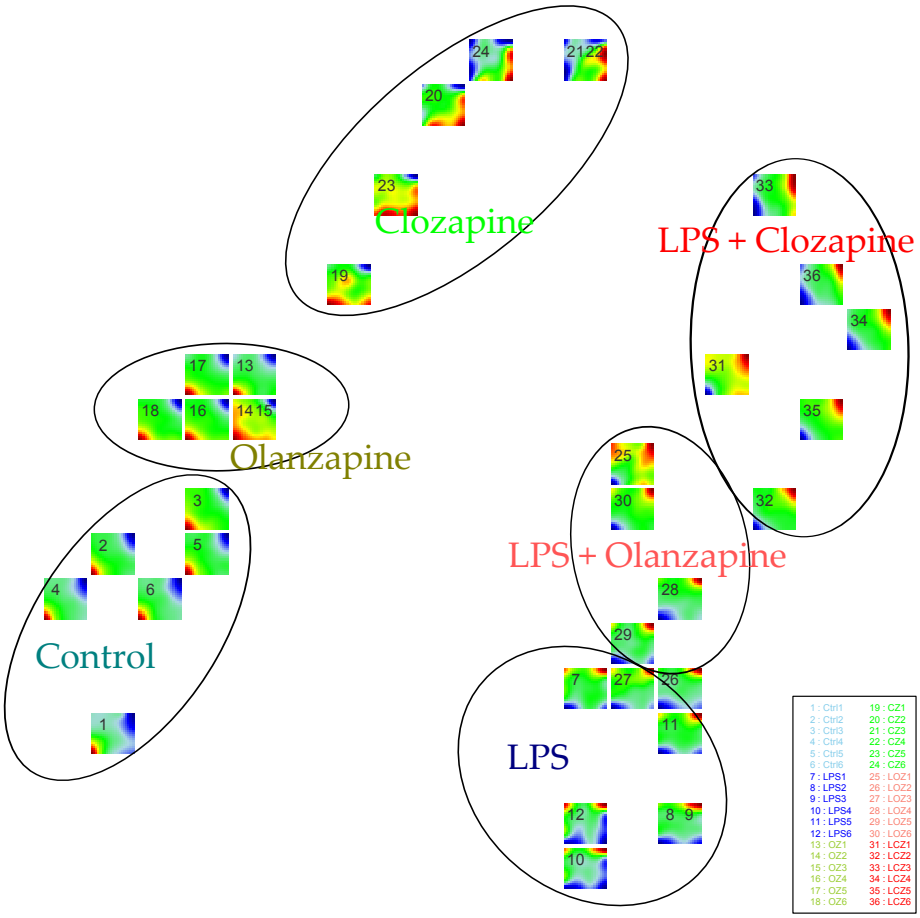

Figure 19: Self organizing maps (SOM) portraits of the microarray samples of the different treatment groups as obtained using 2nd level SOM mapping
(Ctrl= control, OZ = olanzapine, CZ = clozapine, LOZ = LPS+olanzapine, LCZ= LPS+clozapine. The numbers behind these abbreviations indicate the different human livers used (see table 23).

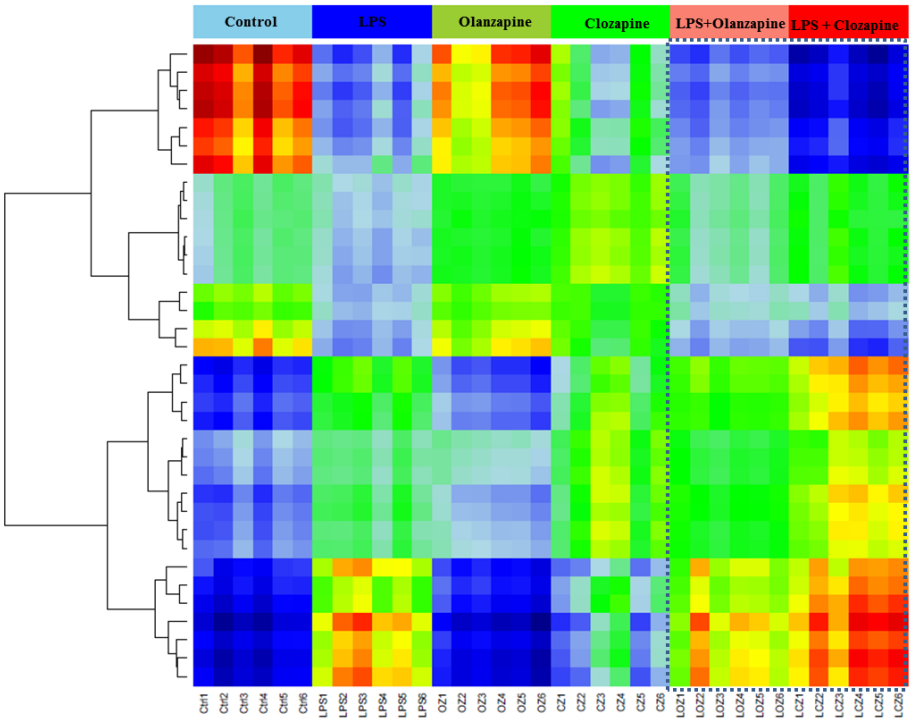

Figure 20: Hierarchical clustering visualization of the gene expression patterns of the treatment groups based on 35 most regulated metagenes

This type of representation visualizes similarity relations between the samples in horizontal direction and between the metagenes in vertical direction.

specifically regulated due to the combination of LPS and clozapine, a Venn diagram of the unique genes of Figure 21A and 21B was made and is given in Figure 21C. A significant number of 719 genes are uniquely regulated due to the combined treatment of LPS and clozapine. These genes may represent information on the mechanism of the synergistic toxicity and thus of IDILI.

PATHWAY ANALYSIS Pathway analysis was performed on all regulated genes of all treatment groups. As it was the aim of the study to test the inflammatory stress hypothesis and to identify the pathways involved, we selected the immune related and cellular stress response pathways in IPA. Canonical signalling pathway comparison revealed the impact of the different treatment groups on the immune related and cellular stress response pathways in IPA (figure 22). It is apparent that LPS+clozapine treatment leads to more extensive activation of most of the pathways than all other treatment groups involved in the comparison. Noticeable differences were also found between treatments with clozapine alone and olanzapine alone. Olanzapine alone did not affect any of these pathways, however clozapine itself already affected several of the pathways, among which the IL8 signaling, Toll-like receptor signaling, HMGB1 signaling, MAPK signaling, IL6 signaling and CD 40 signaling.

Interestingly the NRF2-mediated stress response is inhibited by LPS alone, not affected by clozapine or olanzapine alone or LPS+olanzapine, but is clearly activated by LPS+clozapine. The pathways that were suggested to be associated with idiosyncratic DILI, such as p38 MAPK signalling, HMGB1 signalling, NFkB signalling, and iNOS signalling [187, 189], and NFR2-mediated oxidative stress response [197] were further explored and the regulation of genes in those pathways after exposure to the different treatments are shown in Tables 24-29.

As expected, many of the genes involved in each of the selected pathways are significantly regulated by LPS treatment. Interestingly many of these genes were also regulated by clozapine but not by olanzapine. Moreover they are regulated to a larger extend in the LPS+clozapine group than in any of the other treatment groups (Table 24-29).

To further study the mechanism of the increased toxicity in the LPS+clozapine treatment, further pathway analysis of the 719 genes (figure 21C) that are uniquely regulated due to LPS+clozapine treatment, was performed and revealed that oxidative phosphorylation and mitochondrial dysfunction were the most predominantly affected pathways. The genes involved in the oxidative phosphorylation were downregulated (table 29 and figure 23).

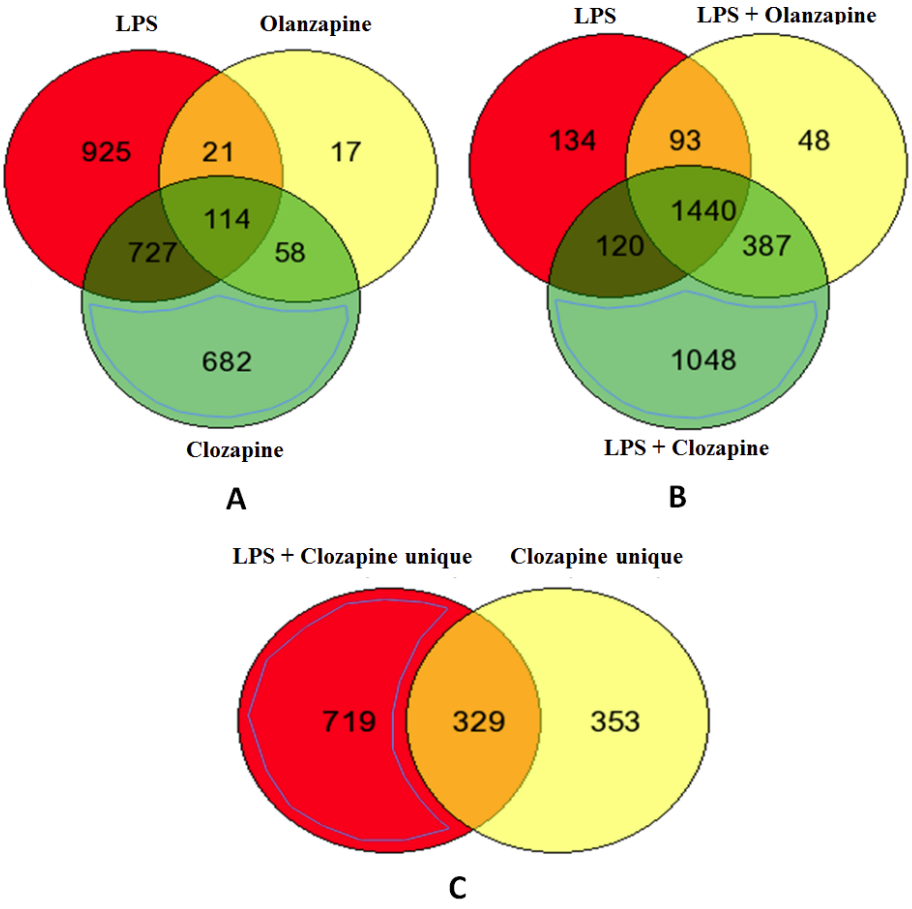

Figure 21: Venn diagram comparison of the significantly regulated genes by different treatment groups

3A: genes regulated due to exposure to LPS, clozapine and olanzapine are compared; 3B: genes regulated due to exposure to LPS, LPS+clozapine and LPS+olanzapine are compared; 3C: Genes uniquely regulated due to clozapine are compared with genes uniquely regulated due to LPS+clozapine.

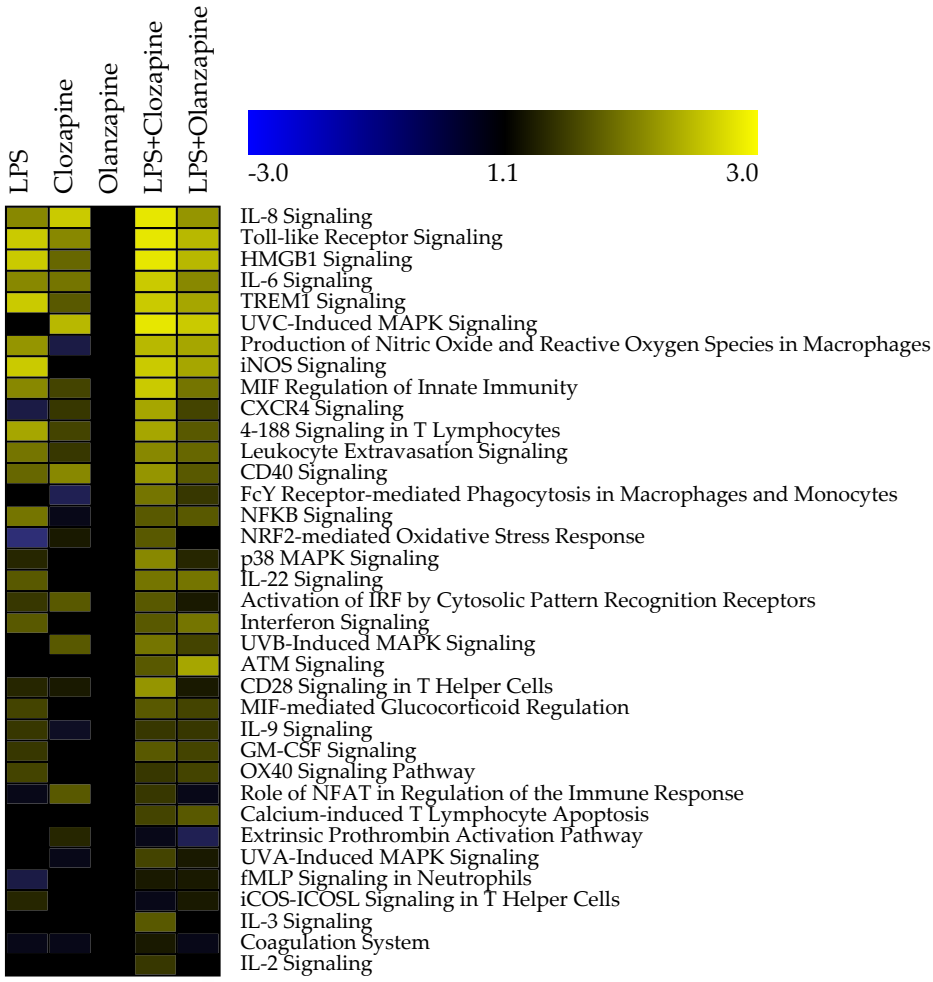

Figure 22: Canonical signalling pathway analysis (immune related and cellular stress response pathways) of the regulated genes in the different treatment groups

Activation z-scores are scaled from 3 to -3 (yellow to blue) indicating positive or negative activation of the corresponding pathways. Intensity of the color represents the relative effect among the different treatment groups.

Table 24: Expression changes of genes involved in the HMGB1 signalling pathway

HMGB1 (High mobility group 1) signalling

Symbol	Entrez Gene Name	LPS	Olanzapine	Clozapine	LPS+Olanzapine	LPS+Clozapine
CSF2	colony stimulating factor 2 (granulocyte-macrophage)	1.8	1.1	1.3	1.6	2.2
FOS	FBJ murine osteosarcoma viral oncogene homolog	1.0	1.1	1.9	1.3	1.7
ICAM1	intercellular adhesion molecule 1	4.5	1.1	1.5	4.4	5.4
IFNGR1	interferon gamma receptor 1	1.4	1.1	1.4	1.6	1.7
IFNG	interferon, gamma	2.9	-1.1	1.0	1.5	2.3
IL1A	interleukin 1, alpha	20.2	1.7	1.5	13.5	20.7
IL1B	interleukin 1, beta	31.0	2.5	2.4	26.4	32.1
IL11	interleukin 11	4.4	-1.1	1.6	3.7	3.9
IL12A	interleukin 12A	1.5	-1.0	1.2	1.3	1.7
IL6	interleukin 6	16.4	1.3	2.2	13.4	15.4
JUN	jun proto-oncogene	1.1	1.1	1.5	1.2	1.6
LIF	leukemia inhibitory factor	6.1	1.2	2.2	6.8	7.8
MAPK13	mitogen-activated protein kinase 13	1.0	1.1	2.0	1.6	2.1
MAPK8	mitogen-activated protein kinase 8	1.7	1.0	1.4	1.7	2.1
NFKB1	nuclear factor of kappa gene enhancer in B-cells 1	2.5	1.1	1.3	2.2	2.6
PLAT	plasminogen activator, tissue	3.4	1.1	1.4	3.2	3.4
RELA	v-rel avian reticuloendotheliosis viral oncogene homolog A	2.1	1.1	1.6	2.0	3.1
RHOQ	ras homolog family member Q	1.3	1.2	1.7	1.5	1.7
RRAS2	related RAS viral (r-ras) oncogene homolog 2	-1.0	1.0	1.7	1.2	1.5
RND3	Rho family GTPase 3	1.4	1.1	2.2	1.7	2.6
SERPINE1	serpin peptidase inhibitor, clade E, member 1	2.1	1.2	2.5	2.8	3.4
TNFRSF1B	tumor necrosis factor receptor superfamily, member 1B	3.0	1.1	1.2	2.9	3.5
IL18	interleukin 18	-1.5	-1.3	-1.5	-1.8	-1.9
PIK3C2G	phosphatidylinositol-4-phosphate 3-kinase, type 2 gamma	-1.3	-1.8	-2.8	-2.6	-3.3
PIK3R1	phosphoinositide-3-kinase, regulatory subunit 1 (alpha)	-1.7	-1.1	-1.6	-1.9	-2.0
VCAM1	vascular cell adhesion molecule 1	1.0	-1.3	-2.6	-2.1	-2.2

Data are presented as fold change values in comparison to vehicle controls. Significantly upregulated genes are highlighted blue and downregulated genes are highlighted orange.

Table 25: Expression changes of genes involved in the P38 MAPK signalling network

p38 MAPK (mitogen activated protein kinase) pathway

Symbol	Entrez Gene Name	LPS	Olanzapine	Clozapine	LPS+Olanzapine	LPS+Clozapine
ATF1	activating transcription factor 1	1.1	1.0	1.6	1.3	2.0
CREB1	cAMP responsive element binding protein 1	1.5	1.1	1.2	1.4	1.5
DAXX	death-domain associated protein	1.4	1.1	1.3	1.4	1.6
DUSP1	dual specificity phosphatase 1	1.8	1.2	2.4	1.9	3.1
DDIT3	DNA-damage-inducible transcript 3	1.2	1.2	2.2	1.5	2.1
FADD	Fas (TNFRSF6)-associated via death domain	1.0	1.2	1.6	1.1	1.5
IL1A	interleukin 1, alpha	20.2	1.7	1.5	13.5	20.7
IL1B	interleukin 1, beta	31.0	2.5	2.4	26.4	32.1
IL1RN	interleukin 1 receptor antagonist	4.0	1.1	2.0	4.2	6.8
IRAK2	interleukin-1 receptor-associated kinase 2	1.8	1.1	1.7	1.9	2.7
MAPK13	mitogen-activated protein kinase 13	1.0	1.1	2.0	1.6	2.1
MAPKAPK2	mitogen-activated protein kinase-activated protein kinase 2	1.5	1.1	1.3	1.5	1.7
MAX	MYC associated factor X	1.2	1.0	1.4	1.2	1.7
TAB2	TGF-beta activated kinase 1/MAP3K7 binding protein 2	1.6	1.0	1.3	1.5	1.9
TIFA	TRAF-interacting protein with forkhead-associated domain	3.1	1.1	1.1	2.4	2.9
TNFRSF1B	tumor necrosis factor receptor superfamily, member 1B	3.0	1.1	1.2	2.9	3.5
TRAF6	TNF receptor-associated factor 6, E3 ubiquitin protein ligase	1.3	1.1	1.5	1.3	1.8
EEF2K	eukaryotic elongation factor 2 kinase	-1.4	1.0	-1.1	-1.5	-1.7
FAS	Fas cell surface death receptor	-1.4	-1.1	-1.6	-1.9	-1.5
IL18	interleukin 18	-1.5	-1.3	-1.5	-1.8	-1.9
MAP3K5	mitogen-activated protein kinase kinase kinase 5	-1.1	-1.1	-1.7	-1.5	-2.0
MEF2C	myocyte enhancer factor 2C	-1.6	-1.1	-1.0	-1.7	-2.0
PLA2G12A	phospholipase A2, group XIIA	-2.0	-1.0	-1.8	-2.1	-3.1
PLA2G12B	phospholipase A2, group XIIB	-8.4	-1.5	-4.3	-9.0	-10.8
TGFBR2	transforming growth factor, beta receptor II (70/80kDa)	-2.3	-1.1	-1.4	-2.4	-2.5

Data are presented as fold change values in comparison to vehicle controls. Significantly upregulated genes are highlighted blue and downregulated genes are highlighted orange.

Table 26: Expression changes of genes involved in the NFkB signalling pathway

NFkB (nuclear factor kappa-light-chain-enhancer of activated B cells) pathway						
Symbol	**Entrez Gene Name**	**LPS**	**Olanzapine**	**Clozapine**	**LPS+Olanzapine**	**LPS+Clozapine**
BCL10	B-cell CLL/lymphoma 10	1.3	1.1	1.9	1.4	2.1
CD40	CD40 molecule, TNF receptor superfamily member 5	2.1	-1.1	-1.0	1.7	2.5
FADD	Fas (TNFRSF6)-associated via death domain	1.0	1.2	1.6	1.1	1.5
IL1A	interleukin 1, alpha	20.2	1.7	1.5	13.5	20.7
IL1B	interleukin 1, beta	31.0	2.5	2.4	26.4	32.1
IL1RN	interleukin 1 receptor antagonist	4.0	1.1	2.0	4.2	6.8
MALT1	MALT1 paracaspase	1.2	-1.0	1.4	1.4	1.6
MAP4K4	mitogen-activated protein kinase kinase kinase kinase 4	1.8	1.2	1.6	1.7	2.1
MAPK8	mitogen-activated protein kinase 8	1.7	1.0	1.4	1.7	2.1
NFKB1	nuclear factor of kappa light polypeptide gene enhancer in B-cells 1	2.5	1.1	1.3	2.2	2.6
NFKBIA	nuclear factor of kappa, alpha	2.5	-1.0	1.4	2.2	2.7
NFKBIB	nuclear factor of kappa, beta	1.3	1.1	1.2	1.4	1.6
NFKBIE	nuclear factor of kappa, epsilon	1.6	1.1	1.4	1.7	2.2
PDGFRA	platelet-derived growth factor receptor, alpha polypeptide	1.9	1.1	1.1	1.7	1.9
PELI1	pellino E3 ubiquitin protein ligase 1	2.3	-1.1	1.2	1.8	2.3
RELA	v-rel avian reticuloendotheliosis viral oncogene homolog A	2.1	1.1	1.6	2.0	3.1
RELB	v-rel avian reticuloendotheliosis viral oncogene homolog B	2.3	1.0	1.5	2.3	3.1
RRAS2	related RAS viral (r-ras) oncogene homolog 2	-1.0	1.0	1.7	1.2	1.5
TAB2	TGF-beta activated kinase 1/MAP3K7 binding protein 2	1.6	1.0	1.3	1.5	1.9
TBK1	TANK-binding kinase 1	1.4	1.0	1.2	1.4	1.6
TLR2	toll-like receptor 2	6.9	-1.2	1.1	4.8	6.1
TNFRSF1B	tumor necrosis factor receptor superfamily, member 1B	3.0	1.1	1.2	2.9	3.5
TRAF3	TNF receptor-associated factor 3	1.6	1.1	1.2	1.7	1.8
TRAF6	TNF receptor-associated factor 6, E3 ubiquitin protein ligase	1.3	1.1	1.5	1.3	1.8
FGFR2	fibroblast growth factor receptor 2	-1.8	-1.4	-1.7	-1.9	-2.0
FGFR3	fibroblast growth factor receptor 3	-2.4	-1.1	-1.9	-2.2	-2.4
GHR	growth hormone receptor	-2.1	-1.4	-2.4	-2.6	-5.3
IL18	interleukin 18	-1.5	-1.3	-1.5	-1.8	-1.9
PIK3C2G	phosphatidylinositol-4-phosphate 3-kinase, catalytic subunit type 2 gamma	-1.3	-1.8	-2.8	-2.6	-3.3
PIK3R1	phosphoinositide-3-kinase, regulatory subunit 1 (alpha)	-1.7	-1.1	-1.6	-1.9	-2.0
PRKCZ	protein kinase C, zeta	-1.2	-1.1	-1.4	-1.2	-1.5
TGFBR2	transforming growth factor, beta receptor II (70/80kDa)	-2.3	-1.1	-1.4	-2.4	-2.5
TGFBR3	transforming growth factor, beta receptor III	-2.8	-1.3	-2.2	-3.2	-3.7
TLR3	toll-like receptor 3	-1.0	-1.3	-2.4	-1.6	-2.2

Data are presented as fold change values in comparison to vehicle controls. Significantly upregulated genes are highlighted blue and downregulated genes are highlighted orange.

Table 27: Expression changes of genes involved in the production of nitric oxide and reactive oxygen species

iNOS (inducible nitric oxide synthase) pathway						
Symbol	**Entrez Gene Name**	**LPS**	**Olanzapine**	**Clozapine**	**LPS+Olanzapine**	**LPS+Clozapine**
IFNG	interferon, gamma	2.9	-1.1	1.0	1.5	2.3
IFNGR2	interferon gamma receptor 2 (interferon gamma transducer 1)	1.6	-1.1	-1.0	1.4	1.4
IRAK2	interleukin-1 receptor-associated kinase 2	1.8	1.1	1.7	1.9	2.7
IRF1	interferon regulatory factor 1	2.7	-1.1	-1.3	1.6	2.6
JAK1	Janus kinase 1	1.9	1.0	1.3	1.8	1.8
JAK2	Janus kinase 2	2.5	-1.0	1.0	1.6	2.0
NFKB1	nuclear factor of kappa gene enhancer in B-cells 1	2.5	1.1	1.3	2.2	2.6
NFKBIA	nuclear factor of kappa, alpha	2.5	-1.0	1.4	2.2	2.7
NFKBIE	nuclear factor of kappa, epsilon	1.6	1.1	1.4	1.7	2.2
NOS2	nitric oxide synthase 2, inducible	2.6	-1.2	-1.1	1.6	2.5
RELA	v-rel avian reticuloendotheliosis viral oncogene homolog A	2.1	1.1	1.6	2.0	3.1
FOS	FBJ murine osteosarcoma viral oncogene homolog	1.0	1.1	1.9	1.3	1.7
IFNGR1	interferon gamma receptor 1	1.4	1.1	1.4	1.6	1.7
JUN	jun proto-oncogene	1.1	1.1	1.5	1.2	1.6
MAPK13	mitogen-activated protein kinase 13	1.0	1.1	2.0	1.6	2.1
NFKBIB	nuclear factor of kappa, beta	1.3	1.1	1.2	1.4	1.6
TRAF6	TNF receptor-associated factor 6, E3 ubiquitin protein ligase	1.3	1.1	1.5	1.3	1.8

Data are presented as fold change values in comparison to vehicle controls. Significantly upregulated genes are highlighted blue and downregulated genes are highlighted orange.

Table 28: Expression changes of genes involved in the NRF2-mediated oxidative stress response

NRF2-mediated Oxidative Stress Response						
Symbol	**Entrez Gene Name**	**LPS**	**Olanzapine**	**Clozapine**	**LPS+Olanzapine**	**LPS+Clozapine**
CDC34	cell division cycle 34	1.1	1.1	1.8	1.3	1.8
DNAJB1	DnaJ (Hsp40) homolog, subfamily B, member 1	1.6	1.4	2.2	2.2	2.4
DNAJB2	DnaJ (Hsp40) homolog, subfamily B, member 2	1.2	1.2	1.8	1.4	1.8
FOS	FBJ murine osteosarcoma viral oncogene homolog	1.0	1.1	1.9	1.3	1.7
GSR	glutathione reductase	1.3	1.3	1.6	1.4	1.6
HMOX1	heme oxygenase 1	1.2	-1.2	1.5	1.5	1.8
JUN	jun proto-oncogene	1.1	1.1	1.5	1.2	1.6
MAFF	musculoaponeurotic fibrosarcoma oncogene homolog F	2.0	1.5	3.1	2.5	3.7
MAFG	musculoaponeurotic fibrosarcoma oncogene homolog G	1.4	1.3	1.5	1.7	1.9
MAFK	musculoaponeurotic fibrosarcoma oncogene homolog K	1.2	1.1	1.5	1.4	1.8
MAP2K1	mitogen-activated protein kinase kinase 1	1.3	1.0	1.2	1.4	1.6
MAPK8	mitogen-activated protein kinase 8	1.7	1.0	1.4	1.7	2.1
NFE2L2	nuclear factor, erythroid 2-like 2	1.2	1.2	1.3	1.4	1.5
PRKCD	protein kinase C, delta	1.3	1.1	1.4	1.5	1.9
PRKCI	protein kinase C, iota	1.4	1.2	1.6	1.6	1.8
PRKD3	protein kinase D3	1.5	-1.0	1.1	1.4	1.5
RRAS2	related RAS viral (r-ras) oncogene homolog 2	-1.0	1.0	1.7	1.2	1.5
TXNRD1	thioredoxin reductase 1	-1.1	1.6	2.0	1.2	1.7
ABCC2	ATP-binding cassette, sub-family C (MRP), member 2	-3.9	1.5	-1.3	-2.2	-3.6
ACTA2	actin, alpha 2, smooth muscle, aorta	-1.7	-1.3	-1.8	-2.3	-2.2
AKR7A2	aldo-keto reductase family 7, member A2	-2.1	-1.1	-1.4	-2.0	-2.4
AKR7A3	aldo-keto reductase family 7, member A3	-5.6	-1.3	-2.5	-5.2	-5.7
AOX1	aldehyde oxidase 1	-3.2	-1.2	-2.6	-3.2	-5.8
CAT	catalase	-3.6	-1.4	-2.5	-3.8	-5.0
CBR1	carbonyl reductase 1	-1.9	1.1	-1.3	-1.8	-1.8
DNAJA3	DnaJ (Hsp40) homolog, subfamily A, member 3	-1.5	1.0	-1.2	-1.5	-1.8
DNAJC19	DnaJ (Hsp40) homolog, subfamily C, member 19	-1.8	-1.2	-1.6	-1.8	-1.9
EPHX1	epoxide hydrolase 1, microsomal (xenobiotic)	-2.9	1.1	-2.1	-2.4	-3.2
FKBP5	FK506 binding protein 5	-1.4	-1.0	-1.3	-1.7	-1.7
GSTA1	glutathione S-transferase alpha 1	-16.0	-1.4	-6.5	-11.6	-13.0
GSTK1	glutathione S-transferase kappa 1	-1.7	-1.2	-1.4	-1.7	-1.8
HACD3	3-hydroxyacyl-CoA dehydratase 3	-2.1	-1.1	-1.7	-2.2	-2.9
MAP3K5	mitogen-activated protein kinase kinase kinase 5	-1.1	-1.1	-1.7	-1.5	-2.0
MGST2	microsomal glutathione S-transferase 2	-1.7	-1.3	-1.8	-1.8	-2.8
MGST3	microsomal glutathione S-transferase 3	-1.6	-1.1	-1.1	-1.6	-1.6
PIK3C2G	phosphatidylinositol-4-phosphate 3-kinase, type 2 gamma	-1.3	-1.8	-2.8	-2.6	-3.3
PIK3R1	phosphoinositide-3-kinase, regulatory subunit 1 (alpha)	-1.7	-1.1	-1.6	-1.9	-2.0
PRKCZ	protein kinase C, zeta	-1.2	-1.1	-1.4	-1.2	-1.5
SCARB1	scavenger receptor class B, member 1	1.2	1.0	-1.5	1.2	-1.6
SOD1	superoxide dismutase 1, soluble	-1.4	-1.0	-1.2	-1.3	-1.6

Data are presented as fold change values in comparison to vehicle controls. Significantly upregulated genes are highlighted blue and downregulated genes are highlighted orange.

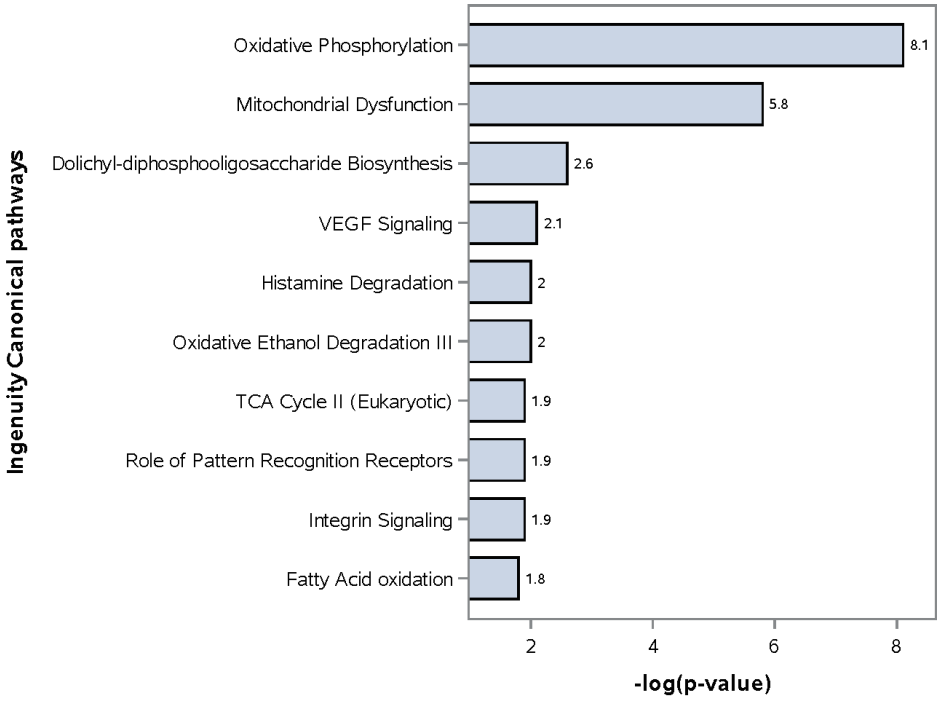

Figure 23: Canonical pathways predominantly affected by the genes uniquely regulated due to LPS+clozapine treatment

Horizontal bars denote the significant values represented as negative logarithm of the p-value (-log(p-value)). -log(p-value) of 1.3 corresponds to p- value 0.05.

Table 29: Expression changes of genes involved in the oxidative phosphorylation

Oxidative phosphorylation pathway						
Symbol	**Entrez Gene Name**	**LPS**	**Olanzapine**	**Clozapine**	**LPS+Olanzapine**	**LPS+Clozapine**
ATP5A1	ATP synthase, H+ transporting, mitochondrial F1 complex, alpha subunit 1	-1.3	-1.1	**-1.6**	**-1.5**	**-2.1**
ATP5B	ATP synthase, H+ transporting, mitochondrial F1 complex, beta polypeptide	-1.4	-1.1	-1.4	**-1.5**	**-1.8**
ATP5C1	ATP synthase, H+ transporting, mitochondrial F1 complex, gamma polypeptide 1	-1.4	-1.1	-1.3	**-1.5**	**-1.8**
ATP5D	ATP synthase, H+ transporting, mitochondrial F1 complex, delta subunit	**-1.5**	-1.1	-1.3	**-1.6**	**-1.8**
ATP5F1	ATP synthase, H+ transporting, mitochondrial Fo complex, subunit B1	-1.4	-1.1	-1.4	**-1.5**	**-1.8**
ATP5G1	ATP synthase, H+ transporting, mitochondrial Fo complex, subunit C1	**-1.5**	-1.1	**-1.5**	**-1.6**	**-2.2**
ATP5G2	ATP synthase, H+ transporting, mitochondrial Fo complex, subunit C2	-1.3	-1.2	-1.2	-1.4	**-1.6**
ATP5G3	ATP synthase, H+ transporting, mitochondrial Fo complex, subunit C3	**-1.6**	-1.2	**-1.5**	**-1.7**	**-2.2**
ATP5J	ATP synthase, H+ transporting, mitochondrial Fo complex, subunit F6	-1.4	-1.1	-1.3	-1.4	**-1.5**
ATP5L	ATP synthase, H+ transporting, mitochondrial Fo complex, subunit G	-1.4	-1.2	-1.3	-1.4	**-1.6**
CYB5A	cytochrome b5 type A (microsomal)	**-2.8**	-1.1	**-2.0**	**-2.7**	**-4.1**
NDUFA3	NADH dehydrogenase (ubiquinone) 1 alpha subcomplex, 3, 9kDa	-1.3	-1.2	-1.4	-1.3	**-1.7**
NDUFB3	NADH dehydrogenase (ubiquinone) 1 beta subcomplex, 3, 12kDa	-1.1	-1.1	**-1.5**	-1.3	**-1.5**
NDUFB5	NADH dehydrogenase (ubiquinone) 1 beta subcomplex, 5, 16kDa	-1.1	-1.2	-1.4	-1.3	**-1.5**
NDUFB6	NADH dehydrogenase (ubiquinone) 1 beta subcomplex, 6, 17kDa	-1.3	-1.2	-1.4	-1.4	**-1.7**
NDUFB7	NADH dehydrogenase (ubiquinone) 1 beta subcomplex, 7, 18kDa	-1.4	-1.3	**-1.5**	**-1.5**	**-1.9**
NDUFB10	NADH dehydrogenase (ubiquinone) 1 beta subcomplex, 10, 22kDa	-1.4	-1.2	-1.3	**-1.5**	**-1.7**
NDUFS1	NADH dehydrogenase (ubiquinone) Fe-S protein 1, 75kDa	-1.2	-1.1	-1.4	-1.4	**-1.7**
NDUFS3	NADH dehydrogenase (ubiquinone) Fe-S protein 3, 30kDa	-1.3	-1.2	-1.4	-1.4	**-1.8**
NDUFS7	NADH dehydrogenase (ubiquinone) Fe-S protein 7, 20kDa	-1.3	-1.1	-1.3	**-1.5**	**-1.6**
NDUFV1	NADH dehydrogenase (ubiquinone) flavoprotein 1, 51kDa	-1.3	-1.1	-1.4	-1.4	**-1.9**
SDHB	succinate dehydrogenase complex, subunit B, iron sulfur (Ip)	-1.3	-1.3	-1.4	-1.3	**-1.6**
SURF1	surfeit 1	-1.2	-1.2	-1.4	-1.3	**-1.6**
UQCRC1	ubiquinol-cytochrome c reductase core protein I	-1.1	-1.1	-1.4	-1.3	**-1.5**
UQCRC2	ubiquinol-cytochrome c reductase core protein II	-1.3	-1.2	**-1.5**	**-1.5**	**-1.8**

Data are presented as fold change values in comparison to vehicle controls. Significantly upregulated genes are highlighted blue and downregulated genes are highlighted orange.

5.4 DISCUSSION

IDILI is a rare but serious side effect of many drug treatments and represents one of the largest undetected liabilities for new drugs in development. Understanding the underlying mechanisms responsible for IDILI is the first step towards identifying its risk in preclinical models. Co-treatment with a small, non-hepatotoxic dose of LPS renders numerous drugs hepatotoxic in rats [186, 187, 14, 198, 26, 199], which is in support of the inflammatory stress hypothesis. As it is generally realized that animal studies have a low predictive value for the human situation, models employing human cells or tissue are currently developed. Several studies employing human cell cultures were reported previously as models for IDILI [136, 200, 201, 202]. Recently Hadi *et al.* were the first to study idiosyncratic drug reactions in human tissue culture *ex vivo* [195] and found that co-incubation of LPS with several IDILI drugs, among which clozapine, resulted in synergistic toxicity, in line with the inflammatory stress hypothesis. In this study, we applied a transcriptomic analysis to the mRNA expression profiles of *ex vivo* human liver slices treated with LPS+clozapine in order to identify pathways that might be involved in IDILI.The synergistic toxicity observed when hPCLS were co-incubated for 24 h with LPS+clozapine but not with LPS+olanzapine was confirmed by ATP content, cytokine release and morphological changes [195]. The selected concentration of clozapine (60 μM) was the same as that of olanzapine (60 μM), both showing minor toxicity. Despite their structural similarity and formation of the same reactive metabolite (a reactive nitrenium ion), administration of an equimolar dose of clozapine, but not olanzapine, in the rat *in vivo* is shown to cause neutropenia [203]. It can be hypothesized that clozapine affects gene expression changes in a manner that makes the response to inflammatory stimuli induced by LPS stronger, resulting in hepatocellular injury. Alternatively, it can be hypothesized that LPS affects the gene expression changes induced by clozapine is such a way that it initiates signaling pathways to hepatocellular injury and synergistic toxicity. This synergistic toxicity does not occur in LPS+olanzapine treated hPCLS, indicating that olanzapine lacks the ability to induce idiosyncratic liver toxicity. IDILI has not been shown for olanzapine in patients, although it should be realized that a much lower dose of olanzapine is used than clozapine [204]. Self-organizing maps and hierarchical clustering analysis was performed to evaluate global differences among different treatment groups (figure 19 and 20). hPCLS treated with LPS+olanzapine could not be distinguished from LPS alone, suggesting that olanzapine co-treatment did not greatly alter LPS-induced gene expression. In contrast, LPS+clozapine treated hPCLS were clustered distantly from either LPS+olanzapine or LPS alone. Similarly, gene expression patterns for clozapine clustered distantly from those for olanzapine or vehicle control. It was observed that LPS alone at a slightly toxic concentration induced significant changes in gene expression patterns compared to the control group, reflecting the inflammatory response. Co-incubation with clozapine further altered the LPS-induced gene expression patterns. Venn comparison of regulated genes also indicates that LPS+clozapine treatment caused regulation of 1048 unique genes which were not regulated with LPS or LPS+olanzapine (figure 21). LPS-induced mild inflammation interacts with drugs that cause human IDILI to cause liver injury in experimental animal inflammation [14]. Inflammation involves the activation of cells of the immune system, coordinated actions of the mediators they produce, and altered inflammatory gene expression and cellular signaling events. We performed pathway analysis using immune-mediated and cellular stress response signalling pathways to compare the

effects in the different treatment groups. This comparison of canonical signalling pathways revealed the enhanced activation of immune related and/or cellular stress related pathways by LPS+clozapine in comparison to LPS or LPS+olanzapine. For instance, Toll-like Receptor signalling is one of the predominantly activated pathways. Toll-Like receptors (TLRs) play a critical role in the early innate immune response and are involved in sensing endogenous danger signals (HMGB1). Stimulation of TLRs by LPS or HMGB1 initiates signaling cascades leading to the activation of downstream signaling molecules like p38MAPK and NFkB which then are translocated into the nucleus where they activate transcription regulators like FOS and JUN leading to the induction of several pro-inflammatory cytokines [205, 206]. HMGB1 is secreted by macrophages and monocytes during inflammatory processes or released passively by hepatocytes due to ischemia reperfusion injury or during drug-induced necrosis [207, 208]. HMGB1 was also released by mouse and human PCLS after treatment with LPS or paracetamol [194, 65]. HMGB1 in turn can activate cell surface receptors on various cell types causing ERK1/2, JNK, and p38 activation and results in the release of proinflammatory cytokines and chemokines (TNF, IL-1A, IL-1B, IL-6, IL-8) and the upregulation of adhesion molecules such as ICAM1. Cytokines involved in the HMGB signalling such as IL1A and IL1B were significantly regulated in the human PCLS after exposure to LPS alone and in combinations with the tested drugs. It is interesting to observe that IL1A and IL1B and ICAM1 expression due to LPS+clozapine was higher than with LPS or LPS+olanzapine (table 24). GM-CSF (CSF2) expression was also enhanced due to LPS+clozapine in comparison with LPS or LPS+olanzapine. A similar trend was observed with measured cytokine levels in the medium of hPCLS [195]. It is also interesting to see that PAI-1 upregulation was higher due to clozapine than to LPS alone and that its expression was further enhanced with LPS+clozapine co-treatment. Several studies reported the role of the hemostatic or coagulation system in LPS+drug induced liver injury [185, 188, 189]. Increased expression of PAI-1 (SERPINE1) *in vivo* causes increased fibrin deposition, leading to tissue hypoxia and hepatocyte cell death. HMGB1 is also known to play a role in the regulation of coagulation by increasing the expression of PAI-1 and PLAT [209]. LPS-induced stabilization of mRNAs encoding for inflammatory mediators requires the downstream p38 pathway member, MAPKAPK-2 [210, 211]. Treatment with neither clozapine nor olanzapine alone, but with LPS caused up-regulation of MAPKAPK2 in the hPCLS, and an additive increase was observed in LPS+clozapine co-treated hPCLS (table 25). Similar enhanced expression of MAPKAPK2 and its target genes was found in LPS+ranitidine co-treated rats *in vivo* [187]. It is possible that the enhanced expression of MAPKAPK-2 in LPS+clozapine co-treated hPCLS stabilizes mRNAs for inflammatory mediators initially expressed after LPS alone. In addition, consistent with its regulation by MAPKAPK2 at the translational level, TNF concentration in the medium was significantly enhanced in LPS+clozapine-treated hPCLS [195]. This enhanced production of inflammatory mediators might result in liver injury represented by necrotic areas in LPS+clozapine-treated hPCLS. Accordingly, identification of genes expressed to a greater degree in LPS+clozapine-treated hPCLS suggested the possibility that p38/MAPKAPK-2 signaling was important for elevated levels of certain cytokine mRNAs. Also, p38 MAPK is known to translocate to the nucleus where it phosphorylates transcription factors like activating transcription factor (ATF1). The activated transcription factors trigger transcription of several stress response genes responsible for cytokine production and apoptosis. ATF1 was upregulated by clozapine but not by olanzapine or LPS and its upreguation was further enhanced by LPS+clozapine treatment. The family of NFkB transcription factors

plays an important role in regulating the expression of many genes involved in cell survival, immunity and inflammatory processes. NFkB transcription factors consist of five known subunits (RELA/p65, c-REL, RELB, NFkB1 and NKB2). The expression of three of them, NFkB1, RELA and RELB, was higher in hPCLS treated with LPS+clozapine than with LPS or LPS+olanzapine. BCL10 involved in activation of NFkB via NIK and IKK was also uniquely regulated due to both clozapine and LPS+clozapine treatments. MALT1, known to enhance the BCL10-induced activation of NFkB, was also uniquely regulated in LPS+clozapine. Amplification of NFkB-mediated gene expression was also observed in an inflammatory stress model (LPS+diclofenac) in rat *in vivo* [189]. Thus, our study also supports the possible involvement of NFkB pathways in IDILI. NFkB, p38 MAPK and IFN signalling pathways lead to induction of iNOS, which was more enhanced by LPS+clozapine than LPS+olanzapine. p38 MAPK mediated activation of AP-1 also leads to induction of iNOS. The transcription factors FOS and JUN of the AP-1 complex were uniquely regulated with clozapine and LPS+clozapine, possibly this reflects the ability of clozapine to induce an idiosyncratic reaction. IFN induces the transcription of iNOS by activating interferon-regulated factor-1 (IRF-1). IFN and IRF1 were upregulated by LPS or LPS+drug combinations but upreguation was higher in LPS+clozapine in contrast to LPS+olanzapine. Together, enhanced expression of NFkB, iNOS, AP-1 and IFN , leading to enhanced activation of iNOS in LPS+clozapine in comparison to LPS+olanzapine, might contribute to the IDILI, due to enhanced production of reactive nitrogen species causing mitochondrial damage [212]. Enhanced activation of Nuclear factor erythroid 2-related factor 2 (NRF2) mediated oxidative stress response was observed due to LPS+clozapine in comparison to other treatments groups. NRF2 is involved in the cellular defense response to oxidative stress by inducing antioxidant and detoxifying enzymes. The NRF2 transcription factor itself was also significantly upregulated only due to LPS+clozapine treatment. Moreover, LPS+clozapine treatment enhanced the expression of NRF2 target genes such as glutathione reductase (GSR) and HMOX1 in comparison to LPS or clozapine alone (Table 28). GSR, a central enzyme in cellular antioxidant defense, involved in glutathione (GSH) production and regeneration, was upregulated by the incubation with clozapine alone, but it was not further enhanced by the coincubation with LPS. Moreover, enhanced expression of genes involved in protein kinase and MAP kinase pathways, which are involved in activation of NRF2, was observed in LPS+clozapine. A recent study using HepG2 cells reported that drugs that are more often associated with DILI cause a strong activation of the NRF2-mediated stress response and a suppression of endogenous NFkB activity [197]. Partly in accordance, we also observed a slight activation of NRF2 stress response but we found no effect on NFkB activity due to clozapine treatment. However, in the presence of an inflammatory stress mediator (LPS), the clozapine-induced NRF2 response was further enhanced and activation of NFkB response was observed (Figure 22). NFkB activation could be ascribed primarily due to treatment with LPS, as clozapine or olanzapine alone did not affect the NFkB pathway. It is noteworthy that enhanced activation of NFkB was also observed due to LPS+diclofenac co-administration in rats [189]. There is also increasing evidence that numerous drugs associated with idiosyncratic drug reactions cause mitochondrial dysfunction [182]. Gene expression profiling in rat *in vivo* revealed the activation of mitochondrial dysfunction in IDILI-associated drugs but not in non-IDILI-associated drugs [136, 184], although recently in a rat *in vivo* model of LPS+diclofenac co-administration, an upregulation of the ATP synthase subunits ATP5J, ATPA, and ATPB was reported [213].

In accordance with the reported mitochondrial dysfunction, pathway analysis of the genes uniquely regulated due to LPS+clozapine treatment (figure 23 and table 29) also revealed that oxidative phosphorylation was the predominantly affected pathway and many genes involved in complex I-V of electron transport chain were downregulated (figure 24). This further strengthens the role of the mitochondrial damage in inflammation-associated IDILI. Genes which are uniquely regulated (719) due to LPS+clozapine treatment could be potential biomarkers for inflammation-associated IDILI. Further studies with other IDILI drugs should elucidate the potential IDILI biomarkers which are not specific for clozapine.

In conclusion, potential gene expression signatures leading to IDILI were identified using a recently validated *ex vivo* model of human PCLS. Mitochondrial dysfunction was identified as a potential mechanism of inflammation-associated IDILI as gene expression changes indicating mitochondrial dysfunction were observed after exposure to LPS+clozapine. In addition, hepatic gene expression analysis suggested the activation of HMGB1, p38 MAPK, and NFkB signalling pathways to be involved in the LPS+clozapine induced IDILI. This study underlines the use of human tissue to elucidate the mechanisms of IDILI in humans and to eventually find human-specific biomarkers for IDILI. The hPCLS seems to be a promising *ex vivo* model for characterizing IDILI. Further research including more IDILI-related drugs together with their non-IDILI-related comparator drugs will elucidate whether the mechanisms of clozapine-induced IDILI found in this study are specific for clozapine or are also involved in liver toxicity induced by other IDILI drugs.

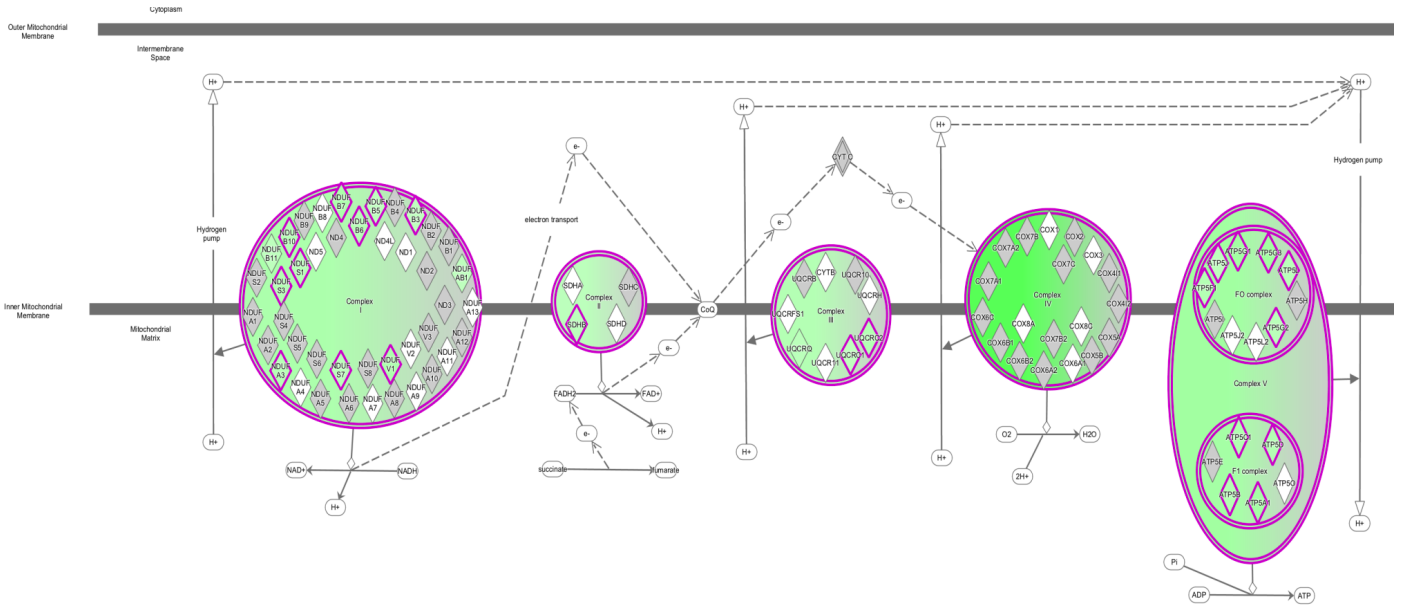

Figure 24: Genes involved in the oxidative phosphorylation that are regulated due to LPS+clozapine exposure Significantly downregulated genes with at least 1.5 fold change are represented as pink colored diamond.

ACKNOWLEDGEMENTS

The authors would like to thank Prof. Dr. Robert Porte and all the surgeons at University Medical Center Groningen for providing human liver tissue. We also thank Marina de Jager, Marjolijn Merema, Miriam Langelaar, Patricia Robbe and Sylvia Blomsma for their help with preparation and incubation of hPCLS. Dr. Willem Schoonen is thanked for providing olanzapine. Lastly, we would like to thank Roel Bijkerk of Leiden University Medical Center for his assistance with the IPA pathway analysis program.

6 SUMMARY, CONCLUSIONS AND FUTURE PERSPECTIVES

The safety assessment of potential drug candidates remains a challenge for the pharmaceutical industry. Hepatotoxicity is one of the major reasons why candidate drugs fail during preclinical or clinical trials. The liver is responsible for the metabolism of drugs and toxic compounds, thus it is the most vulnerable organ for drug-induced toxicity. Drug-induced hepatotoxicity can be intrinsic (dose-dependent) or idiosyncratic (low incidence and largely dose-independent). Preclinical *in vivo* testing of drug toxicity is accompanied by severe animal suffering and discomfort and is only partly predictive for human toxicity because of species differences. This emphasizes the need for the development of new screening methods that address the toxicological hazards early in the drug discovery process. Therefore, great effort is put in developing new screening methods in order to find novel and more accurate preclinical and clinical biomarkers. This will lead to a safer and more efficient drug discovery and development process. With the traditional biomarkers for liver injury, the differentiation between different classes of hepatotoxicity is difficult. Moreover there is a need for reliable *in vitro* toxicity screening tests, which improve the prediction, characterization and understanding of drug-induced hepatotoxicity. A prerequisite for a proper prediction is that the model used has adequate drug metabolizing capacity, as drug-related liver toxicity often results from toxic metabolites formed in the liver. In addition, such methods are developed to be applicable to human tissue in order to better predict liver toxicity in man by avoiding interspecies extrapolation. The Precision-Cut Liver Slice (PCLS) model has been shown to be adequate to study drug metabolism and toxicity [34]. This model can be positioned between *in vivo* experiments and the currently used cell culture models and can be regarded as an *ex vivo* model, with all the different cell types of the liver present in their natural architecture and with intact cell-cell and cell-matrix contacts. For toxicity studies this is of great importance because drug-induced toxicity is currently recognized as a multi-cellular process, where in addition to hepatocyte functions, also cell-cell interactions and non-parenchymal cell functions are considered to be important contributors to the toxicity process [31].

The application of transcriptomics enables investigating the changes in gene expression of the complete genome induced by drug exposure. Through the measurements of the global gene expression it is possible to identify phenotype specific hepatotoxic pathways and mechanisms. In addition, it is possible to select similar endpoints *in vivo* and *in vitro*, facilitating to perform *in vitro* to *in vivo* comparisons. Even if the endpoints are not similar they could be predictive if a good correlation between the *in vivo* and *in vitro* endpoints can be established. Thus, the application of transcriptomics facilitates the development and use of *ex vivo* or *in vitro* models for the prediction of hepatotoxic responses in humans. Also, a correct classification of the hepatotoxicants based on their hepatotoxic phenotype is instrumental for the safety assessment of drugs. Drug-induced liver injury may result in different toxicity phenotypes such as hepatic cholestasis, i.e. impairment of bile flow and increase in intracellular accumulation of bile salts, necrosis, i.e. a form of premature cell

death due to damage by for instance free radicals and/or toxic metabolites, or fibrosis, i.e. the accumulation of collagen..

The aim of this thesis was to obtain insight in the use of PCLS as *ex vivo* model in combination with transcriptomics for the identification and classification of hepatotoxic compounds, and in the elucidation of the mechanisms of the hepatotoxic effects of those compounds at the gene and pathway level. For this aim we analyzed gene expression profiles of PCLS exposed to compounds inducing fibrosis, necrosis, cholestasis and idiosyncratic liver injury.

Validation of rat PCLS as model to study fibrosis

In chapter 2, we aimed to further characterize PCLS as a suitable model to identify whether early changes in gene expression could give an indication of the phenotype of long-term toxicity induced by hepatotoxicants inducing necrosis or fibrosis. In this study, we performed the comparative analysis of the gene expression profiles of rat PCLS induced by paracetamol (APAP) and carbon tetrachloride (CCl_4), which are known to induce toxicity by different mechanisms, being necrosis and fibrosis respectively. The comparison was performed using gene expression patterns, regulated genes, and pathway and upstream regulator analysis of the regulated genes. Gene expression pattern analysis revealed characteristic changes in expression patterns due to exposure to a toxic concentration of each of the compounds compared to the corresponding control. Comparison of the regulated genes showed that there is considerable overlap among the genes regulated by both toxins but there is also a significant number of genes uniquely regulated due to either APAP or CCl_4. Some of those genes uniquely regulated due to CCl_4 treatment include genes related to fibrogenesis. Genes involved in the hepatic stellate cell activation and the onset of fibrogenesis such as CRYAB (alpha-B crystallin), KLF6 (Kruppel-Like Factor 6) and HSP47 (Heat shock protein 47) were upregulated indicating initiation of the fibrotic processes in CCl_4 treated slices, as was shown before [72, 74, 73, 115, 116, 85]. The growth factor TGF-β1 (Transforming growth factor beta 1) plays a key role in fibrosis via hepatic stellate cell activation [214]. From the TGF-β1 gene network resulting from the analysis of the regulated genes due to APAP or CCl_4 treatment, it can be seen that genes that are causally linked to TGF-β1 and have a clear role in fibrosis such as JUN (Jun Proto-Oncogene), LITAF (Lipopolysaccharide-induced tumor necrosis factor) and SERPINE1(Serpin Peptidase Inhibitor, Clade E, Member 1), were upregulated only in the case of exposure to CCl_4, but not to APAP. This observation indicates a substantial involvement of TGF-β1 in the toxicity process initiated by CCl_4 but not by APAP, and gives an indication that early fibrotic processes are activated within 16 h due to exposure to a toxic concentration of CCl_4. Upstream regulator analysis revealed several regulators that are known to control the expression of the regulated genes and that are known to be related to hepatic fibrosis. In conclusion, the early gene expression changes after short-term exposure to CCl_4 and APAP reflect the characteristic difference between these compounds in their ability to induce liver fibrosis after chronic dosing *in vivo*. This study indicates that transcriptomic analysis of PCLS can be used to identify the early events in PCLS that are indicative of a pathology (fibrosis) that develops after chronic injury. Further studies with more fibrotic and non-fibrotic compounds are needed to verify this finding and to identify a set of biomarkers that can be used in the future in drug- induced toxicity screening.

Validation of human PCLS to study drug-induced cholestatic injury (DICI)

In chapter 3, we aimed to validate human PCLS as an *ex vivo* model that reflects the drug-induced cholestasis processes using transcriptomic analysis. To date, human PCLS were not used for studies on cholestasis. Hepatotoxicants that are known to induce cholestasis in humans, such as cyclosporine, chlorpromazine, ethinyl estradiol and methyl testosterone were tested. In addition, ANIT (alpha-naphthyl isothiocyanate), a well-known cholestatic compound in rats, was included in the study. For many cholestatic drugs, the primary causative event involved in cholestasis is the inhibition of BSEP (Bile salt export pump) resulting in the intracellular accumulation of bile acids. It was hypothesized that incubation of PCLS in conventional culture medium would not be very sensitive to the toxic effects of these BSEP inhibition, as they would only be exposed to the newly synthesized bile acids. Therefore, a non-toxic bile acid mixture (60μM) was added to the incubation medium in order to create an environment similar to the physiological concentration in the portal vein of man *in vivo* [119]. Pilot experiments showed that indeed the bile acid concentration in the slices is maintained during incubation with bile acids whereas it is strongly decreased during incubation in conventional medium. Transcriptomic analysis revealed that cholestatic drugs clearly induced the regulation of genes and pathways associated with cholestasis in human PCLS when incubated in the presence of bile acids (60μM of bile acid mix). Also, the observed gene expression pattern of cholestatic injury was concentration dependent for all drugs. Hepatic cholestasis was among the top 5 regulated pathways. The majority of the pathways regulated in the human PCLS are represented in the Adverse Outcome Pathway (AOP) for cholestasis as proposed by Vinken et al., including the primary direct cellular responses and secondary adaptive responses involved in bile acid induced cholestatic injury [16, 17, 18], such as NRF2 (Nuclear factor (erythroid-derived 2)-like 2) mediated oxidative stress response, inflammation mediated hepatic fibrosis, endoplasmic reticulum stress, and activation of the coagulation and complement system. It is well known that adaptive responses to intracellular bile acid accumulation are mediated via FXR (Farnesoid X receptor), LXR (Liver X receptor), PXR (Pregnane X receptor), and VDR (Vitamin D receptor) nuclear receptors. As expected, in the PCLS exposed to the cholestatic drugs, signaling pathways such as FXR, LXR, PXR and VDR as well as the related cholesterol biosynthesis pathways were affected. Activation of nuclear receptors such as FXR, LXR, PXR and VDR, triggers cellular adaption to counteract bile acid accumulation and thus cholestatic liver injury [19]. In contrast with the expected activation of FXR as indicated in the AOP, the target genes in the FXR pathway were downregulated in the human PCLS including genes known to play a role in cholestasis such as MDR3 (Multiple Drug Resistance 3), BSEP (ABCB11) and SHP (Small Heterodimer Partner). Downregulation of BSEP may indicate a direct effect of the tested cholestatic drugs, as potent BSEP inhibitors have been shown to downregulate BSEP expression in primary human hepatocytes [128]. Moreover the decreased expression of FXR can at least partly explain this reduced FXR signalling. This is in line with the finding that both FXR and SHP expression was reduced by 90% or more in cholestatic patients [15]. Thus, based on our findings it can be postulated that exposure to cholestatic compounds could lead to compromised FXR mediated adaptive responses, causing cholestatic injury. Also, downregulation of genes involved in cholesterol transport such as ABCG5 and ABCG8 indicate a loss of the protective action of LXR. In addition, also several genes in the PXR and VDR pathways were mostly downregulated. Together, the reduced activation of FXR,

LXR, PXR and VDR could be responsible for reduced adaptive responses to the effects of the cholestatic drugs and lead to development of cholestatic injury.

Compromised adaptive responses could lead to deleterious cellular effects via toxicity processes such as oxidative stress and endoplasmic reticulum (ER) stress. Oxidative stress is implicated to play a role in the pathogenesis of drug-induced cholestasis as a result of bile acid accumulation. We observed the activation of NRF2 mediated oxidative stress response in the human PCLS treated with cholestatic drugs. This indicates that detoxifying mechanisms are activated in the PCLS to alleviate the oxidative stress probably due to accumulating bile acids. Whether indeed the bile acids accumulate in the slices after exposure to a cholestatic drug remains to be established and is currently under investigation in our lab.

A recent study showed that ER stress is involved in the bile acid induced hepatocellular injury [124]. In line with this, we also observed that ER stress, unfolded protein response (UPR) and protein ubiquitination pathways were among the most affected pathways. The UPR signaling pathway is activated in response to ER stress and promotes cell survival and adaptation. There is increasing evidence for the involvement of ER stress in cholestasis [215, 176, 177, 149, 124]. Our results suggest that ER stress, protein ubiquitination and UPR may be early cellular effects in drug-induced cholestasis. Further studies will be necessary to elucidate the exact role of these processes in bile acid mediated cholestasis.

Hepatic fibrosis and hepatic stellate cell activation was also observed in human PCLS due to exposure to the cholestatic drugs. Indeed, accumulation of bile acids by obstructive cholestasis [134], was shown to lead to an inflammatory response *in vivo* which in turn leads to activation of hepatic stellate cells and liver fibrosis.

The genes involved in cholesterol biosynthesis, the starting material for the synthesis of bile acids in the liver were downregulated in human PCLS indicating the adaptive response of hepatocytes to decrease cholesterol synthesis as a response to cholestatic drugs. Interestingly, this was also observed in mouse PCLS exposed to cholestatic drugs [112, 113].

We also compared our findings with gene expression data obtained from liver samples of patients with cholestasis due to biliary atresia and intrahepatic not drug-induced cholestasis [123]. Comparison of the affected pathways between human PCLS and the patient samples revealed that there was good overlap with respect to the processes involved in cholestasis, although more pathways were affected *in vivo*. For instance, tight junction signalling was affected in patient samples but not in human PCLS. An explanation for the observed differences between *in vivo* data and the *ex vivo* data could be due to the different causes of cholestasis or the large difference in time frame as the patient samples represent fully developed cholestatic disease in infants. Human PCLS should therefore preferably be validated by comparing with human liver tissue of patients suffering from drug-induced cholestasis, but to our knowledge such data has not been published to date.

In conclusion, the transcriptomic analysis of human PCLS exposed to cholestatic drugs in the presence of bile acids revealed that this model reflects the primary toxicity and adaptive processes associated with hepatic cholestasis. The results suggest that decreased adaptive responses mediated via nuclear receptors are associated with these cholestatic effects and lead to the subsequent toxicity processes such as oxidative stress, ER stress and UPR response. Our study demonstrates that human PCLS is a suitable model for future application in drug screening for cholestasis and to identify possible mechanisms of toxicity of cholestatic compounds, when incubated in the presence of a physiological concentration of bile acids. Further studies may reveal biomarkers for DICI. Insights gained from the pathway

analysis such as decreased activation of the FXR pathway, downregulation of cholesterol biosynthesis, increased ER stress response and NRF2 mediated oxidative stress response, could be included in the adverse outcome pathway of cholestasis.

Classification of cholestasis and necrosis inducing drugs

In chapter 4, we aimed to classify hepatotoxicants according to their known phenotype of toxicity, cholestasis or necrosis, based on the gene expression profiles after exposure of human precision-cut liver slices and to identify possible classifier or marker genes. In addition to the five cholestatic compounds studied in chapter 3, the human PCLS were exposed to five hepatotoxicants: acetaminophen, benziodarone, chloramphenicol, colchicine, and nitroso-diethylamine known to induce hepatic necrosis. In all these experiments the PCLS were exposed to the toxic compounds in the presence of the physiological bile acid mix. Machine learning analysis on gene expression data of PCLS exposed to these five cholestatic and five necrotic compounds resulted in four classification models based on two different algorithms namely SVM (Support vector machine) and RF (Random forest) and two different tested concentrations (low and medium), which were 70-80 % accurate in predicting the phenotype of the hepatotoxicants. Interestingly, chloramphenicol was consistently classified as cholestatic compound despite the fact that it is generally considered a direct acting necrotic compound. However, some studies indicated that chloramphenicol can also cause cholestasis [157]. In spite of the fact that the compounds were chosen based on their literature reported phenotype of liver toxic phenotype, it is well known that cholestasis often presents as mixed cholestatic and hepatocellular injury [141]. Further, recent evidence suggests that inflammatory cell-mediated necrosis might also accompany cholestasis. Steiner *et al.,* reported that this overlap of mechanisms involved in the toxicity of necrotic and cholestatic compounds further complicates the classification of hepatotoxicants into the correct phenotype of toxicity [150]. However, despite the complexity owing to overlap of mechanisms in toxicity for the classification of necrosis and cholestasis, the developed classification models were able to classify the hepatotixicants with relatively good accuracy. The low concentration gene expression profiles gave better prediction accuracy than the medium concentration, which can probably be due to the accompanying necrosis at higher concentrations of the cholestatic compounds. In conclusion, although all four models gave a reasonably comparable overall performance in compound class prediction accuracy, the SVM low concentration model shows the highest prediction accuracy in correctly classifying all 5 cholestatic compounds and the classifier genes identified by this model are consistent across concentrations and not too sensitive for inter-individual variation, which supports the reliability of this model in future settings. Further analysis of the function of the classifier genes identified by the SVM low model showed that they are involved in ER stress, oxidative stress and unfolded protein response (UPR), and lipid and cholesterol metabolism including a Sodium/Bile Acid Cotransporter, which is well in line with the findings of chapter 3. Classifier genes identified in our human PCLS model were compared with cholestasis-specific classifier genes reported in different rat *in vivo* studies [150, 147, 52, 29, 30]. No overlap was observed among the classifiers genes between rat *in vivo* and human *ex vivo.* This lack of concordance could be partly due to species differences and underlines the importance of the human cells or tissues to identify human specific biomarkers. It should also be mentioned that there was also little or no overlap among the classifier genes found for

the cholestasis phenotype between different rat *in vivo* studies [150, 147, 52, 29, 30]. The lack of concordance in these studies further questions the applicability of the identified markers and could be partly due to overfitting of the data.

In conclusion, gene expression profiling after *ex vivo* exposure of precision-cut human liver slices to hepatotoxicants known to induce either cholestasis or necrosis resulted in a classification model that showed good accuracy in distinguishing cholestasis from necrosis. Despite the limitation of the low number of compounds studied at a single time point (24 h), the developed models were able to classify the hepatotoxicants based on their phenotype or mechanism of toxicity with a good accuracy and the identified classifier genes are associated with the phenotype of toxicity. The identified classifiers were mechanistically involved in endoplasmic reticulum stress, unfolded protein response and other stress response pathways, phenomena shown to play a role in cholestasis (chapter 3). They appeared consistent across different concentration levels, different predictive algorithms and inter-individual variation in response. Hence, the human PCLS model is a useful model to study the mechanisms of drug-induced toxicity and to classify toxins based on their mechanism of toxicity and to identify and validate classifiers responsible for drug-induced liver toxicity in humans. A limitation of our study is the low sample size and further validation of the identified classifiers by incorporating additional compounds will be necessary.

Human PCLS to study mechanisms involved in drug induced in idiosyncratic toxicity

In chapter 5, we applied transcriptomic analysis to understand the possible mechanisms or pathways that might be involved in idiosyncratic drug induced liver injury (IDILI). Several hypotheses have been tested in animal or human models to study IDILI and associated mechanisms. Among the hypothesis tested the inflammatory stress hypothesis is of particular interest due to its inter-relation to other hypothesis such as mitochondrial stress hypothesis [26] as it was reported that inflammatory mediators induced during inflammation could induce mitochondrial dysfunction [216, 217, 218]. Recently, Hadi *et al.* were the first to study the inflammatory stress hypothesis in human and mouse precision-cut liver slices *ex vivo* [195] and found that co-incubation of LPS (Lipopolysaccharide) with several IDILI drugs, among which clozapine, resulted in synergistic toxicity. To further understand the possible mechanisms involved in clozapine induced IDLI, we compared the gene expression profiles of clozapine with its non-IDILI analogue olanzapine in the presence and absence of LPS. Pathway analysis using immune-mediated and cellular stress response signalling pathways to compare the effects in the different treatment groups revealed the enhanced activation of toll-like receptor signalling, HMGB1 (High-mobility group box 1) signalling, iNOS (Inducible nitric oxide synthase) signalling, p38-MAPK (Mitogen-activated protein kinase) and NRF2 oxidative stress response in LPS+clozapine. Several inflammatory mediators involved in the different inflammatory signalling pathways such as IL1A (Interleukin-1 alpha), IL1B (Interleukin-1 beta), ICAM1 (Intercellular adhesion molecule 1), GM-CSF (Granulocyte-macrophage colony-stimulating factor), MAPKAPK-2 (MAPK-activated protein kinase 2) and PAI-1 (Plasminogen activator inhibitor-1) were significantly regulated with enhanced expression in LPS+clozapine co-treated human PCLS compared to the human PCLS exposed to LPS or clozapine alone, or to LPS+olanzapine. This enhanced production of inflammatory mediators might contribute to the liver injury represented by necrotic areas in LPS+clozapine-treated human PCLS. Also, the enhanced

expression of NFkB, iNOS, AP-1 and IFN , leading to enhanced activation of iNOS in LPS+clozapine, might contribute to the IDILI by enhanced production of reactive nitrogen species causing mitochondrial damage [212]. Drugs that are more often associated with IDILI are shown to cause strong activation of NRF2 mediated stress response [197]. In our results, clozapine showed activation of NRF2 stress response but not LPS or olanzapine and the clozapine-induced NRF2 response was further enhanced in the presence of an inflammatory stress condition (LPS). There is also increasing evidence that numerous drugs associated with idiosyncratic drug reactions cause mitochondrial dysfunction [182, 184]. In accordance, pathway analysis of the 719 genes uniquely regulated due to LPS+clozapine treatment also revealed that oxidative phosphorylation was the predominantly affected pathway and many genes involved in complex I-V of the electron transport chain were downregulated. This further strengthens the role of the mitochondrial damage in inflammation-associated IDILI. In addition, hepatic gene expression analysis suggested the activation of HMGB1, p38 MAPK, NFkB signalling pathways to be possibly involved in the LPS+clozapine induced IDILI.

In conclusion, the human PCLS seems to be a promising *ex vivo* model for characterizing IDILI and toxic mechanisms associated with it. Inflammatory-associated mitochondrial dysfunction was identified as a potential mechanism of inflammation-associated IDILI. Further research including more IDILI-related drugs together with their non-IDILI-related comparator drugs would be necessary to confirm the findings.

Limitations and future perspectives

In the studies described in this thesis, the precision-cut liver slice model is validated as a model to study compound or drug induced toxicity mechanisms. Moreover, the transcriptomic analysis revealed that the PCLS can serve as a useful model to identify intrinsic drug induced toxicity phenotypes such as necrosis, cholestasis, and fibrosis as well as IDILI.

One of the main limitations in these studies is that a limited number of compounds were studied, in a limited number of human liver samples, mainly due to practical reasons such as limited availability of human tissue, and the costs for the microarray measurements. Further studies with an additional set of compounds are necessary to confirm the findings reported in this thesis. The limited availability of human donors for human liver slices in turn limits the use of PCLS for toxicogenomics research. However, the results of our studies confirm that even with 5 different liver samples a fairly good characterization of hepatotoxicity can be obtained. Although the human livers show quite some variation in basic gene expression, the changes in gene expression due to exposure to a toxic compound are rather consistent, thus showing the feasibility of this type of experiments with a limited number of human samples.

Gene expression microarrays only measure the response at the mRNA transcription level of a gene, which only gives a rather rough estimate of its corresponding changes in protein expression level and the subsequent metabolic changes. Proteomics studies, aiming to characterize the expression of all proteins in a cell, tissue or organism are needed to understand the functional relevance of proteins regulated due to a toxic insult. In addition, metabolomics studies, aiming to characterize the global metabolite profiles in a system (cell, tissue or organism) under a given set of conditions, may elucidate the effects of the induced changes in protein expression. The liver is responsible for the production and secretion of

a large variety of plasma proteins and endogenous molecules and is also a major target for drug-induced toxicity. Hence, secreted protein or metabolite profiles can also reveal relevant toxicity signatures. To obtain a broader insight about the drug induced liver injury and to discover clinically significant biomarkers, comparison of data from transcriptomics, proteomics and metabolomics experiments would be necessary.

Further gene expression studies using RNA-Seq (RNA sequencing) can be considered for the better prediction of biomarkers for DILI. RNA-Seq can look at different populations of RNA, which include total RNA, small RNA, such as microRNA, transferRNA, and ribosomal profiling, in addition to mRNA transcripts. MicroRNAs (miRNA) are non-coding RNAs that play key roles in the post-transcriptional regulation of gene expression and participate in physiological and pathological regulatory processes, including liver diseases. Changes in the expression levels of specific miRNAs have been reported in different liver diseases, indicating their potential use as biomarkers for DILI [219, 220, 221]. Other advantages of RNA-Seq compared to microarrays include high sensitivity; discovery of novel genes; ability to quantify a large dynamic range of expression levels allowing the identification of more differentially expressed genes with higher fold changes [222].

So far, toxicogenomics studies using PCLS model were scarcely reported in the literature. The presence of all the different liver cell types in the PCLS model allows for studying the interaction between different cells in response to a toxic insult but at the same can also contributes to an extra level of complexity in the study. Gene expression is invariably heterogeneous between different cell types, and it is sometimes difficult to attribute the observed changes in gene expression to any of the different cell types. Single cell transcriptome studies using for instance Laser Scanning Dissection Microscopy, would provide information about the response of each of the different cell types and identify the most responsive cell types in the PCLS [223]. The limited lifetime of the PCLS model was also considered as one of the main disadvantage and limited their extensive use in the toxicology research in comparison to other *in vitro* models. However, recently, significant improvements in the incubation medium were reported which facilitate the extension of the viability of the PCLS up to 5 days [224]. So with the increased viability up to five days, it seems that sub-chronic toxicity studies can be performed in the near future.

The results of the studies described in this thesis show the ability of human PCLS to properly reflect drug-induced liver injury as observed in the clinic and to identify human specific toxicity markers using toxicogenomics analysis. The use of human tissue will not only greatly contribute to the replacement, reduction and refinement (3R's) of animals for scientific purposes, but also enables a better risk assessment by avoiding interspecies extrapolation.

SAMENVATTING, CONCLUSIES EN TOEKOMSTPERSPECTIEVEN

De veiligheidsbeoordeling van potentiële kandidaat-geneesmiddelen is een uitdaging voor de farmaceutische industrie. Hepatotoxiciteit is een van de belangrijke redenen waarom kandidaatgeneesmiddelen falen in preklinische en klinische testen. De blootstelling van de lever is hoog en de lever is grotendeels verantwoordelijk voor het metabolisme van geneesmiddelen wat tot toxische verbindingen kan leiden, en daardoor is de lever het meest kwetsbare orgaan voor geneesmiddel-geïnduceerde toxiciteit. Geneesmiddel-geïnduceerde hepatotoxiciteit kan intrinsiek (dosis-afhankelijk) of idiosyncratisch (lage incidentie en grotendeels dosis-onafhankelijk) zijn. Preklinische in vivo testen van geneesmiddeltoxiciteit gaan gepaard met ernstig dierenleed en ongemak, en zijn slechts gedeeltelijk voorspellend voor humane toxiciteit als gevolg van verschillen tussen mens en dier. Dit benadrukt de noodzaak van de ontwikkeling van nieuwe screeningsmethoden die het toxicologische risico in begin van het geneesmiddel ontdekkingsproces beter in kaart kunnen brengen. Daarnaast wordt veel energie gestoken in het ontwikkelen van nieuwe en accurate preklinische en klinische biomarkers. Dit zal leiden tot een veiliger en efficiënter geneesmiddelontdekking en ontwikkelingsproces. Met de traditionele biomarkers voor leverbeschadiging is het onderscheid tussen verschillende klassen van hepatotoxiciteit moeilijk te maken. Bovendien is er behoefte aan betrouwbare in vitro toxiciteitstesten, waarbij de voorspelling, de karakterisering en het begrip van het mechanisme van geneesmiddel-geïnduceerde hepatotoxiciteit verbeteren. Een voorwaarde voor een goede voorspelling is dat het gebruikte model een goede geneesmiddelmetaboliserende capaciteit heeft, omdat geneesmiddelgerelateerde levertoxiciteit vaak het gevolg is van toxische metabolieten gevormd in de lever. Bovendien is het van belang om dergelijke methoden te ontwikkelen voor toepassing op humaan weefsel om levertoxiciteit in mensen beter te voorspellen door het vermijden van interspecies extrapolatie. Van het Precision-Cut Liver Slices (PCLS) model is aangetoond dat het in staat is om metabolisme en toxiciteit van geneesmiddelen in de lever goed te representeren [69]. Dit model kan worden geplaatst tussen de in vivo experimenten en de momenteel gebruikte celkweek modellen, en kan worden beschouwd als een ex vivo model met al de verschillende celtypen van de lever aanwezig in hun natuurlijke architectuur en met intacte cel-cel en cel-matrix contacten. Voor toxiciteitstudies is dit van groot belang, omdat geneesmiddel-geïnduceerde toxiciteit wordt gezien als een multi-cellulair proces, waar naast hepatocyt-functies ook cel-cel interacties en niet-parenchymale celfuncties worden beschouwd als belangrijke factoren in het toxiciteits proces [31].

De toepassing van transcriptomics maakt het onderzoeken van de veranderingen in genexpressie van het volledige genoom, geïnduceerd door blootstelling aan geneesmiddelen, mogelijk. Door het meten van de globale genexpressie is het mogelijk om hepatotoxische pathways en mechanismen van een specifiek fenotype van toxiciteit te identificeren. Bovendien is het mogelijk om soortgelijke eindpunten te selecteren in vivo en in vitro/ex vivo wat het vergelijken van in vitro/ex vivo en in vivo studies mogelijk maakt. Zelfs als de eindpunten niet hetzelfde zijn, kunnen de gevonden in vitro/ex vivo

eindpunten voorspellend zijn, mits een goede correlatie tussen in vivo en in vitro/ex vivo eindpunten kan worden vastgesteld. De toepassing van transcriptomics kan dus bijdragen aan de ontwikkeling en het gebruik van ex vivo of in vitro modellen voor het voorspellen van hepatotoxische reacties bij mensen. Ook is een juiste classificatie van de hapatotoxische stoffen op basis van hun hepatotoxische fenotype een randvoorwaarde voor de veiligheidsbeoordeling van geneesmiddelen. Geneesmiddelgeïnduceerde leverschade kan resulteren in verschillende toxische fenotypen, zoals hepatische cholestase (verminderde galstroom en een toename van intracellulaire ophoping van galzouten), necrose (een vorm van vroegtijdige celdood als gevolg van schade door bijvoorbeeld vrije radicalen en/of tosiche metabolieten), of fibrose (de ophoping van collageen).

Het doel van dit proefschrift was om inzicht te krijgen in het gebruik van PCLS als ex vivo model in combinatie met transcriptomics voor de identificatie en classificatie van hepatotoxische verbindingen, en in de opheldering van de mechanismen van de hepatotoxische effecten van die verbindingen op gen- en pathwayniveau. Voor dit doel onderzochten we de genexpressie profielen van PCLS die waren blootgesteld aan verbindingen die fibrose, necrose, cholestase en idiosyncratische leverschade induceren.

VALIDATIE VAN PCLS RAT ALS MODEL OM FIBROSE TE BESTUDEREN

In hoofdstuk 2 was het doel om PCLS verder te karakteriseren als een geschikt model om te bepalen of vroege veranderingen in genexpressie een indicatie kunnen geven van het fenotype van toxiciteit op lange termijn dat wordt veroorzaakt door levertoxische stoffen die necrose of fibrose induceren. In deze studie is een vergelijkende analyse uitgevoerd van de genexpressieprofielen van rat PCLS geïnduceerd door paracetamol (APAP) en koolstoftetrachloride (CCl_4), waarvan bekend is dat deze leverschade induceren via verschillende mechanismen, respectievelijk necrose en fibrose. De vergelijking werd uitgevoerd met behulp van genexpressiepatronen, gereguleerde genen, en pathway en upstream regulator analyse van de gereguleerde genen. Analyse van de genexpressiepatronen onthulde kenmerkende veranderingen in de expressiepatronen als gevolg van blootstelling aan een toxische concentratie van elk van de verbindingen vergeleken met de overeenkomstige controle. Vergelijking van de gereguleerde genen toonde aan dat er een aanzienlijke overlap is tussen de genen die gereguleerd worden door beide toxinen, maar er is ook een significant aantal genen dat uniek wordt gereguleerd door ofwel APAP of CCl_4. Van sommige van die genen die alleen gereguleerd worden door CCl_4 behandeling is bekend dat ze zijn betrokken bij fibrogenese. Genen betrokken bij de activatie van stellaatcellen en van fibrogenese zoals CRYAB (alfa-B crystalline), KLF6 (Krüppel-Like Factor 6) en HSP47 (heat shock protein 47) werden opgereguleerd, wat aangeeft dat fibrotische processen in de met CCl_4 behandelde slices worden geïnitieerd, zoals eerder ook met andere methoden werd aangetoond [72, 73]. De groeifactor TGF-β1 (Transforming growth factor beta 1) speelt een sleutelrol in fibrose via activatie van de stellaatcellen [214]. Uit het genetische netwerk van TGF-β1, dat volgde uit de analyse van de gereguleerde genen door APAP of CCl_4 behandeling, kan men zien dat de genen die causaal zijn verbonden met TGF-β1 en een duidelijke rol hebben in fibrose, zoals JUN (Jun Proto-Oncogene), LITAF (lipopolysaccharide geïnduceerde tumor necrosis factor) en

SERPINE1 (Serpin Peptidase Inhibitor, Clade E, lid 1), alleen werden opgereguleerd na blootstelling aan CCl_4, maar niet door APAP. Deze waarneming duidt op een aanzienlijke betrokkenheid van TGF-β1 in het toxiciteitsproces, geïnitieerd door CCl_4 en niet door APAP, en geeft een indicatie dat vroege fibrotische processen binnen 16 uur na blootstelling aan een toxische concentratie van CCl_4 worden geactiveerd. Bovendien bleek uit upstream regulator analyse van de CCl_4-behandelde PCLS, dat verschillende regulatoren waarvan bekend is dat deze de expressie van de gereguleerde genen controleren, gerelateerd zijn aan leverfibrose. Kortom, de vroege genexpressie veranderingen na kortdurende blootstelling aan CCl_4 en APAP ex vivo weerspiegelen het karakteristieke verschil tussen deze verbindingen in hun vermogen om leverfibrose te induceren na chronische dosering in vivo. Deze studie geeft aan dat transcriptoom analyse van PCLS kan worden gebruikt om de vroege gebeurtenissen in PCLS, die indicatief zijn voor een pathologie (fibrose) die ontwikkelt na chronisch letsel, te identificeren. Verdere studies, met meer fibrotische en niet- fibrotische verbindingen zijn nodig om deze bevinding te verifiëren en een reeks biomarkers te identificeren die in de toekomst kunnen worden gebruikt in de screening van nieuwe geneesmiddelen voor geneesmiddel geïnduceerde toxiciteit.

VALIDATIE VAN HUMANE PCLS OM GENEESMIDDEL-GEÏNDUCEERDE CHOLESTATISCHE (DICI) SCHADE TE BESTUREN

In hoofdstuk 3 was het doel om humane PCLS te valideren als een ex vivo model dat de geneesmiddel-geïnduceerde cholestase processen weerspiegelt met behulp van transcriptoom analyse. Tot op heden werden humane PCLS niet gebruikt voor onderzoek naar cholestase. Hepatotoxische stoffen waarvan bekend is dat deze cholestase induceren bij mensen, zoals cyclosporine, chloropromazine, ethinylestradiol en methyltestosteron zijn getest in humane PCLS. Bovendien werd ANIT (a-naftyl-isothiocyanaat), een bekende cholestatische verbinding bij ratten, opgenomen in de studie. Voor veel cholestatische geneesmiddelen is de remming van BSEP (galzuuruitscheidingspomp) de primaire oorzakelijke gebeurtenis leidend tot cholestasis, wat resulteert in de intracellulaire ophoping van galzuren. De hypothese was dat incubatie van PCLS in het gebruikelijke cultuurmedium niet erg gevoelig zou zijn voor de toxische effecten van deze BSEP remming, omdat ze nietworden blootgesteld aan externe galzuren maar alleen aan nieuw gesynthetiseerde galzuren. Daarom werd een niet-toxisch galzuur mengsel (60 μM) aan het incubatiemedium toegevoegd om een omgeving te creëen die vergelijkbaar is met de fysiologische concentratie in de poortader van de mens in vivo [119]. Pilot experimenten toonden aan dat de galzuurconcentratie in de slices inderdaad nagenoeg gelijk blijft tijdens incubatie met galzuren, terwijl het sterk vermindert tijdens incubatie in het gebruikelijke medium zonder galzouten. Transcriptoom analyse in humane PCLS toonde aan dat cholestatische geneesmiddelen duidelijk de regulering van genen en pathways veroorzaken die geassocieerd zijn met cholestase bij incubatie in aanwezigheid van galzuren. Daarnaast was het waargenomen genexpressie patroon van cholestatische schade concentratieafhankelijk voor alle geneesmiddelen. Lever-cholestase was een van de top 5 gereguleerde pathways. De meeste van de pathways gereguleerd in de humane PCLS komen voor in de Adverse Outcome Pathway (AOP) voor cholestase zoals voorgesteld door

Vinken et al., inclusief de primaire directe cellulaire reacties en secundaire adaptieve reacties betrokken bij galzuur-geïnduceerde cholestatische schade [16], zoals NRF2 (Nucleaire factor (erythroide-afgeleide 2)-like 2) gemedieerde oxidatieve stressrespons, ontsteking gemedieerde hepatische fibrose, endoplasmatisch reticulum stress en activering van de stolling en het complementsysteem. Het is welbekend dat adaptieve reacties op intracellulaire galzuur ophoping worden gemedieerd via de nucleaire receptoren FXR (farnesoid X receptor), LXR (lever X-receptor), PXR (pregnaan X receptor) en VDR (vitamine D receptor). Zoals verwacht, waren deze signaleringsroutes en de bijbehorende cholesterol biosynthese pathways aangetast in PCLS blootgesteld aan cholestatische geneesmiddelen. Activering van deze nucleaire receptoren activeert cellulaire aanpassing om galzuur ophoping, en dus cholestatische leverschade, tegen te gaan [142, 19]. In tegenstelling tot de verwachte activatie van FXR zoals in de AOP werd aangegeven, waren de doelgenen van de FXR pathway verlaagd in humane PCLS, waaronder genen waarvan bekend is dat deze een rol spelen in cholestase zoals MDR3 (Multiple Drug Resistance 3), BSEP (ABCB11) en SHP (Small Heterodimeer Partner). Afname van BSEP expressie zou een direct effect kunnen zijn van de geteste cholestatische stoffen, immers van potente BSEP remmers is gebleken dat zij de BSEP expressie in primaire humane hepatocyten verminderen [128]. Bovendien kan de gevonden verminderde expressie van FXR tenminste gedeeltelijk de verminderde FXR signalering verklaren. Dit is in overeenstemming met de bevinding dat zowel FXR als SHP expressie werd gereduceerd met 90% of meer in cholestatische patiënten [15]. Daarom, gebaseerd op onze bevindingen kan worden gesteld dat blootstelling aan cholestatische verbindingen kan leiden tot een verminderde FXR gemedieerde adaptieve responsen, waardoor cholestatische schade ontstaat. Daarnaast lijken downregulatie van genen betrokken bij cholesteroltransport zoals ABCG5 en ABCG8 een verlies van de beschermende werking van LXR te geven. Verder waren verschillende genen in de PXR en VDR pathways meestal gereduceerd. Tezamen zouden de verlaagde activatie van FXR, LXR, PXR en VDR verantwoordelijk kunnen zijn voor een beperkte adaptieve respons op de effecten van de cholestatische stoffen en leiden tot de ontwikkeling van cholestatisch letsel.

Gecompromitteerde adaptieve reacties kunnen leiden tot schadelijke cellulaire effecten via toxiciteitsprocessen zoals oxidatieve stress en endoplasmatisch reticulum (ER) stress. Van oxidatieve stress is bekend dat het een rol speelt in de pathogenese van geneesmiddel-geïnduceerde cholestase als gevolg van galzuurophoping. We zagen ook de activering van een NRF2 gemedieerde oxidatieve stress respons in de humane PCLS behandeld met cholestatische geneesmiddelen. Dit geeft aan dat ontgiftende mechanismen worden geactiveerd in de PCLS om de oxidatieve stress, wellicht als gevolg van accumulatie van galzuren, te verlichten. Of de galzuren inderdaad ophopen in de slices na blootstelling aan een cholestatisch geneesmiddel zal nog moeten worden vastgesteld en wordt momenteel onderzocht in ons laboratorium.

Een recente studie toonde aan dat ER stress betrokken is bij galzuur-geïnduceerde hepatocellulaire schade [124]. In overenkomst hiermee, zagen we ook dat ER stress, unfolded protein respons (UPR) en eiwit ubiquitinatie pathways een van de zwaarst getroffen pathways waren. De UPR signaleringsroute wordt geactiveerd in een reactie op ER stress en bevordert de overleving en de adaptatie van de cel. Er is steeds meer bewijs voor de betrokkenheid van ER stress in cholestase [215, 149, 124]. Onze resultaten suggereren dat ER stress, eiwit ubiquitinilering en UPR vroege cellulaire effecten van

geneesmiddel-geïnduceerde cholestase kunnen zijn. Verdere studies zijn nodig om de precieze rol van die processen in galzuur-gemedieerde cholestase op te helderen.

Leverfibrose en stellaatcel activering werd ook waargenomen in humane PCLS als gevolg van blootstelling aan cholestatische geneesmiddelen. Inderdaad, accumulatie van galzuren door obstructieve cholestase [134] bleek te leiden tot een ontstekingsreactie in vivo wat vervolgens leidt tot activatie van hepatische stellaatcellen en leverfibrose.

De genen betrokken bij cholesterol biosynthese, het uitgangsmateriaal voor de synthese van galzuren in de lever, kwamen verminderd tot expressie in humane PCLS, hetgeen duidt op een adaptieve respons van hepatocyten door de cholesterolsynthese te laten dalen als reactie op cholestatische drugs. Interessant genoeg werd dit ook waargenomen in muizen PCLS die werden blootgesteld aan cholestatische drugs [113].

We hebben onze bevindingen eveneens vergeleken met genexpressie data verkregen uit de lever monsters van patiënten met cholestase als gevolg van galgangatresie en intrahepatische, niet door geneesmiddelen-geïnduceerde cholestase [123]. Na vergelijking van de aangetaste pathways tussen humane PCLS en patiënt monsters bleek dat er een goede overlap was in de veranderingen in de cholestase gerelateerde genen, hoewel in vivo meer pathways werden beïnvloed. Zo bleek de tight junction signalering beïnvloed in patiëntmonsters, maar niet in de humane PCLS. De waargenomen verschillen tussen in vivo en ex vivo gegevens kunnen zijn veroorzaakt door de verschillende oorzaken van cholestase of het grote verschil in tijdsduur van de ziekte, omdat het in de patiënt chronische cholestatische aandoeningen betreft en de PCLS slechts 24 uur werden blootgesteld aan cholestatische stoffen. Humane PCLS moeten bij voorkeur worden gevalideerd door het vergelijken met humaan leverweefsel van patiënten die lijden aan geneesmiddel-geïnduceerde cholestase, maar voor zover ons bekend zijn zulke gegevens tot nu toe nog niet in de literatuur verschenen. De waarnemingen in onze studie komen wel overeen met de verwachte genexpressiepatronen bij cholestase.

Tot slot, de transcriptoom analyse van humane PCLS die zijn blootgesteld aan cholestatische geneesmiddelen in aanwezigheid van galzuren toonde aan dat dit model de primaire toxiciteit en adaptieve processen die geassocieerd zijn met levercholestase weerspiegelt. De resultaten suggereren dat de verminderde adaptieve responsen, gemedieerd via nucleaire receptoren, in verband staan met deze cholestatische effecten en leiden tot de daaropvolgende toxische processen zoals oxidatieve stress, ER stress en UPR respons. Onze studie toont aan dat de humane PCLS geïncubeerd in aanwezigheid van een fysiologische concentratie van galzuren, een geschikt model is voor toekomstige toepassing in screening van geneesmiddelen op mogelijke cholestatische bijwerkingen en voor identificatie van mogelijke mechanismen van toxiciteit van cholestatische verbindingen. Verdere studies kunnen biomarkers onthullen voor geneesmiddel-geïnduceerde cholestase. Inzichten verkregen uit de pathway analyse, zoals verminderde activering van de FXR pathway, verminderde regulatie van de cholesterol biosynthese, verhoogde ER stressreactie en NRF2 gemedieerde oxidatieve stress respons, kunnen worden opgenomen in de adverse outcome pathway van cholestase.

CLASSIFICATIE VAN CHOLESTASE EN NECROSE INDUCERENDE GENEESMIDDELEN

In hoofdstuk 4 waren we gericht op het classificeren van hepatotoxicants naar hun bekende toxische fenotype (cholestase of necrose) op basis van de genexpressieprofielen na blootstelling van humane PCLS en op de identificatie van mogelijke classificatie of markergenen. Naast de vijf cholestatische verbindingen die werden onderzocht in hoofdstuk 3, werden de humane PCLS blootgesteld aan vijf hepatotoxicants: paracetamol, benziodarone, chlooramfenicol, colchicine en nitroso-diethylamine waarvan bekend is dat deze hepatische necrose veroorzaken. In al deze experimenten werden de PCLS blootgesteld aan de toxische verbindingen in aanwezigheid van de fysiologische galzuurmix. Machine learning analyse van de genexpressie gegevens van PCLS blootgesteld aan deze vijf cholestatische en vijf necrotische verbindingen resulteerde in vier classificatie modellen op basis van twee verschillende algoritmes, namelijk SVM (Support Vector Machine) en RF (Random Forest), en twee verschillende geteste concentraties (lage en middelhoge), die voor 70-80% nauwkeurig het fenotype van de door de hepatotoxische stoffen veroorzaakte schade voorspellen. Interessant genoeg werd chlooramfenicol steeds geklasseerd als cholestatische verbinding ondanks dat het algemeen wordt beschouwd als een direct werkende necrotische verbinding. Echter, sommige oudere studies hebben aangetoond dat chlooramfenicol ook kan leiden tot cholestase [41, 157]. Ondanks het feit dat de verbindingen werden gekozen op basis van hun in de literatuur gerapporteerde toxische lever fenotype is algemeen bekend dat cholestase zich vaak presenteert als een combinatie van cholestatische en hepatocellulaire schade [141]. Verder zijn er aanwijzingen dat inflammatoire necrose ook kan leiden tot cholestase [225]. Deze overlappende mechanismen betrokken bij de toxiciteit van necrotische en cholestatische verbindingen bemoeilijken de indeling van hepatotoxische stoffen op grond van het juiste fenotype van toxiciteit [150]. Echter, ondanks de complexiteit als gevolg van overlap van de mechanismen in de toxiciteit voor de classificatie van necrose en cholestase, waren de ontwikkelde classificatiemodellen in staat om de hepatotixische stoffen te classificeren als necrotisch of cholestatisch met een relatief goede nauwkeurigheid. De classificatie gebaseerd op genexpressieprofielen van PCLS werden blootgesteld aan een lage concentratie van de toxische stoffen bleek nauwkeuriger dan wanneer de PCLS waren blootgesteld aan een hogere concentratie, wat waarschijnlijk zou kunnen worden veroorzaakt door de bijkomende necrose bij hogere concentraties van de cholestatische verbindingen. Tenslotte, hoewel alle vier de modellen een redelijk vergelijkbare prestatie gaven wat betreft de nauwkeurigheid van de voorspelling van het fenotype van schade van de toxische verbindingen, gaf het zogenaamde SVM lage concentratie model de meest nauwkeurige voorspelling van de juiste classificatie van alle 5 cholestatische verbindingen, en de classificatiegenen geïdentificeerd door dit model werden consistent gevonden bij alle concentraties en bleken niet erg gevoelig voor inter-individuele variatie, wat de betrouwbaarheid van dit model voor toekomstig gebruik ondersteunt. Verdere analyse van de functie van de geïdentificeerde 4 classificatiegenen toonde aan dat ze betrokken zijn bij ER stress, oxidatieve stress en ongevouwen eiwit respons (UPR), en het lipide en cholesterol metabolisme (inclusief een natrium / galzuur cotransporter) wat in overeenstemming is met de bevindingen in hoofdstuk 3. Classificatiegenen, geïdentificeerd in ons humane PCLS model, werden vergeleken met cholestase-specifieke classificatiegenen die vermeld zijn in verschillende rat in vivo studies [150, 52, 30]. Onder de classificatiegenen werd geen overlap

waargenomen bij vergelijking van rat in vivo en humane ex vivo gevonden genen. Dit gebrek aan overeenkomst kan deels te wijten zijn aan verschillen tussen mens en rat en onderstreept het belang van humane cellen of weefsels om specifieke humane biomarkers te identificeren. Daarnaast moet worden vermeld dat er ook weinig of geen overlap gevonden werd onder de classificatiegenen die gevonden waren voor het cholestase fenotype tussen verschillende rat in vivo studies onderling [150, 52, 226]. Het is nog onduidelijk hoe dit ontbreken van overeenstemming in deze onderzoeken kan worden verklaard, maar het kan deels te wijten zijn aan het overfitten van de gegevens.

Tot slot, de genexpressie profilering na blootstelling van humane PCLS ex vivo aan hepatotoxische stoffen waarvan bekend is dat deze ofwel cholestase of necrose induceren, resulteerde in een classificatiemodel dat een goede nauwkeurigheid toonde in het onderscheiden van cholestase en necrose. Ondanks de beperking van het lage aantal onderzochte verbindingen op één tijdstip (24 uur), waren de ontwikkelde modellen in staat de hepatotoxische stoffen te classificeren op basis van hun fenotype of toxiciteitsmechanisme met een goede nauwkeurigheid en de geïdentificeerde classificatiegenen zijn geassocieerd met het toxische fenotype. De geïdentificeerde classificicatiegenen zijn mechanistisch betrokken bij endoplasmatisch reticulum stress, ongevouwen eiwit respons en andere stressreactie pathways, fenomenen waarvan is aangetoond dat deze een rol spelen bij cholestase (hoofdstuk 3). Ze bleken consistent bij verschillende concentraties, verschillende voorspellende algoritmen en bij de verschillende individuele levermonsters. Daarom is het humane PCLS model een nuttig model om de mechanismen van geneesmiddel-geïnduceerde toxiciteit te bestuderen, toxines op basis van hun mechanisme van toxiciteit te classificeren en de classificatiegenen verantwoordelijk voor geneesmiddel-geïnduceerde levertoxiciteit bij mensen te identificeren en te valideren. Een beperking van onze studie is de lage aantal stoffen en humane weefselmonsters, en verdere validatie van de geïdentificeerde classifiers door het opnemen van additionele verbindingen is nodig.

HUMANE PCLS OM DE MECHANISMEN TE BESTUDEREN DIE BETROKKEN ZIJN BIJ GENEESMIDDEL-GEÏNDUCEERDE IDIOSYNCRATISCHE TOXICITEIT

In hoofdstuk 5, hebben we transcriptoom analyse toegepast om de mogelijke mechanismen of pathways te ontdekken die betrokken zouden kunnen zijn in idiosyncratische geneesmiddel-geinduceerde levertoxiciteit (IDILI). Verschillende hypotheses zijn recent getest in dierlijke of humane modellen om IDILI en bijbehorende mechanismen te onderzoeken. Onder de geteste hypothesen is de inflammatoire stress hypothese, die onder mer gerelateerd is aande mitochondriale stress hypothese [198]. Zo werd gemeld dat ontstekingsmediatoren die geïnduceerd worden tijdens ontstekingen mitochondriële dysfunctie kunnen induceren [216, 217, 218]. Recentelijk waren Hadi et al. de eersten die de inflammatoire stress hypothese in humane en muis PCLS ex vivo hebben bestudeerd [195], waarbij zij ontdekten dat co-incubatie van de LPS (lipopolysaccharide) met verscheidene IDILI geneesmiddelen, waaronder clozapine, resulteerde in synergistische toxiciteit. Om de mogelijke mechanismen betrokken bij clozapine-geïnduceerde IDILI beter te begrijpen, vergeleken we de genexpressie profielen van clozapine met de niet-IDILI analoog olanzapine, in de aanwezigheid en afwezigheid van LPS. Pathway-analyse met name van immuun

gemedieerde en signaaltransductie pathways van cellulaire stress respons toonde activatie aan van Toll-like receptor-signalering, HMGB1 (High-mobiliteit groep box 1) signalering, iNOS (Inducible nitric oxide synthase) signalering, p38-MAPK (Mitogen-activated protein kinase) en NRF2 oxidatieve stress respons in de LPS + clozapine groep. Verschillende inflammatoire mediatoren betrokken bij de verschillende inflammatoire signaalwegen zoals IL1A (interleukin-1 alfa), IL1B (interleukine-1 beta), ICAM1 (Intercellulaire adhesie molecuul 1), GM-CSF (granulocyt-macrofaag-koloniestimulerende factor), MAPKAPK-2 (MAPK-activated protein kinase 2) en PAI-1 (plasminogeen activator inhibitor-1) werden gereguleerd met significant verhoogde expressie in LPS + clozapine behandelde humane PCLS vergeleken met de humane PCLS blootgesteld aan LPS of clozapine alleen, of LPS + olanzapine. Deze verhoogde productie van ontstekingsmediatoren zou kunnen bijdragen aan de leverbeschadiging die voorkomt in necrotische gebieden in humane PCLS behandeld met LPS + clozapine. Ook zou de verhoogde expressie van NFkB, iNOS, AP-1 en IFNy, in LPS + clozapine, kunnen bijdragen aan IDILI door de verhoogde productie van reactief stikstofmono-oxide die mitochondriale schade kan veroorzaken [197]. Geneesmiddelen die vaker geassocieerd worden met IDILI blijken een sterke activatie van de NRF2 gemedieerde stressrespons te veroorzaken [197]. In onze studie veroorzaakte clozapine (maar niet LPS of olanzapine) activatie van de NRF2 stressrespons en de clozapine-geïnduceerde NRF2 reactie werd verder versterkt door de aanwezigheid van een inflammatoire stress toestand (LPS). Er is ook steeds meer bewijs dat een groot aantal geneesmiddelen, die in verband worden gebracht met idiosyncratische bijwerkingen, mitochondriële dysfunctie veroorzaakt [182, 184]. In overeenstemming hiermee, toonde pathway-analyse van de 719 genen die uniek gereguleerd zijn als gevolg van LPS + clozapine behandeling aan dat oxidatieve fosforylering de meest getroffen pathway was en veel genen betrokken bij complex IV van de elektron transport keten werden gereduceerd. Dit bevestigt de rol van de mitochondriële schade in ontstekingsgerelateerde IDILI. Daarnaast toonde de genexpressie analyse aan dat de activering van HMGB1, p38 MAPK, en NFkB signaalwegen eventueel betrokken is bij LPS+clozapine geïnduceerde IDILI.

Samenvattend, humane PCLS lijkt een veelbelovend ex vivo model voor het karakteriseren van IDILI en toxische mechanismen die daarbij betrokken zijn. Mitochondriële dysfunctie werd geïdentificeerd als een potentieel mechanisme van ontstekingsgerelateerde IDILI. Verder onderzoek met meer IDILI gerelateerde geneesmiddelen in vergelijking met hun niet-IDILI-gerelateerde analogen is nodig om de bevindingen te bevestigen.

BEPERKINGEN EN TOEKOMSTPERSPECTIEVEN

Met de in dit proefschrift beschreven studies is het PCLS model gevalideerd als een model om de effecten van mogelijke levertoxische stoffen en de mechanismen van geneesmiddel-geïnduceerde toxiciteit te bestuderen. Bovendien is uit de transcriptoom analyse gebleken dat de PCLS een nuttig model kan zijn voor het identificeren van intrinsieke geneesmiddel-geïnduceerde toxische fenotypen zoals necrose, cholestase en fibrose alsook IDILI.

Een van de belangrijkste beperkingen van deze studies is dat slechts een beperkt aantal verbindingen werd bestudeerd in een beperkt aantal humane levermonsters, voornamelijk vanwege praktische redenen zoals een beperkte beschikbaarheid van menselijk weefsel, de

beperkte beschikbare tijd en de hoge kosten voor microarray metingen. Verdere studies met een extra set van verbindingen zijn nodig om de bevindingen in dit proefschrift te bevestigen. De beperkte beschikbaarheid van menselijke donoren voor humane lever slices zou beperkend kunnen zijn voor het gebruik van PCLS voor onderzoek naar toxicogenomics. Maar de resultaten van onze studies bevestigen dat zelfs met 5 verschillende levermonsters een redelijk goede karakterisering van hepatotoxiciteit kan worden verkregen. Hoewel de humane levers behoorlijk wat variatie vertonen in basale genexpressie, zijn de veranderingen in genexpressie als gevolg van blootstelling aan een toxische verbinding vrij consistent, wat de mogelijkheden aangeeft van de haalbaarheid van dit type experimenten met een beperkt aantal humane monsters.

Microarrays meten alleen de respons op mRNA-transcriptieniveau van genen, wat alleen een nogal ruwe schatting geeft van de corresponderende veranderingen op eiwitexpressie-niveau en de daaropvolgende metabolische veranderingen. Proteomics onderzoek, gericht op het meten van de expressie van alle eiwitten in een cel, weefsel of organisme en vervolgens functionele studies van de gevonden eiwitten, is nodig om het functionele belang begrijpen van eiwitten die gereguleerd worden door een toxische insult. Daarnaast kunnen metabolomics studies, gericht op het karakteriseren van de globale metabolietprofielen in een systeem (cel, weefsel of organisme) onder een gegeven set van omstandigheden, de effecten van de geïnduceerde veranderingen in eiwitexpressie ophelderen. De lever is verantwoordelijk voor de productie en secretie van een grote verscheidenheid aan plasma-eiwitten en endogene moleculen en is ook een belangrijke target voor geneesmiddel-geïnduceerde toxiciteit. Daarom kunnen uitgescheiden eiwit- of metabolietprofielen ook relevante toxische kenmerken onthullen. Om een breder inzicht te verkrijgen in de geneesmiddel-geïnduceerde leverschade en klinisch significante biomarkers te ontdekken, is vergelijking van de uitkomsten van transcriptomics, proteomics en metabolomics experimenten nodig.

Verdere genexpressie studies met behulp van RNA-Seq (RNA sequencing) kunnen worden overwogen voor betere voorspelling van biomarkers voor DILI. RNA-Seq kan kijken naar verschillende RNA populaties, waaronder totaal RNA, klein RNA (zoals microRNA), transferRNA en ribosomale profilering, alsook naar mRNA transcripten. MicroRNA (miRNA) zijn niet-coderende RNA's die een belangrijke rol spelen in de post-transcriptionele regulatie van genexpressie en participeren in fysiologische en pathologische regulatie processen, waaronder leverziekten. Veranderingen in de expressie van specifieke miRNAs zijn gemeld bij verschillende leverziekten, wat een indicatie is voor hun potentieel gebruik als biomarkers voor DILI [227, 219, 221]. Andere voordelen van RNA-Seq vergeleken met microarrays zijn de hoge gevoeligheid, de ontdekking van nieuwe genen, en de capaciteit om een groot dynamisch bereik van expressieniveaus te kwantificeren [222].

Tot nu toe werden toxicogenomics studies die gebruik maken van het PCLS model nauwelijks vermeld in de literatuur. De aanwezigheid van alle verschillende leverceltypes in het PCLS model maakt het bestuderen van de interactie tussen verschillende cellen in reactie op een toxisch insult mogelijk, maar draagt tegelijk bij aan een extra niveau van complexiteit in de studie. Genexpressie is altijd heterogeen tussen verschillende celtypen, en het is soms moeilijk de waargenomen veranderingen in genexpressie toe te kennen aan elk van de verschillende celtypen. Single cel transcriptoom studies met gebruik van bijvoorbeeld Laser Scanning Microscopy Dissection, zou informatie kunnen verstrekken over de reactie van elk van de verschillende celtypen en de meest reagerende celtypen in de PCLS vaststellen

[223]. De beperkte levensduur van het PCLS model werd ook beschouwd als een van de belangrijkste nadelen en beperkte hun uitgebreide gebruik in toxicologisch onderzoek in vergelijking met andere in vitro modellen. Onlangs zijn echter aanzienlijke verbeteringen in het incubatiemedium gerapporteerd die de verlenging van de levensvatbaarheid van PCLS tot 5 dagen mogelijk maken [224]. Met de verhoogde levensvatbaarheid tot vijf dagen, lijkt het erop dat sub-chronische toxiciteitsstudies in de nabije toekomst kunnen worden uitgevoerd.

De resultaten van de in dit proefschrift beschreven studies tonen het vermogen van de humane PCLS om geneesmiddel-geïnduceerde leverschade zoals waargenomen in de kliniek weer te geven en humaan specifieke toxiciteitsmarkers te identificeren met behulp van toxicogenomics analyse. Het gebruik van humaan weefsel zal een belangrijke bijdrage leveren aan de vervanging, vermindering en verbetering (3R's) van dieren voor wetenschappelijke doeleinden, en kan daarnaast tot een betere risico-evaluatie leiden door het vermijden van de vertaling van resultaten van proefdieren naar de mens.

LIST OF FIGURES

LIST OF TABLES

BIBLIOGRAPHY

[1] H. FRIIS and P. B. ANDREASEN. Drug-induced hepatic injury: an analysis of 1100 cases reported to The Danish Committee on Adverse Drug Reactions between 1978 and 1987. *Journal of Internal Medicine*, 232(2):133–138, aug 1992. (Cited on page 1.)

[2] Catherine Sgro, François Clinard, Kader Ouazir, Henry Chanay, Christian Allard, Christian Guilleminet, Claude Lenoir, Alain Lemoine, and Patrick Hillon. Incidence of drug-induced hepatic injuries: a French population-based study. *Hepatology (Baltimore, Md.)*, 36(2):451–455, aug 2002. (Cited on page 1.)

[3] Naga Chalasani, Robert J. Fontana, Herbert L. Bonkovsky, Paul B. Watkins, Timothy Davern, Jose Serrano, Hongqiu Yang, and James Rochon. Causes, Clinical Features, and Outcomes From a Prospective Study of Drug-Induced Liver Injury in the United States. *Gastroenterology*, 135(6):1924–1934.e4, dec 2008. (Cited on page 1.)

[4] Lauren Bell and Naga Chalasani. Epidemiology of Idiosyncratic Drug-Induced Liver Injury. *Seminars in Liver Disease*, 29(04):337–347, nov 2009. (Cited on page 1.)

[5] George Ostapowicz, Robert J Fontana, Frank V Schiødt, Anne Larson, Timothy J Davern, Steven H B Han, Timothy M McCashland, A Obaid Shakil, J Eileen Hay, Linda Hynan, Jeffrey S Crippin, Andres T Blei, Grace Samuel, Joan Reisch, and William M Lee. Results of a prospective study of acute liver failure at 17 tertiary care centers in the United States. *Annals of internal medicine*, 137(12):947–954, dec 2002. (Cited on page 1.)

[6] Jinghai J Xu, Dolores Diaz, and Peter J O'Brien. Applications of cytotoxicity assays and pre-lethal mechanistic assays for assessment of human hepatotoxicity potential. *Chemico-biological interactions*, 150(1):115–128, nov 2004. (Cited on page 1.)

[7] Jerry Avorn. The $2.6 Billion Pill - Methodologic and Policy Considerations. *New England Journal of Medicine*, 372(20):1877–1879, may 2015. (Cited on page 1.)

[8] M. Chen, M. Zhang, J. Borlak, and W. Tong. A Decade of Toxicogenomic Research and Its Contribution to Toxicological Science. *Toxicological Sciences*, 130(2):217–228, dec 2012. (Cited on pages 1 and 9.)

[9] Varun Ahuja and Sharad Sharma. Drug safety testing paradigm, current progress and future challenges: an overview. *Journal of Applied Toxicology*, 34(6):576–594, jun 2014. (Cited on page 1.)

[10] Harry Olson, Graham Betton, Jeffrey Stritar, and Denise Robinson. The predictivity of the toxicity of pharmaceuticals in humans from animal data an interim assessment. *Toxicology Letters*, 102-103:535–538, dec 1998. (Cited on page 1.)

[11] Laura Suter, Susanne Schroeder, Kirstin Meyer, Jean-Charles Gautier, Alexander Amberg, Maria Wendt, Hans Gmuender, Angela Mally, Eric Boitier, Heidrun Ellinger-Ziegelbauer, Katja Matheis, and Friedlieb Pfannkuch. EU framework 6 project: predictive toxicology (PredTox)-overview and outcome. *Toxicology and applied pharmacology*, 252(2):73–84, apr 2011. (Cited on pages 1 and 9.)

[12] Thomas Hartung. Food for Thought Look Back in Anger - What Clinical Studies Tell Us About Preclinical Work. *ALTEX*, 30(3):275–291. (Cited on page 1.)

[13] Ignazio Grattagliano. Biochemical mechanisms in drug-induced liver injury: Certainties and doubts. *World Journal of Gastroenterology*, 15(39):4865, 2009. (Cited on page 2.)

[14] Xiaomin Deng, Robert F Stachlewitz, Michael J Liguori, Eric A G Blomme, Jeffrey F Waring, James P Luyendyk, Jane F Maddox, Patricia E Ganey, and Robert A Roth. Modest inflammation enhances diclofenac hepatotoxicity in rats: role of neutrophils and bacterial translocation. *The Journal of pharmacology and experimental therapeutics*, 319(3):1191–1199, dec 2006. (Cited on pages 2 and 93.)

[15] Christine Demeilliers, Emmanuel Jacquemin, Véronique Barbu, Martine Mergey, François Paye, Laura Fouassier, Nicolas Chignard, Chantal Housset, and Nour-Eddine Lomri. Altered hepatobiliary gene expressions in PFIC1: ATP8B1 gene defect is associated with CFTR downregulation. *Hepatology (Baltimore, Md.)*, 43(5):1125–1134, may 2006. (Cited on pages 2, 44, 103, and 114.)

[16] M Vinken, M Maes, T Vanhaecke, and V Rogiers. Drug-induced liver injury: mechanisms, types and biomarkers. *Current medicinal chemistry*, 20(24):3011–3021, jan 2013. (Cited on pages 2, 33, 43, 103, and 114.)

[17] Mathieu Vinken. The adverse outcome pathway concept: A pragmatic tool in toxicology. *Toxicology*, 312:158–165, 2013. (Cited on pages 2, 33, 43, and 103.)

[18] Mathieu Vinken, Brigitte Landesmann, Marina Goumenou, Stefanie Vinken, Imran Shah, Hartmut Jaeschke, Catherine Willett, Maurice Whelan, and Vera Rogiers. Development of an Adverse Outcome Pathway From Drug-Mediated Bile Salt Export Pump Inhibition to Cholestatic Liver Injury. *Toxicological Sciences*, 136(1):97–106, aug 2013. (Cited on pages 2, 3, 33, 43, 103, and 121.)

[19] Martin Wagner, Gernot Zollner, and Michael Trauner. New molecular insights into the mechanisms of cholestasis. *Journal of hepatology*, 51(3):565–580, oct 2009. (Cited on pages 2, 43, 103, and 114.)

[20] Antonella Pellicoro, Prakash Ramachandran, John P Iredale, and Jonathan A Fallowfield. Liver fibrosis and repair: immune regulation of wound healing in a solid organ. *Nature reviews. Immunology*, 14(3):181–194, mar 2014. (Cited on page 2.)

[21] Ursula E Lee and Scott L Friedman. Mechanisms of hepatic fibrogenesis. *Best practice {&} research. Clinical gastroenterology*, 25(2):195–206, apr 2011. (Cited on page 2.)

[22] Mathieu Vinken. Adverse Outcome Pathways and Drug-Induced Liver Injury Testing. *Chemical research in toxicology*, 28(7):1391–1397, jul 2015. (Cited on pages 2, 3, and 121.)

[23] Christothea Constandinou, Neil Henderson, and John P. Iredale. Modeling Liver Fibrosis in Rodents. In *Fibrosis Research*, pages 237–250. Humana Press, Totowa, NJ, 2005. (Cited on page 2.)

[24] Karen E Lasser. Timing of New Black Box Warnings and Withdrawals for Prescription Medications. *JAMA*, 287(17):2215, may 2002. (Cited on page 4.)

[25] Jack Uetrecht. Idiosyncratic drug reactions: current understanding. *Annual review of pharmacology and toxicology*, 47:513–539, jan 2007. (Cited on page 4.)

[26] Patrick J Shaw, Patricia E Ganey, and Robert A Roth. Idiosyncratic drug-induced liver injury and the role of inflammatory stress with an emphasis on an animal model of trovafloxacin hepatotoxicity. *Toxicological sciences : an official journal of the Society of Toxicology*, 118(1):7–18, nov 2010. (Cited on pages 4, 93, 106, and 121.)

[27] Jack Uetrecht and Dean J Naisbitt. Idiosyncratic adverse drug reactions: current concepts. *Pharmacological reviews*, 65(2):779–808, apr 2013. (Cited on page 4.)

[28] H Olson, G Betton, D Robinson, K Thomas, A Monro, G Kolaja, P Lilly, J Sanders, G Sipes, W Bracken, M Dorato, K Van Deun, P Smith, B Berger, and A Heller. Concordance of the toxicity of pharmaceuticals in humans and in animals. *Regulatory toxicology and pharmacology : RTP*, 32(1):56–67, aug 2000. (Cited on page 5.)

[29] Zhichao Liu, Qiang Shi, Don Ding, Reagan Kelly, Hong Fang, and Weida Tong. Translating Clinical Findings into Knowledge in Drug Safety Evaluation - Drug Induced Liver Injury Prediction System (DILIps). *PLoS Computational Biology*, 7(12):e1002310, dec 2011. (Cited on pages 5, 57, 72, 105, and 106.)

[30] Jiangang Liu, Robert A Jolly, Aaron T Smith, George H Searfoss, Keith M Goldstein, Vladimir N Uversky, Keith Dunker, Shuyu Li, Craig E Thomas, and Tao Wei. Predictive Power Estimation Algorithm (PPEA)-a new algorithm to reduce overfitting for genomic biomarker discovery. *PloS one*, 6(9):e24233, jan 2011. (Cited on pages 5, 57, 72, 105, 106, and 116.)

[31] Valerie Y Soldatow, Edward L Lecluyse, Linda G Griffith, and Ivan Rusyn. In vitro models for liver toxicity testing. *Toxicology research*, 2(1):23–39, jan 2013. (Cited on pages 5, 101, and 111.)

[32] Brian G Lake and Roger J Price. Evaluation of the metabolism and hepatotoxicity of xenobiotics utilizing precision-cut slices. *Xenobiotica; the fate of foreign compounds in biological systems*, 43(1):41–53, jan 2013. (Cited on page 5.)

[33] Christiane Guguen-Guillouzo, Anne Corlu, and Andre Guillouzo. Stem cell-derived hepatocytes and their use in toxicology. *Toxicology*, 270(1):3–9, mar 2010. (Cited on page 5.)

[34] John H Ansede, William R Smith, Cassandra H Perry, Robert L St Claire, and Kenneth R Brouwer. An in vitro assay to assess transporter-based cholestatic hepatotoxicity using sandwich-cultured rat hepatocytes. *Drug metabolism and disposition: the biological fate of chemicals*, 38(2):276–280, mar 2010. (Cited on pages 5, 33, 36, 58, 59, 81, and 101.)

[35] Anne M Larson, Julie Polson, Robert J Fontana, Timothy J Davern, Ezmina Lalani, Linda S Hynan, Joan S Reisch, Frank V Schiødt, George Ostapowicz, A Obaid Shakil, and William M Lee. Acetaminophen-induced acute liver failure: results of a United States multicenter, prospective study. *Hepatology (Baltimore, Md.)*, 42(6):1364–1372, dec 2005. (Cited on page 7.)

[36] M. Fung, A. Thornton, K. Mybeck, J. H.-h. Wu, K. Hornbuckle, and E. Muniz. Evaluation of the Characteristics of Safety Withdrawal of Prescription Drugs from Worldwide Pharmaceutical Markets-1960 to 1999. *Therapeutic Innovation & Regulatory Science*, 35(1):293–317, jan 2001. (Cited on page 7.)

[37] Priska Kaufmann, Michael Török, Anya Hänni, Paul Roberts, Rodolfo Gasser, and Stephan Krähenbühl. Mechanisms of benzarone and benzbromarone-induced hepatic toxicity. *Hepatology (Baltimore, Md.)*, 41(4):925–935, apr 2005. (Cited on page 7.)

[38] A B Saba, Ola Davies O, M O Oyeyemi, and Ajala O. The toxic effects of prolonged administration of chloramphenicol on the liver and kidney of rats. *African Journal of Biomedical Research*, 3(3):133–137, 2000. (Cited on page 7.)

[39] R Salm. Acute necrosis of the liver following chloramphenicol therapy. *Edinburgh medical journal*, 60(7):334–336, jul 1953. (Cited on page 7.)

[40] E. Olatunde Farombi. Antioxidant Status and Hepatic Lipid Peroxidation in Chloramphenicol-Treated Rats. *The Tohoku Journal of Experimental Medicine*, 194(2):91–98, 2001. (Cited on page 7.)

[41] E. C. Foot and W. B. Thomson. Cholestatic Jaundice After Chloramphenicol. *British Medical Journal*, 1(5327):403–404, 1963. (Cited on pages 7 and 116.)

[42] M W Stanley, J D Taurog, and D C Snover. Fatal colchicine toxicity: report of a case. *Clinical and experimental rheumatology*, 2(2):167–171, jan 1989. (Cited on page 7.)

[43] M Levy, M Spino, and S E Read. Colchicine: a state-of-the-art review. *Pharmacotherapy*, 11(3):196–211, jan 1991. (Cited on page 7.)

[44] C C Travis, T W McClain, and P D Birkner. Diethylnitrosamine-induced hepatocarcinogenesis in rats: a theoretical study. *Toxicology and applied pharmacology*, 109(2):289–304, jun 1991. (Cited on page 7.)

[45] Veena Sharma and Pracheta Janmeda. Protective Assessment of Euphorbia neriifolia and its Isolated Flavonoid Against N-nitrosodiethylamine-induced Hepatic Carcinogenesis in Male Mice: A Histopathological Analysis. *Toxicology international*, 21(1):37–43, jan 2014. (Cited on page 7.)

[46] P J Hertzog, P S Bhathal, P R Dorling, R N Le Page, and R N Le Page. Alpha-naphthyl-isothiocyanate-induced cholestasis in the rat: studies of liver plasma membrane enzymes. *Pathology*, 7(1):13–23, jul 1975. (Cited on page 8.)

[47] Gerd A Kullak-Ublick. Drug-Induced Cholestatic Liver Disease, 2000. (Cited on page 8.)

[48] M Soresi, V Sparacino, G Pisciotta, G Bonfissuto, F Caputo, A Carroccio, S Calabrese, and G Montalto. [Effects of cyclosporin A on various indices of cholestasis in kidney transplant recipients]. *Minerva urologica e nefrologica = The Italian journal of urology and nephrology*, 47(2):65–69, jun 1995. (Cited on page 8.)

[49] A Myara, J F Cadranel, R Dorent, F Lunel, E Bouvier, M Gerhardt, B Bernard, J J Ghoussoub, A Cabrol, I Gandjbakhch, P Opolon, and F Trivin. Cyclosporin A-mediated cholestasis in patients with chronic hepatitis after heart transplantation. *European journal of gastroenterology {&} hepatology*, 8(3):267–271, mar 1996. (Cited on page 8.)

[50] Ryan E Morgan, Michael Trauner, Carlo J van Staden, Paul H Lee, Bharath Ramachandran, Michael Eschenberg, Cynthia A Afshari, Charles W Qualls, Ruth Lightfoot-Dunn, and Hisham K Hamadeh. Interference with bile salt export pump function is a susceptibility factor for human liver injury in drug development. *Toxicological sciences : an official journal of the Society of Toxicology*, 118(2):485–500, dec 2010. (Cited on page 8.)

[51] F Borhan-Manesh and J B Farnum. Methyltestosterone-induced cholestasis. The importance of disproportionately low serum alkaline phosphatase level. *Archives of internal medicine*, 149(9):2127–2129, sep 1989. (Cited on page 8.)

[52] M Hirode, A Horinouchi, T Uehara, A Ono, T Miyagishima, H Yamada, T Nagao, Y Ohno, and T Urushidani. Gene expression profiling in rat liver treated with compounds inducing elevation of bilirubin. *Human {&} experimental toxicology*, 28(4):231–244, apr 2009. (Cited on pages 8, 57, 72, 105, 106, 116, and 117.)

[53] Robert A Roth, James P Luyendyk, Jane F Maddox, and Patricia E Ganey. Inflammation and drug idiosyncrasy-is there a connection? *The Journal of pharmacology and experimental therapeutics*, 307(1):1–8, oct 2003. (Cited on page 8.)

[54] J. P. Buchweitz. Underlying Endotoxemia Augments Toxic Responses to Chlorpromazine: Is There a Relationship to Drug Idiosyncrasy? *Journal of Pharmacology and Experimental Therapeutics*, 300(2):460–467, feb 2002. (Cited on page 8.)

[55] Istvan Bitter, Martin R.K Dossenbach, Shlomo Brook, Peter D Feldman, Stephen Metcalfe, Carlo A Gagiano, János Füredi, György Bartko, Zoltan Janka, Csaba M Banki, Gabor Kovacs, and Alan Breier. Olanzapine versus clozapine in treatment-resistant or treatment-intolerant schizophrenia. *Progress in Neuro-Psychopharmacology and Biological Psychiatry*, 28(1):173–180, jan 2004. (Cited on page 8.)

[56] Gilbert S Omenn. Toxicogenomics: Principles and Applications, nov 2004. (Cited on page 9.)

[57] Laura Suter, Lee E Babiss, and Eric B Wheeldon. Toxicogenomics in predictive toxicology in drug development. *Chemistry {&} biology*, 11(2):161–171, feb 2004. (Cited on page 9.)

[58] Yi Yang, Eric A G Blomme, and Jeffrey F Waring. Toxicogenomics in drug discovery: from preclinical studies to clinical trials. *Chemico-biological interactions*, 150(1):71–85, nov 2004. (Cited on page 9.)

[59] Jens Hrach. Toxicogenomic approaches for the prediction of hepatotoxicity in vitro, mar 2009. (Cited on page 9.)

[60] Urs A Meyer, Ulrich M Zanger, and Matthias Schwab. Omics and drug response. *Annual review of pharmacology and toxicology*, 53:475–502, jan 2013. (Cited on page 9.)

[61] E F Nuwaysir, M Bittner, J Trent, J C Barrett, and C A Afshari. Microarrays and toxicology: the advent of toxicogenomics. *Molecular carcinogenesis*, 24(3):153–159, mar 1999. (Cited on page 9.)

[62] S Bulera. RNA expression in the early characterization of hepatotoxicants in Wistar rats by high-density DNA microarrays. *Hepatology*, 33(5):1239–1258, may 2001. (Cited on page 9.)

[63] Kirsten A. Baken, Joanna Arkusz, Jeroen L.A. Pennings, Rob J. Vandebriel, and Henk van Loveren. In vitro immunotoxicity of bis(tri-n-butyltin)oxide (TBTO) studied by toxicogenomics. *Toxicology*, 237(1-3):35–48, jul 2007. (Cited on page 9.)

[64] Kirsten A. Baken, Jeroen L.A. Pennings, Martijs J. Jonker, Mirjam M. Schaap, Annemieke de Vries, Harry van Steeg, Timo M. Breit, and Henk van Loveren. Overlapping gene expression profiles of model compounds provide opportunities for immunotoxicity screening. *Toxicology and Applied Pharmacology*, 226(1):46–59, jan 2008. (Cited on page 9.)

[65] Mackenzie Hadi. *Precision-Cut Liver Slices as a Model for Intrinsic and Idiosyncratic Drug-Induced Liver Injury*. PhD thesis, 2012. (Cited on pages 10, 79, and 94.)

[66] D L Laskin, C R Gardner, V F Price, and D J Jollow. Modulation of macrophage functioning abrogates the acute hepatotoxicity of acetaminophen. *Hepatology (Baltimore, Md.)*, 21(4):1045–1050, 1995. (Cited on page 15.)

[67] C A Rivera, B U Bradford, K J Hunt, Y Adachi, L W Schrum, D R Koop, E R Burchardt, R A Rippe, and R G Thurman. Attenuation of CCl(4)-induced hepatic fibrosis by GdCl(3) treatment or dietary glycine. *American journal of physiology. Gastrointestinal and liver physiology*, 281(1):G200–G207, 2001. (Cited on page 15.)

[68] Adam K Rowden, Jeffrey Norvell, David L Eldridge, and Mark A Kirk. Acetaminophen poisoning, 2006. (Cited on page 15.)

[69] Inge A M de Graaf, Peter Olinga, Marina H de Jager, Marjolijn T Merema, Ruben de Kanter, Esther G van de Kerkhof, and Geny M M Groothuis. Preparation and incubation of precision-cut liver and intestinal slices for application in drug metabolism and toxicity studies. *Nature Protocols*, 5(9):1540–1551, sep 2010. (Cited on pages 15 and 111.)

[70] S Ekins. Past, present, and future applications of precision-cut liver slices for in vitro xenobiotic metabolism. *Drug metabolism reviews*, 28(4):591–623, nov 1996. (Cited on page 15.)

[71] M G L Elferink, P Olinga, A L Draaisma, M T Merema, S Bauerschmidt, J Polman, W G Schoonen, and G M M Groothuis. Microarray analysis in rat liver slices correctly predicts in vivo hepatotoxicity. *Toxicology and applied pharmacology*, 229(3):300–309, jun 2008. (Cited on pages 15, 16, 26, 34, 58, and 79.)

[72] Marja van de Bovenkamp, Geny M M Groothuis, Annelies L Draaisma, Marjolijn T Merema, Judith I Bezuijen, Marit J van Gils, Dirk K F Meijer, Scott L Friedman, and Peter Olinga. Precision-cut liver slices as a new model to study toxicity-induced hepatic stellate cell activation in a physiologic milieu. *Toxicological Sciences*, 85(1):632–638, 2005. (Cited on pages 15, 16, 26, 34, 44, 102, and 112.)

[73] Inge M Westra, Dorenda Oosterhuis, Geny M M Groothuis, and Peter Olinga. The effect of antifibrotic drugs in rat precision-cut fibrotic liver slices. *PloS one*, 9(4):e95462, jan 2014. (Cited on pages 15, 34, 44, 102, and 112.)

[74] Nandini Raghavan, Dhammika Amaratunga, Alex Y Nie, and Michael McMillian. Class prediction in toxicogenomics. *Journal of biopharmaceutical statistics*, 15(2):327–341, jan 2005. (Cited on pages 15, 16, 26, 34, 44, and 102.)

[75] Peter Olinga, Ingrid H Hof, Marjolijn T Merema, Maaike Smit, Marina H De Jager, Piet J Swart, Maarten J H Slooff, Dirk K F Meijer, and Geny M M Groothuis. The applicability of rat and human liver slices to the study of mechanisms of hepatic drug uptake. *Journal of Pharmacological and Toxicological Methods*, 45(1):55–63, 2001. (Cited on pages 15 and 79.)

[76] Peter Olinga, Marjolijn T Merema, Marina H De Jager, Frans Derks, Barbro N Melgert, Han Moshage, M J H Slooff, D K F Meijer, Klaas Poelstra, and G M M Groothuis. Rat liver slices as a tool to study LPS-induced inflammatory response in the liver. *Journal of Hepatology*, 35(2):187–194, 2001. (Cited on pages 15 and 79.)

[77] P Olinga, M T Merema, M H de Jager, F Derks, B N Melgert, H Moshage, M J Slooff, D K Meijer, K Poelstra, and G M Groothuis. Rat liver slices as a tool to study LPS-induced inflammatory response in the liver. *Journal of hepatology*, 35(2):187–194, aug 2001. (Cited on pages 15 and 79.)

[78] Marieke G L Elferink, Peter Olinga, Annelies L Draaisma, Marjolijn T Merema, Klaas Nico Faber, Maarten J H Slooff, Dirk K F Meijer, and Geny M M Groothuis. LPS-induced downregulation of MRP2 and BSEP in human liver is due to a posttranscriptional process. *American journal of physiology. Gastrointestinal and liver physiology*, 287(5):G1008–16, nov 2004. (Cited on pages 15 and 79.)

[79] Haude Clouzeau-Girard, Christelle Guyot, Chantal Combe, Valérie Moronvalle-Halley, Chantal Housset, Thierry Lamireau, Jean Rosenbaum, and Alexis Desmoulière. Effects of bile acids on biliary epithelial cell proliferation and portal fibroblast activation using rat liver slices. *Laboratory investigation; a journal of technical methods and pathology*, 86(3):275–285, 2006. (Cited on page 15.)

[80] Diana Jung, Marieke G L Elferink, Frans Stellaard, and Geny M M Groothuis. Analysis of bile acid-induced regulation of FXR target genes in human liver slices. *Liver international : official journal of the International Association for the Study of the Liver*, 27(1):137–144, feb 2007. (Cited on pages 15 and 43.)

[81] Andreas Schroeder, Odilo Mueller, Susanne Stocker, Ruediger Salowsky, Michael Leiber, Marcus Gassmann, Samar Lightfoot, Wolfram Menzel, Martin Granzow, and Thomas Ragg. The RIN: an RNA integrity number for assigning integrity values to RNA measurements. *BMC molecular biology*, 7:3, 2006. (Cited on page 16.)

[82] Yilin Dai, Ling Guo, Meng Li, and Yi-Bu Chen. Microarray US: a user-friendly graphical interface to Bioconductor tools that enables accurate microarray data analysis and expedites comprehensive functional analysis of microarray results. *BMC research notes*, 5:282, jan 2012. (Cited on page 17.)

[83] Rainer Breitling, Patrick Armengaud, Anna Amtmann, and Pawel Herzyk. Rank products: a simple, yet powerful, new method to detect differentially regulated genes in replicated microarray experiments. *FEBS letters*, 573(1-3):83–92, aug 2004. (Cited on pages 17 and 18.)

[84] Gabriel S Eichler, Sui Huang, and Donald E Ingber. Gene Expression Dynamics Inspector (GEDI): for integrative analysis of expression profiles. *Bioinformatics*, 19(17):2321–2322, nov 2003. (Cited on page 17.)

[85] Inge M Westra, Dorenda Oosterhuis, Geny M M Groothuis, and Peter Olinga. Precision-cut liver slices as a model for the early onset of liver fibrosis to test antifibrotic drugs. *Toxicology and Applied Pharmacology*, 274(2):328–338, 2014. (Cited on pages 17, 34, 44, and 102.)

[86] Andreas Krämer, Jeff Green, Jack Pollard, and Stuart Tugendreich. Causal analysis approaches in Ingenuity Pathway Analysis. *Bioinformatics (Oxford, England)*, 30(4):523–530, feb 2014. (Cited on page 18.)

[87] Huan Cai, Hongyu Chen, Tie Yi, Caitlin M Daimon, John P Boyle, Chris Peers, Stuart Maudsley, and Bronwen Martin. VennPlex-a novel Venn diagram program for comparing and visualizing datasets with differentially regulated datapoints. *PloS one*, 8(1):e53388, jan 2013. (Cited on page 18.)

[88] Asish K Ghosh and Douglas E Vaughan. PAI-1 in tissue fibrosis. *Journal of cellular physiology*, 227(2):493–507, feb 2012. (Cited on page 21.)

[89] Yao Hsiao, Tie Zou, Chang-Chun Ling, Hua Hu, Xian-Mei Tao, and Hou-Yan Song. Disruption of tissue-type plasminogen activator gene in mice aggravated liver fibrosis. *Journal of gastroenterology and hepatology*, 23(7 Pt 2):e258–64, jul 2008. (Cited on page 21.)

[90] Can-Jie Guo, Qin Pan, Tao Cheng, Bo Jiang, Guang-Yu Chen, and Ding-Guo Li. Changes in microRNAs associated with hepatic stellate cell activation status identify signaling pathways. *The FEBS journal*, 276(18):5163–5176, sep 2009. (Cited on page 21.)

[91] Johannes Kluwe, Jean-Philippe Pradere, Geum-Youn Gwak, Ali Mencin, Samuele De Minicis, Christoph H Osterreicher, Jordi Colmenero, Ramon Bataller, and Robert F Schwabe. Modulation of hepatic fibrosis by c-Jun-N-terminal kinase inhibition. *Gastroenterology*, 138(1):347–359, jan 2010. (Cited on page 21.)

[92] David E Smart, Karen Green, Fiona Oakley, Jonathan B Weitzman, Moshe Yaniv, Gary Reynolds, Jelena Mann, Harry Millward-Sadler, and Derek A Mann. JunD is a profibrogenic transcription factor regulated by Jun N-terminal kinase-independent phosphorylation. *Hepatology (Baltimore, Md.)*, 44(6):1432–1440, dec 2006. (Cited on page 21.)

[93] S Ceccarelli, N Panera, C De Stefanis, D Gnani, A Crudele, C Rychlicki, S Petrini, M Mina, C Furlanello, S De Minicis, G Svegliati-Baroni, V Nobili, and A Alisi. P280 LPS-INDUCED TRANSCRIPTION FACTORS INVOLVED IN NON-ALCOHOLIC LIVER DISEASE (NAFLD) INFLAMMATORY AND PRO-FIBROGENIC PATTERN. *Journal of Hepatology*, 60(1):S159, apr 2014. (Cited on page 21.)

[94] V Ratziu, A Lalazar, L Wong, Q Dang, C Collins, E Shaulian, S Jensen, and S L Friedman. Zf9, a Kruppel-like transcription factor up-regulated in vivo during early hepatic fibrosis. *Proceedings of the National Academy of Sciences of the United States of America*, 95(16):9500–9505, aug 1998. (Cited on page 21.)

[95] Yoshiyuki Takahara, Mitsuo Takahashi, Hiroki Wagatsuma, Fumihiko Yokoya, Qing-Wei Zhang, Mutsuyo Yamaguchi, Hiroyuki Aburatani, and Norifumi Kawada. Gene expression profiles of hepatic cell-type specific marker genes in progression of liver fibrosis. *World journal of gastroenterology : WJG*, 12(40):6473–6499, oct 2006. (Cited on page 21.)

[96] Koichi Matsuzaki. Smad phosphoisoform signals in acute and chronic liver injury: similarities and differences between epithelial and mesenchymal cells. *Cell and tissue research*, 347(1):225–243, jan 2012. (Cited on page 26.)

[97] Jiansheng Huang, Navin Viswakarma, Songtao Yu, Yuzhi Jia, Liang Bai, Aurore Vluggens, Mustapha Cherkaoui-Malki, Mushfiquddin Khan, Inderjit Singh, Gongshe Yang, M Sambasiva Rao, Jayme Borensztajn, and Janardan K Reddy. Progressive endoplasmic reticulum stress contributes to hepatocarcinogenesis in fatty acyl-CoA oxidase 1-deficient mice. *The American journal of pathology*, 179(2):703–713, aug 2011. (Cited on page 27.)

[98] T Ohyama, K Sato, K Kishimoto, Y Yamazaki, N Horiguchi, T Ichikawa, S Kakizaki, H Takagi, T Izumi, and M Mori. Azelnidipine is a calcium blocker that attenuates liver fibrosis and may increase antioxidant defence. *British journal of pharmacology*, 165(4b):1173–1187, feb 2012. (Cited on page 27.)

[99] H-Y Yue, C Yin, J-L Hou, X Zeng, Y-X Chen, W Zhong, P-F Hu, X Deng, Y-X Tan, J-P Zhang, B-F Ning, J Shi, X Zhang, H-Y Wang, Y Lin, and W-F Xie. Hepatocyte nuclear factor 4alpha attenuates hepatic fibrosis in rats. *Gut*, 59(2):236–246, feb 2010. (Cited on page 27.)

[100] Efrat Sharvit, Shirley Abramovitch, Shimon Reif, and Rafael Bruck. Amplified inhibition of stellate cell activation pathways by PPAR-γ, RAR and RXR agonists. *PloS one*, 8(10):e76541, jan 2013. (Cited on page 27.)

[101] Keiko Iwaisako, Michael Haimerl, Yong-Han Paik, Kojiro Taura, Yuzo Kodama, Claude Sirlin, Elizabeth Yu, Ruth T Yu, Michael Downes, Ronald M Evans, David A Brenner, and Bernd Schnabl. Protection from liver fibrosis by a peroxisome proliferator-activated receptor δ agonist. *Proceedings of the National Academy of Sciences of the United States of America*, 109(21):E1369–76, may 2012. (Cited on page 27.)

[102] Tetsuya Toyama, Hideki Nakamura, Yuichi Harano, Norihito Yamauchi, Atsuhiro Morita, Toshihiko Kirishima, Masahito Minami, Yoshito Itoh, and Takeshi Okanoue. PPARalpha ligands activate antioxidant enzymes and suppress hepatic fibrosis in rats. *Biochemical and biophysical research communications*, 324(2):697–704, nov 2004. (Cited on page 27.)

[103] Eduardo L Guimaraes, Jan Best, Laurent Dolle, Mustapha Najimi, Etienne Sokal, and Leo A van Grunsven. Mitochondrial uncouplers inhibit hepatic stellate cell activation. *BMC gastroenterology*, 12:68, jan 2012. (Cited on page 27.)

[104] Cheng Ji, Neil Kaplowitz, Mo Yin Lau, Eddy Kao, Lydia M Petrovic, and Amy S Lee. Liver-specific loss of glucose-regulated protein 78 perturbs the unfolded protein response and exacerbates a spectrum of liver diseases in mice. *Hepatology (Baltimore, Md.)*, 54(1):229–239, jul 2011. (Cited on page 27.)

[105] Núria Tarrats, Anna Moles, Albert Morales, Carmen García-Ruiz, José C Fernández-Checa, and Montserrat Marí. Critical role of tumor necrosis factor receptor 1, but not 2, in hepatic stellate cell proliferation, extracellular matrix remodeling, and liver fibrogenesis. *Hepatology (Baltimore, Md.)*, 54(1):319–327, jul 2011. (Cited on page 27.)

[106] Elisabetta A Renzoni, David J Abraham, Sarah Howat, Xu Shi-Wen, Piersante Sestini, George Bou-Gharios, Athol U Wells, Srihari Veeraraghavan, Andrew G Nicholson, Christopher P Denton, Andrew Leask, Jeremy D Pearson, Carol M Black, Kenneth I Welsh, and Roland M du Bois. Gene expression profiling reveals novel TGFbeta targets in adult lung fibroblasts. *Respiratory research*, 5(1):24, jan 2004. (Cited on page 27.)

[107] Juling Ji, Feng Yu, Qiuhong Ji, Zhiyao Li, Kuidong Wang, Jinsheng Zhang, Jinbiao Lu, Li Chen, Qun E, Yaoying Zeng, Yuhua Ji, and E Qun. Comparative proteomic analysis of rat hepatic stellate cell activation: a comprehensive view and suppressed immune response. *Hepatology (Baltimore, Md.)*, 56:332–349, 2012. (Cited on page 28.)

[108] Eiichiro Ogimura, Shuichi Sekine, and Toshiharu Horie. Bile salt export pump inhibitors are associated with bile acid-dependent drug-induced toxicity in sandwich-cultured hepatocytes. *Biochemical and biophysical research communications*, 416(3-4):313–317, dec 2011. (Cited on page 33.)

[109] Sagnik Chatterjee, Ingrid T G W Bijsmans, Saskia W C van Mil, Patrick Augustijns, and Pieter Annaert. Toxicity and intracellular accumulation of bile acids in sandwich-cultured rat hepatocytes: role of glycine conjugates. *Toxicology in vitro : an international journal published in association with BIBRA*, 28(2):218–230, mar 2014. (Cited on page 33.)

[110] Sagnik Chatterjee, Lysiane Richert, Patrick Augustijns, and Pieter Annaert. Hepatocyte-based in vitro model for assessment of drug-induced cholestasis. *Toxicology and applied pharmacology*, 274(1):124–136, jan 2014. (Cited on page 33.)

[111] J Fraczek, J Bolleyn, T Vanhaecke, V Rogiers, and M Vinken. Primary hepatocyte cultures for pharmaco-toxicological studies: at the busy crossroad of various anti-dedifferentiation strategies. *Archives of toxicology*, 87(4):577–610, apr 2013. (Cited on page 33.)

[112] Ewa Szalowska, Geert Stoopen, Maria J Groot, Peter J M Hendriksen, and Ad A C M Peijnenburg. Treatment of mouse liver slices with cholestatic hepatotoxicants results in down-regulation of Fxr and its target genes. *BMC medical genomics*, 6(1):39, jan 2013. (Cited on pages 33, 43, 45, and 104.)

[113] Ewa Szalowska, Geert Stoopen, Jeroen C W Rijk, Si Wang, Peter J M Hendriksen, Maria J Groot, Jan Ossenkoppele, and Ad A C M Peijnenburg. Effect of oxygen concentration and selected protocol factors on viability and gene expression of mouse liver slices. *Toxicology in vitro : an international journal published in association with BIBRA*, 27(5):1513–1524, aug 2013. (Cited on pages 33, 43, 45, 104, and 115.)

[114] M G L Elferink, P Olinga, E M van Leeuwen, S Bauerschmidt, J Polman, W G Schoonen, S H Heisterkamp, and G M M Groothuis. Gene expression analysis of precision-cut human liver slices indicates stable expression of ADME-Tox related genes. *Toxicology and applied pharmacology*, 253(1):57–69, may 2011. (Cited on pages 34, 58, and 79.)

[115] Inge M Westra. The p38-Mapk pathway is involved in fibrogenesis in rat precision-cut liver slices. *submitted for publication*, 2014. (Cited on pages 34, 44, and 102.)

[116] Inge M Westraa, Mackenzie Hadia, Dorenda Oosterhuisb, and Koert P de Jongc. Human precision-cut liver slices as an ex vivo model to test antifibrotic drugs in the early onset and end-stage of liver fibrosis. *Precision-cut liver slices: an ex vivo model for the early onset and end-stage of liver fibrosis*, page 97, 2014. (Cited on pages 34, 44, and 102.)

[117] Suresh Vatakuti, Willem G E J Schoonen, Marieke L G Elferink, Geny M M Groothuis, and Peter Olinga. Acute toxicity of CCl4 but not of paracetamol induces a transcriptomic signature of fibrosis in precision-cut liver slices. *Toxicology in vitro : an international journal published in association with BIBRA*, 29(5):1012–1020, apr 2015. (Cited on pages 34, 44, 58, 60, 71, and 79.)

[118] Inge Am de Graaf, Geny Mm Groothuis, and Peter Olinga. Precision-cut tissue slices as a tool to predict metabolism of novel drugs. *Expert opinion on drug metabolism {&} toxicology*, 3(6):879–898, dec 2007. (Cited on page 35.)

[119] Max Scherer, Carsten Gnewuch, Gerd Schmitz, and Gerhard Liebisch. Rapid quantification of bile acids and their conjugates in serum by liquid chromatography-tandem mass spectrometry. *Journal of chromatography. B, Analytical technologies in the biomedical and life sciences*, 877(30):3920–3925, nov 2009. (Cited on pages 36, 60, 103, and 113.)

[120] Lars M T Eijssen, Magali Jaillard, Michiel E Adriaens, Stan Gaj, Philip J de Groot, Michael Müller, and Chris T Evelo. User-friendly solutions for microarray quality control and pre-processing on ArrayAnalysis.org. *Nucleic acids research*, 41(Web Server issue):W71–6, jul 2013. (Cited on pages 37 and 82.)

[121] Martin Lauss, Ilhami Visne, Albert Kriegner, Markus Ringnér, Göran Jönsson, and Mattias Höglund. Monitoring of technical variation in quantitative high-throughput datasets. *Cancer informatics*, 12:193–201, jan 2013. (Cited on pages 37 and 82.)

[122] M E Ritchie, B Phipson, D Wu, Y Hu, C W Law, W Shi, and G K Smyth. limma powers differential expression analyses for RNA-sequencing and microarray studies. *Nucleic Acids Research*, pages gkv007–, jan 2015. (Cited on page 37.)

[123] Kazuhiko Bessho, Reena Mourya, Pranavkumar Shivakumar, Stephanie Walters, John C Magee, Marepalli Rao, Anil G Jegga, and Jorge A Bezerra. Gene expression signature for biliary atresia and a role for interleukin-8 in pathogenesis of experimental disease. *Hepatology (Baltimore, Md.)*, 60(1):211–223, jul 2014. (Cited on pages 37, 45, 104, and 115.)

[124] Tetsuo Adachi, Tomoyuki Kaminaga, Hiroyuki Yasuda, Tetsuro Kamiya, and Hirokazu Hara. The involvement of endoplasmic reticulum stress in bile acid-induced hepatocellular injury. *Journal of clinical biochemistry and nutrition*, 54(2):129–135, mar 2014. (Cited on pages 38, 44, 72, 104, and 114.)

[125] M Makishima, A Y Okamoto, J J Repa, H Tu, R M Learned, A Luk, M V Hull, K D Lustig, D J Mangelsdorf, and B Shan. Identification of a nuclear receptor for bile acids. *Science (New York, N.Y.)*, 284(5418):1362–1365, may 1999. (Cited on page 43.)

[126] Jinghua Yu, Jane-L Lo, Li Huang, Annie Zhao, Edward Metzger, Alan Adams, Peter T Meinke, Samuel D Wright, and Jisong Cui. Lithocholic acid decreases expression of bile salt export pump through farnesoid X receptor antagonist activity. *The Journal of biological chemistry*, 277(35):31441–31447, aug 2002. (Cited on page 43.)

[127] Jane-L Lew, Annie Zhao, Jinghua Yu, Li Huang, Nuria De Pedro, Fernando Peláez, Samuel D Wright, and Jisong Cui. The farnesoid X receptor controls gene expression in a ligand- and promoter-selective fashion. *The Journal of biological chemistry*, 279(10):8856–8861, mar 2004. (Cited on page 43.)

[128] Brandy Garzel, Hui Yang, Lei Zhang, Shiew-Mei Huang, James E Polli, and Hongbing Wang. The role of bile salt export pump gene repression in drug-induced cholestatic liver toxicity. *Drug metabolism and disposition: the biological fate of chemicals*, 42(3):318–322, mar 2014. (Cited on pages 44, 103, and 114.)

[129] Hirdesh Uppal, Simrat P S Saini, Antonio Moschetta, Ying Mu, Jie Zhou, Haibiao Gong, Yonggong Zhai, Songrong Ren, George K Michalopoulos, David J Mangelsdorf, and Wen Xie. Activation of LXRs prevents bile acid toxicity and cholestasis in female mice. *Hepatology (Baltimore, Md.)*, 45(2):422–432, feb 2007. (Cited on page 44.)

[130] Marielle Gascon-Barré, Christian Demers, Ali Mirshahi, Stéphane Néron, Sylvia Zalzal, and Antonio Nanci. The normal liver harbors the vitamin D nuclear receptor in nonparenchymal and biliary epithelial cells. *Hepatology (Baltimore, Md.)*, 37(5):1034–1042, may 2003. (Cited on page 44.)

[131] Yuji Tanaka, Lauren M Aleksunes, Yue Julia Cui, and Curtis D Klaassen. ANIT-induced intrahepatic cholestasis alters hepatobiliary transporter expression via Nrf2-dependent and independent signaling. *Toxicological sciences : an official journal of the Society of Toxicology*, 108(2):247–257, apr 2009. (Cited on page 44.)

[132] Bryan L Copple, Hartmut Jaeschke, and Curtis D Klaassen. Oxidative stress and the pathogenesis of cholestasis. *Seminars in liver disease*, 30(2):195–204, may 2010. (Cited on page 44.)

[133] Sébastien Anthérieu, Pamela Bachour-El Azzi, Julie Dumont, Ziad Abdel-Razzak, Christiane Guguen-Guillouzo, Bernard Fromenty, Marie-Anne Robin, and André Guillouzo. Oxidative stress plays a major role in chlorpromazine-induced cholestasis in human HepaRG cells. *Hepatology (Baltimore, Md.)*, 57(4):1518–1529, apr 2013. (Cited on page 44.)

[134] Carmen G Tag, Sibille Sauer-Lehnen, Sabine Weiskirchen, Erawan Borkham-Kamphorst, René H Tolba, Frank Tacke, and Ralf Weiskirchen. Bile duct ligation in mice: induction of inflammatory liver injury and fibrosis by obstructive cholestasis. *Journal of visualized experiments : JoVE*, (96), jan 2015. (Cited on pages 44, 104, and 115.)

[135] Xuebin Qin and Bin Gao. The complement system in liver diseases. *Cellular {&} molecular immunology*, 3(5):333–340, oct 2006. (Cited on page 45.)

[136] Michael J Liguori, Mark G Anderson, Stanley Bukofzer, James McKim, Jeffrey F Pregenzer, Jacques Retief, Brian B Spear, and Jeffrey F Waring. Microarray analysis in human hepatocytes suggests a mechanism for hepatotoxicity induced by trovafloxacin. *Hepatology (Baltimore, Md.)*, 41(1):177–186, jan 2005. (Cited on pages 45, 93, and 95.)

[137] Jiali Li, Parinaz C Pircher, Ira G Schulman, and Stefan K Westin. Regulation of complement C_3 expression by the bile acid receptor FXR. *The Journal of biological chemistry*, 280(9):7427–7434, mar 2005. (Cited on page 45.)

[138] Omar M E Abdel-Salam, Ayman R Baiuomy, Amany Ameen, and Nabila S Hassan. A study of unfractionated and low molecular weight heparins in a model of cholestatic liver injury in the rat. *Pharmacological research : the official journal of the Italian Pharmacological Society*, 51(1):59–67, jan 2005. (Cited on page 45.)

[139] James P Luyendyk, Glenn H Cantor, Daniel Kirchhofer, Nigel Mackman, Bryan L Copple, and Ruipeng Wang. Tissue factor-dependent coagulation contributes to alpha-naphthylisothiocyanate-induced cholestatic liver injury in mice. *American journal of physiology. Gastrointestinal and liver physiology*, 296(4):G840–9, apr 2009. (Cited on page 45.)

[140] M B Fallon, A Mennone, and J M Anderson. Altered expression and localization of the tight junction protein ZO-1 after common bile duct ligation. *The American journal of physiology*, 264(6 Pt 1):C1439–47, jun 1993. (Cited on page 45.)

[141] Manmeet S Padda, Mayra Sanchez, Abbasi J Akhtar, and James L Boyer. Drug-induced cholestasis. *Hepatology (Baltimore, Md.)*, 53(4):1377–1387, apr 2011. (Cited on pages 57, 70, 105, and 116.)

[142] Gernot Zollner and Michael Trauner. Molecular mechanisms of cholestasis. *Wiener medizinische Wochenschrift (1946)*, 156(13-14):380–385, jul 2006. (Cited on pages 57 and 114.)

[143] Christiane Pauli-Magnus and Peter J Meier. Hepatobiliary transporters and drug-induced cholestasis. *Hepatology (Baltimore, Md.)*, 44(4):778–787, oct 2006. (Cited on page 57.)

[144] Gernot Zollner and Michael Trauner. Mechanisms of cholestasis. *Clinics in liver disease*, 12(1):1–26, vii, 2008. (Cited on page 57.)

[145] Larry C Mattheakis. Predicting hepatotoxicity using cell based assays, oct 2010. (Cited on page 57.)

[146] J Hrach, S O Mueller, and P Hewitt. Development of an in vitro liver toxicity prediction model based on longer term primary rat hepatocyte culture. *Toxicology letters*, 206(2):189–196, oct 2011. (Cited on page 57.)

[147] Georges Natsoulis. Cholestasis signature, jul 2008. (Cited on pages 57, 72, 105, and 106.)

[148] G A Ramm, S C Carr, K R Bridle, L Li, R S Britton, D H Crawford, C A Vogler, B R Bacon, and T F Tracy. Morphology of liver repair following cholestatic liver injury: resolution of ductal hyperplasia, matrix deposition and regression of myofibroblasts. *Liver*, 20(5):387–396, oct 2000. (Cited on page 57.)

[149] Wim F P M Van den Hof, Anke Van Summeren, Arjen Lommen, Maarten L J Coonen, Karen Brauers, Marcel van Herwijnen, Will K W H Wodzig, and Jos C S Kleinjans. Integrative cross-omics analysis in primary mouse hepatocytes unravels mechanisms of cyclosporin A-induced hepatotoxicity. *Toxicology*, 324:18–26, oct 2014. (Cited on pages 58, 72, 104, and 114.)

[150] Guido Steiner, Laura Suter, Franziska Boess, Rodolfo Gasser, Maria Cristina de Vera, Silvio Albertini, Stefan Ruepp, Maria Cristina de Vera, Silvio Albertini, and Stefan Ruepp. Discriminating Different Classes of Toxicants By Transcript Profiling. *Environmental Health Perspectives*, 112(12):1236–1248, aug 2004. (Cited on pages 58, 70, 72, 105, 106, 116, and 117.)

[151] Geny; Vatakuti, Suresh; Olinga, Peter;Pennings, Jeroen; Groothuis, Suresh Vatakuti, Peter Olinga, Jeroen Pennings, and Geny Groothuis. Validation of precision cut liver slices to study drug-induced cholestasis A transcriptomics approach. (Cited on page 58.)

[152] Wei Shi, Alicia Oshlack, and Gordon K Smyth. Optimizing the noise versus bias trade-off for Illumina whole genome expression BeadChips. *Nucleic acids research*, 38(22):e204, dec 2010. (Cited on page 61.)

[153] Qiang Shi, Huixiao Hong, John Senior, and Weida Tong. Biomarkers for drug-induced liver injury. *Expert review of gastroenterology {&} hepatology*, 4(2):225–234, apr 2010. (Cited on page 61.)

[154] Robert C Gentleman, Vincent J Carey, Douglas M Bates, Ben Bolstad, Marcel Dettling, Sandrine Dudoit, Byron Ellis, Laurent Gautier, Yongchao Ge, Jeff Gentry, Kurt Hornik, Torsten Hothorn, Wolfgang Huber, Stefano Iacus, Rafael Irizarry, Friedrich Leisch, Cheng Li, Martin Maechler, Anthony J Rossini, Gunther Sawitzki, Colin Smith, Gordon Smyth, Luke Tierney, Jean Y H Yang, and Jianhua Zhang. Bioconductor: open software development for computational biology and bioinformatics. *Genome biology*, 5(10):R80, jan 2004. (Cited on page 61.)

[155] Nuno L Barbosa-Morais, Mark J Dunning, Shamith A Samarajiwa, Jeremy F J Darot, Matthew E Ritchie, Andy G Lynch, and Simon Tavaré. A re-annotation pipeline for Illumina BeadArrays: improving the interpretation of gene expression data. *Nucleic acids research*, 38(3):e17, jan 2010. (Cited on page 61.)

[156] Alison E M Vickers, Robyn Fisher, Peter Olinga, and Sharon Dial. Repair pathways evident in human liver organ slices. *Toxicology in vitro : an international journal published in association with BIBRA*, 25(7):1485–1492, oct 2011. (Cited on page 65.)

[157] E Gjone and O M Orning. Jaundice due to chloramphenicol. *Acta hepato-splenologica*, 13(5):288–292, jan 1996. (Cited on pages 70, 105, and 116.)

[158] Maria-J Perez and Oscar Briz. Bile-acid-induced cell injury and protection. *World journal of gastroenterology : WJG*, 15(14):1677–1689, apr 2009. (Cited on page 70.)

[159] Lucas Maillette de Buy Wenniger and Ulrich Beuers. Bile salts and cholestasis. *Digestive and liver disease : official journal of the Italian Society of Gastroenterology and the Italian Association for the Study of the Liver*, 42(6):409–418, jun 2010. (Cited on page 70.)

[160] A E M Vickers and R L Fisher. Evaluation of drug-induced injury and human response in precision-cut tissue slices. *Xenobiotica*, 43(1):29–40, 2013. (Cited on page 70.)

[161] P J Utz, M Hottelet, T M Le, S J Kim, M E Geiger, W J van Venrooij, and P Anderson. The 72-kDa component of signal recognition particle is cleaved during apoptosis. *The Journal of biological chemistry*, 273(52):35362–35370, dec 1998. (Cited on page 71.)

[162] Alison E M Vickers and Robyn L Fisher. Evaluation of drug-induced injury and human response in precision-cut tissue slices. *Xenobiotica*, dec 2012. (Cited on page 71.)

[163] Jin Choi, Sonia Djebbar, Andréa Fournier, and Claude Labrie. The co-chaperone DNAJC12 binds to Hsc70 and is upregulated by endoplasmic reticulum stress. *Cell stress {&} chaperones*, 19(3):439–446, may 2014. (Cited on page 71.)

[164] Ying Shen, Laurent Meunier, and Linda M Hendershot. Identification and characterization of a novel endoplasmic reticulum (ER) DnaJ homologue, which stimulates ATPase activity of BiP in vitro and is induced by ER stress. *The Journal of biological chemistry*, 277(18):15947–15956, may 2002. (Cited on page 71.)

[165] Nobuko Hosokawa, Ikuo Wada, Koji Nagasawa, Tatsuya Moriyama, Katsuya Okawa, and Kazuhiro Nagata. Human XTP3-B forms an endoplasmic reticulum quality control scaffold with the HRD1-SEL1L ubiquitin ligase complex and BiP. *The Journal of biological chemistry*, 283(30):20914–20924, jul 2008. (Cited on page 71.)

[166] Gia K Voeltz, William A Prinz, Yoko Shibata, Julia M Rist, and Tom A Rapoport. A class of membrane proteins shaping the tubular endoplasmic reticulum. *Cell*, 124(3):573–586, feb 2006. (Cited on page 71.)

[167] Tatiana Claro Da Silva, James E Polli, and Peter W Swaan. The solute carrier family 10 (SLC10): Beyond bile acid transport. *Molecular Aspects of Medicine*, 34(2-3):252–269, jan 2013. (Cited on page 71.)

[168] Beth A Dombroski, Renuka R Nayak, Kathryn G Ewens, Wendy Ankener, Vivian G Cheung, and Richard S Spielman. Gene expression and genetic variation in response to endoplasmic reticulum stress in human cells. *American journal of human genetics*, 86(5):719–729, may 2010. (Cited on page 71.)

[169] Sujit Nair, Changjiang Xu, Guoxiang Shen, Vidya Hebbar, Avantika Gopalakrishnan, Rong Hu, Mohit Raja Jain, Celine Liew, Jefferson Y Chan, and Ah-Ng Tony Kong. Toxicogenomics of endoplasmic reticulum stress inducer tunicamycin in the small intestine and liver of Nrf2 knockout and C57BL/6J mice. *Toxicology letters*, 168(1):21–39, jan 2007. (Cited on page 71.)

[170] Sujatha Muralidharan and Pranoti Mandrekar. Cellular stress response and innate immune signaling: integrating pathways in host defense and inflammation. *Journal of leukocyte biology*, 94(6):1167–1184, dec 2013. (Cited on page 71.)

[171] Peter Reinhardt, Benjamin Schmid, Lena F Burbulla, David C Schöndorf, Lydia Wagner, Michael Glatza, Susanne Höing, Gunnar Hargus, Susanna A Heck, Ashutosh Dhingra, Guangming Wu, Stephan Müller, Kathrin Brockmann, Torsten Kluba, Martina Maisel, Rejko Krüger, Daniela Berg, Yaroslav Tsytsyura, Cora S Thiel, Olympia-Ekaterini Psathaki, Jürgen Klingauf, Tanja Kuhlmann, Marlene Klewin, Heiko Müller, Thomas Gasser, Hans R Schöler, and Jared Sterneckert. Genetic correction of a LRRK2 mutation in human iPSCs links parkinsonian neurodegeneration to ERK-dependent changes in gene expression. *Cell stem cell*, 12(3):354–367, mar 2013. (Cited on page 71.)

[172] Harmeet Malhi and Randal J Kaufman. Endoplasmic reticulum stress in liver disease. *Journal of hepatology*, 54(4):795–809, apr 2011. (Cited on page 72.)

[173] Si Chen, William B Melchior, and Lei Guo. Endoplasmic reticulum stress in drug- and environmental toxicant-induced liver toxicity. *Journal of environmental science and health. Part C, Environmental carcinogenesis {&} ecotoxicology reviews*, 32(1):83–104, jan 2014. (Cited on page 72.)

[174] X Y Chen, R Li, M Wang, and Z Y Geng. Identification of differentially expressed genes in hypothalamus of chicken during cold stress. *Molecular biology reports*, 41(4):2243–2248, apr 2014. (Cited on page 72.)

[175] Si Chen, Jiekun Xuan, Letha Couch, Advait Iyer, Yuanfeng Wu, Quan-Zhen Li, and Lei Guo. Sertraline induces endoplasmic reticulum stress in hepatic cells. *Toxicology*, 322:78–88, aug 2014. (Cited on page 72.)

[176] Anke Van Summeren. *Analysis of protein expression patterns induced by classifying hepatotoxicants in primary mouse hepatocytes*. PhD thesis, 2014. (Cited on pages 72 and 104.)

[177] Wim F P M Van den Hof, Maarten L J Coonen, Marcel van Herwijnen, Karen Brauers, Will K W H Wodzig, Joost H M van Delft, and Jos C S Kleinjans. Classification of Hepatotoxicants Using HepG2 Cells: A Proof of Principle Study. *Chemical Research in Toxicology*, 27(3):433–442, mar 2014. (Cited on pages 72 and 104.)

[178] Ahmad Sharanek, Pamela B.-E. Bachour-El Azzi, Houssein Al-Attrache, Camille C Savary, Lydie Humbert, Dominique Rainteau, Christiane Guguen-Guillouzo, and André Guillouzo. Different dose-dependent mechanisms are involved in early cyclosporine a-induced cholestatic effects in hepaRG cells. *Toxicological sciences : an official journal of the Society of Toxicology*, 141(1):244–253, sep 2014. (Cited on page 72.)

[179] Anke Van Summeren, Johan Renes, Daneida Lizarraga, Freek G Bouwman, Jean-Paul Noben, Joost H M van Delft, Jos C S Kleinjans, and Edwin C M Mariman. Screening for drug-induced hepatotoxicity in primary mouse hepatocytes using acetaminophen, amiodarone, and cyclosporin a as model compounds: an omics-guided approach. *OMICS: A Journal of Integrative Biology*, 17(2):71–83, feb 2013. (Cited on page 72.)

[180] C Ju and J P Uetrecht. Mechanism of idiosyncratic drug reactions: reactive metabolite formation, protein binding and the regulation of the immune system. *Current drug metabolism*, 3(4):367–377, aug 2002. (Cited on page 79.)

[181] M Pirmohamed, S Madden, and B K Park. Idiosyncratic drug reactions. Metabolic bioactivation as a pathogenic mechanism. *Clinical pharmacokinetics*, 31(3):215–230, sep 1996. (Cited on page 79.)

[182] Urs A Boelsterli and Priscilla L K Lim. Mitochondrial abnormalities A link to idiosyncratic drug hepatotoxicity? *Toxicology and Applied Pharmacology*, 220(1):92–107, apr 2007. (Cited on pages 79, 95, 107, and 118.)

[183] Derick Han, Lily Dara, Sanda Win, Tin Aung Than, Liyun Yuan, Sadeea Q Abbasi, Zhang-Xu Liu, and Neil Kaplowitz. Regulation of drug-induced liver injury by signal transduction pathways: critical role of mitochondria. *Trends in pharmacological sciences*, 34(4):243–253, apr 2013. (Cited on page 79.)

[184] Daphna Laifenfeld, Luping Qiu, Rachel Swiss, Jennifer Park, Michael Macoritto, Yvonne Will, Husam S Younis, and Michael Lawton. Utilization of causal reasoning of hepatic gene expression in rats to identify molecular pathways of idiosyncratic drug-induced liver injury. *Toxicological sciences : an official journal of the Society of Toxicology*, 137(1):234–248, jan 2014. (Cited on pages 79, 95, 107, and 118.)

[185] James P Luyendyk, Patrick J Shaw, Christopher D Green, Jane F Maddox, Patricia E Ganey, and Robert A Roth. Coagulation-mediated hypoxia and neutrophil-dependent hepatic injury in rats given lipopolysaccharide and ranitidine. *The Journal of pharmacology and experimental therapeutics*, 314(3):1023–1031, sep 2005. (Cited on pages 79 and 94.)

[186] Jeffrey F Waring, Michael J Liguori, James P Luyendyk, Jane F Maddox, Patricia E Ganey, Robert F Stachlewitz, Colin North, Eric A G Blomme, and Robert A Roth. Microarray analysis of lipopolysaccharide potentiation of trovafloxacin-induced liver injury in rats suggests a role for proinflammatory chemokines and neutrophils. *The Journal of pharmacology and experimental therapeutics*, 316(3):1080–1087, mar 2006. (Cited on pages 79 and 93.)

[187] James P Luyendyk, Lois D Lehman-McKeeman, David M Nelson, Vasanthi M Bhaskaran, Timothy P Reilly, Bruce D Car, Glenn H Cantor, Jane F Maddox, Patricia E Ganey, and Robert A Roth. Unique gene expression and hepatocellular injury in the lipopolysaccharide-ranitidine drug idiosyncrasy rat model: comparison with famotidine. *Toxicological sciences : an official journal of the Society of Toxicology*, 90(2):569–585, apr 2006. (Cited on pages 79, 86, 93, and 94.)

[188] Patrick J Shaw, Aaron M Fullerton, Michael A Scott, Patricia E Ganey, and Robert A Roth. The role of the hemostatic system in murine liver injury induced by coexposure to lipopolysaccharide and trovafloxacin, a drug with idiosyncratic liability. *Toxicology and applied pharmacology*, 236(3):293–300, may 2009. (Cited on pages 79 and 94.)

[189] Susanne Ramm and Angela Mally. Role of drug-independent stress factors in liver injury associated with diclofenac intake. *Toxicology*, 312:83–96, oct 2013. (Cited on pages 79, 86, 94, and 95.)

[190] Kyle L Poulsen, Jesus Olivero-Verbel, Kevin M Beggs, Patricia E Ganey, and Robert A Roth. Trovafloxacin enhances lipopolysaccharide-stimulated production of tumor necrosis factor-α by macrophages: role of the DNA damage response. *The Journal of pharmacology and experimental therapeutics*, 350(1):164–170, jul 2014. (Cited on page 79.)

[191] Kyle L Poulsen, Ryan P Albee, Patricia E Ganey, and Robert A Roth. Trovafloxacin potentiation of lipopolysaccharide-induced tumor necrosis factor release from RAW 264.7 cells requires extracellular signal-regulated kinase and c-Jun N-Terminal Kinase. *The Journal of pharmacology and experimental therapeutics*, 349(2):185–191, may 2014. (Cited on page 79.)

[192] Franziska Boess, Markus Kamber, Simona Romer, Rodolfo Gasser, Dieter Muller, Silvio Albertini, and Laura Suter. Gene expression in two hepatic cell lines, cultured primary hepatocytes, and liver slices compared to the in vivo liver gene expression in rats: possible implications for toxicogenomics use of in vitro systems. *Toxicological sciences : an official journal of the Society of Toxicology*, 73(2):386–402, jun 2003. (Cited on page 79.)

[193] E Evdokimova, H Taper, and P Buc Calderon. Effects of bacterial endotoxin (lipopolysaccharides) on survival and metabolism of cultured precision-cut rat liver slices. *Toxicology in vitro : an international journal published in association with BIBRA*, 16(1):47–54, feb 2002. (Cited on page 79.)

[194] Mackenzie Hadi, Yixi Chen, Viktoriia Starokozhko, Marjolijn T Merema, and Geny M M Groothuis. Mouse precision-cut liver slices as an ex vivo model to study idiosyncratic drug-induced liver injury. *Chemical research in toxicology*, 25(9):1938–1947, sep 2012. (Cited on pages 79 and 94.)

[195] Mackenzie Hadi, Inge M. Westra, Viktoriia Starokozhko, Sanja Dragovic, Marjolijn T. Merema, and Geny M. M. Groothuis. Human Precision-Cut Liver Slices as an ex Vivo Model to Study Idiosyncratic Drug-Induced Liver Injury. *Chemical Research in Toxicology*, 26(5):710–720, may 2013. (Cited on pages 79, 80, 81, 83, 93, 94, 106, and 117.)

[196] Henry Löffler-Wirth, Martin Kalcher, and Hans Binder. oposSOM: R-package for high-dimensional portraying of genome-wide expression landscapes on Bioconductor. *Bioinformatics (Oxford, England)*, jun 2015. (Cited on page 82.)

[197] Bram Herpers, Steven Wink, Lisa Fredriksson, Zi Di, Giel Hendriks, Harry Vrieling, Hans de Bont, and Bob van de Water. Activation of the Nrf2 response by intrinsic hepatotoxic drugs correlates with suppression of NF-κB activation and sensitizes toward TNFα-induced cytotoxicity. *Archives of toxicology*, may 2015. (Cited on pages 86, 95, 107, and 118.)

[198] Patrick J Shaw, Marie J Hopfensperger, Patricia E Ganey, and Robert A Roth. Lipopolysaccharide and trovafloxacin coexposure in mice causes idiosyncrasy-like liver injury dependent on tumor necrosis factor-alpha. *Toxicological sciences : an official journal of the Society of Toxicology*, 100(1):259–266, nov 2007. (Cited on pages 93 and 117.)

[199] Jingtao Lu, A Daniel Jones, Jack R Harkema, Robert A Roth, and Patricia E Ganey. Amiodarone exposure during modest inflammation induces idiosyncrasy-like liver injury in rats: role of tumor necrosis factor-alpha. *Toxicological sciences : an official journal of the Society of Toxicology*, 125(1):126–133, jan 2012. (Cited on page 93.)

[200] Benjamin D Cosgrove, Bracken M King, Maya A Hasan, Leonidas G Alexopoulos, Paraskevi A Farazi, Bart S Hendriks, Linda G Griffith, Peter K Sorger, Bruce Tidor, Jinghai J Xu, and Douglas A Lauffenburger. Synergistic drug-cytokine induction of hepatocellular death as an in vitro approach for the study of inflammation-associated idiosyncratic drug hepatotoxicity. *Toxicology and applied pharmacology*, 237(3):317–330, jun 2009. (Cited on page 93.)

[201] Benjamin D Cosgrove, Leonidas G Alexopoulos, Ta-chun Hang, Bart S Hendriks, Peter K Sorger, Linda G Griffith, and Douglas A Lauffenburger. Cytokine-associated drug toxicity in human hepatocytes is associated with signaling network dysregulation. *Molecular bioSystems*, 6(7):1195–1206, jul 2010. (Cited on page 93.)

[202] Richard A Thompson, Emre M Isin, Yan Li, Lars Weidolf, Ken Page, Ian Wilson, Steve Swallow, Brian Middleton, Simone Stahl, Alison J Foster, Hugues Dolgos, Richard Weaver, and J Gerry Kenna. In vitro approach to assess the potential for risk of idiosyncratic adverse reactions caused by candidate drugs. *Chemical research in toxicology*, 25(8):1616–1632, aug 2012. (Cited on page 93.)

[203] Winnie Ng, Rossoune Kennar, and Jack Uetrecht. Effect of Clozapine and Olanzapine on Neutrophil Kinetics: Implications for Drug-Induced Agranulocytosis. *Chemical Research in Toxicology*, 27(7):1104–1108, jul 2014. (Cited on page 93.)

[204] K N Chengappa, B G Pollock, H Parepally, J Levine, M A Kirshner, J S Brar, and R A Zoretich. Anticholinergic differences among patients receiving standard clinical doses of olanzapine or clozapine. *Journal of clinical psychopharmacology*, 20(3):311–316, jun 2000. (Cited on page 93.)

[205] Jinsheng Guo and Scott L Friedman. Toll-like receptor 4 signaling in liver injury and hepatic fibrogenesis. *Fibrogenesis {&} tissue repair*, 3(1):21, jan 2010. (Cited on page 94.)

[206] Jong Sung Park, John Arcaroli, Ho-Kee Yum, Huan Yang, Haichao Wang, Kuang-Yao Yang, Kang-Hyeon Choe, Derek Strassheim, Todd M Pitts, Kevin J Tracey, and Edward Abraham. Activation of gene expression in human neutrophils by high mobility group box 1 protein. *American journal of physiology. Cell physiology*, 284(4):C870–9, apr 2003. (Cited on page 94.)

[207] John R Klune, Rajeev Dhupar, Jon Cardinal, Timothy R Billiar, and Allan Tsung. HMGB1: endogenous danger signaling. *Molecular medicine (Cambridge, Mass.)*, 14(7-8):476–484, jan 2008. (Cited on page 94.)

[208] John Evankovich, Sung W Cho, Ruilin Zhang, Jon Cardinal, Rajeev Dhupar, Lemeng Zhang, John R Klune, Jason Zlotnicki, Timothy Billiar, and Allan Tsung. High mobility group box 1 release from hepatocytes during ischemia and reperfusion injury is mediated by decreased histone deacetylase activity. *The Journal of biological chemistry*, 285(51):39888–39897, dec 2010. (Cited on page 94.)

[209] Carmen Fiuza, Michael Bustin, Shefali Talwar, Margaret Tropea, Eric Gerstenberger, James H Shelhamer, and Anthony F Suffredini. Inflammation-promoting activity of HMGB1 on human microvascular endothelial cells. *Blood*, 101(7):2652–2660, apr 2003. (Cited on page 94.)

[210] Simon Rousseau, Nick Morrice, Mark Peggie, David G Campbell, Matthias Gaestel, and Philip Cohen. Inhibition of SAPK2a/p38 prevents hnRNP A0 phosphorylation by MAPKAP-K2 and its interaction with cytokine mRNAs. *The EMBO journal*, 21(23):6505–6514, dec 2002. (Cited on page 94.)

[211] Jonathan L E Dean, Gareth Sully, Andrew R Clark, and Jeremy Saklatvala. The involvement of AU-rich element-binding proteins in p38 mitogen-activated protein kinase pathway-mediated mRNA stabilisation. *Cellular signalling*, 16(10):1113–1121, oct 2004. (Cited on page 94.)

[212] E Anggård. Nitric oxide: mediator, murderer, and medicine. *Lancet (London, England)*, 343(8907):1199–1206, may 1994. (Cited on pages 95 and 107.)

[213] S Ramm, B Morissey, B Hernandez, C Rooney, S R Pennington, and A Mally. Application of a discovery to targeted LC-MS proteomics approach to identify deregulated proteins associated with idiosyncratic liver toxicity in a rat model of LPS/diclofenac co-administration. *Toxicology*, 331:100–111, may 2015. (Cited on page 95.)

[214] Andrew Leask and David J Abraham. TGF-beta signaling and the fibrotic response. *FASEB journal : official publication of the Federation of American Societies for Experimental Biology*, 18(7):816–827, may 2004. (Cited on pages 102 and 112.)

[215] Anke Van Summeren, Johan Renes, Freek G Bouwman, Jean-Paul Noben, Joost H M van Delft, Jos C S Kleinjans, and Edwin C M Mariman. Proteomics investigations of drug-induced hepatotoxicity in HepG2 cells. *Toxicological sciences : an official journal of the Society of Toxicology*, 120(1):109–122, mar 2011. (Cited on pages 104 and 114.)

[216] Yoshifumi Watanabe, Osamu Suzuki, Takahiro Haruyama, and Toshihiro Akaike. Interferon-gamma induces reactive oxygen species and endoplasmic reticulum stress at the hepatic apoptosis. *Journal of cellular biochemistry*, 89(2):244–253, may 2003. (Cited on pages 106 and 117.)

[217] Nithya Mariappan, Carrie M Elks, Bruno Fink, and Joseph Francis. TNF-induced mitochondrial damage: a link between mitochondrial complex I activity and left ventricular dysfunction. *Free radical biology {&} medicine*, 46(4):462–470, feb 2009. (Cited on pages 106 and 117.)

[218] María J López-Armada, Romina R Riveiro-Naveira, Carlos Vaamonde-García, and Marta N Valcárcel-Ares. Mitochondrial dysfunction and the inflammatory response. *Mitochondrion*, 13(2):106–118, mar 2013. (Cited on pages 106 and 117.)

[219] Jose J G Marin, Luis Bujanda, and Jesus M Banales. MicroRNAs and cholestatic liver diseases. *Current opinion in gastroenterology*, 30(3):303–309, may 2014. (Cited on pages 108 and 119.)

[220] Qiaoli Liu, Yun Qian, Feng Chen, Xiaoming Chen, Zhi Chen, and Min Zheng. EGCG attenuates pro-inflammatory cytokines and chemokines production in LPS-stimulated Lo2 hepatocyte. *Acta biochimica et biophysica Sinica*, 46(1):31–39, jan 2014. (Cited on page 108.)

[221] Li-Min Li, Dong Wang, and Ke Zen. MicroRNAs in Drug-induced Liver Injury. *Journal of clinical and translational hepatology*, 2(3):162–169, sep 2014. (Cited on pages 108 and 119.)

[222] Shanrong Zhao, Wai-Ping Fung-Leung, Anton Bittner, Karen Ngo, and Xuejun Liu. Comparison of RNA-Seq and microarray in transcriptome profiling of activated T cells. *PloS one*, 9(1):e78644, jan 2014. (Cited on pages 108 and 119.)

[223] Fuchou Tang, Kaiqin Lao, and M Azim Surani. Development and applications of single-cell transcriptome analysis. *Nature methods*, 8(4 Suppl):S6–11, apr 2011. (Cited on pages 108 and 120.)

[224] Viktoriia Starokozhko, Getahun B Abza, Hedy C Maessen, Marjolijn T Merema, Frieke Kuper, and Geny M M Groothuis. Viability, function and morphological integrity of precision-cut liver slices during prolonged incubation: Effects of culture medium. *Toxicology in vitro : an international journal published in association with BIBRA*, oct 2015. (Cited on pages 108 and 120.)

[225] Benjamin L Woolbright and Hartmut Jaeschke. Novel insight into mechanisms of cholestatic liver injury. *World journal of gastroenterology : WJG*, 18(36):4985–4993, sep 2012. (Cited on page 116.)

[226] Yang Liu, Li-Feng Wang, Hai-Feng Zou, Xiao-Yan Song, Hua-Feng Xu, Ping Lin, Hai-Hong Zheng, and Xiao-Guang Yu. Expression and location of Smad2, 4 mRNAs during and after liver fibrogenesis of rats. *World journal of gastroenterology : WJG*, 12(10):1577–1582, 2006. (Cited on page 117.)

[227] Yu Yamaura, Miki Nakajima, Shingo Takagi, Tatsuki Fukami, Koichi Tsuneyama, and Tsuyoshi Yokoi. Plasma microRNA profiles in rat models of hepatocellular injury, cholestasis, and steatosis. *PloS one*, 7(2):e30250, jan 2012. (Cited on page 119.)

ABBREVIATIONS

ACOX1 Peroxisomal acyl-coenzyme A oxidase 1

AKT1 Protein Kinase B Alpha

APAP Acetaminophen/ Paracetamol

BRCA1 Breast Cancer 1, early onset

C2ORF30/ERLEC1 Endoplasmic reticulum lectin 1

CADPS2 Calcium-dependent activator protein for secretion 2

CCl4 Carbon tetrachloride

DNAJB9/ERDJ4 DnaJ Hsp40 Homolog, Subfamily B, Member 9

EDN1 Endothelin-1

FGF2 Fibroblast growth factor

GMCSF- Granulocyte-macrophage colony stimulating factor

HACL1 2-Hydroxyacyl-CoA Lyase 1

HMGB1 High mobility group protein box-1

HNF1A Hepatocyte nuclear factor 1 homeobox A

HNF4A Hepatocyte nuclear factor 4 alpha

hPCLS Human precision-cut liver slices

HSC Hepatic stellate cell

IDILI Idiosyncratic drug-induced liver injury

IL1A- Interleukin-1 alpha

iNOS Inducible nitric oxide synthase

LPS Lipopolysaccharide

NFkB Nuclear factor kappa-light-chain-enhancer of activated B cells

NFXL1 Nuclear transcription factor, X-box binding-like

NUPR1 Nuclear Protein 1

p38 MAPK p38 Mitogen activated protein kinase

PAN2 Poly (A) Specific Ribonuclease Subunit

PCLS Precision-cut liver slices

PKD1 Polycystin-1

PPARA Peroxisome proliferator-activated receptor alpha

PPARD Peroxisome proliferator-activated receptor delta

PPARG Peroxisome proliferator-activated receptor gamma

pSmadL/C Dually phosphorylated smad

REEP5 Receptor expression enhancing protein 5

RXRA Retinoid X receptor alpha

SLC10A7 Sodium/Bile Acid Cotransporter 7

SORL1 Sortilin-Related Receptor 1

TFAM Mitochondrial transcription factor A

TGFB1 Transforming Growth Factor Beta 1

TLR4 Toll like receptor 4

TMED7 Transmembrane p24 trafficking protein 7

TMEM-117 Transmembrane protein 117

TNF Tumor necrosis factor

TP53 Tumor protein p53

UW University of Wisconsin organ preservation solution

WME William's medium E

DANKWOORD/ACKNOWLEDGEMENTS

"We must find time to stop and thank the people who make a difference in our lives." - **John F. Kennedy**

Ten eerste wil ik mijn oprechte en welgemeende dankbaarheid tonen aan mijn promotoren Prof. Geny Groothuis en Prof. Peter Olinga. Ik ben diep dankbaar voor jullie geduld, samenwerking, stimulatie en opbouwende kritiek. Jullie moedigden mij aan om met mijn eigen oplossingen te komen en hielden mijn motivatie hoog. Ik kon altijd bij jullie aan de deur kloppen zonder afspraak en kreeg snel oplossingen voor al mijn vragen. Geny, naast een geweldige wetenschapper bent u ook een geweldige persoon. Ik bewonder uw zorg voor al de mederwerkers binnen het lab. Het doet me goed dat het nieuwe 'Groothuis slicing lab' naar u genoemd is, u heb het verdiend! Het beste toegewenst voor al uw plannen na uw wetenschappelijke carrière. Peter, ik ben onder de indruk van de bijna exponentiële groei van medewerkers in uw groep. Ik wens u het alle beste in alle toekomstige bezigheden.

It is indeed great pleasure to express my deep sense of gratitude and humble thanks to Prof.Jeroen Pennings. I really enjoyed working in collaboration with you and I could always get instant solutions for my queries.

I would further like to express my sincere thanks to the members of the thesis reading committee for their kind gesture to evaluate this thesis.I thank Prof.Bob Van de Water, Prof.Klaas Nico Faber and Prof.Pieter Annaert for their time and providing valuable suggestions for its improvement.

I would like to extend my acknowledgement to Prof.Klaas Poelstra, Dr.Hans Proost, Prof.Angela Casini and Prof.Barbro Melgert, Dr.Inge de Graaf, Dr.Anna Salvati and Dr. Leonie Belaars for your valuable discussions and suggestions during the research meetings and it was great pleasure talking to you during social gatherings.

Marina, Marjolijn and Miriam, many thanks for assisting me with everything in the lab. Marina and Marjolijn, I really admire your patience and interest in teaching the slicing technique to students and visiting scientists. You both doing an amazing job. Thanks for the nice time. Inge, you also played a great role in improving the slice technique. Thanks for your advices and I like your cool attitude.

My special thanks goes to Prof.dr.Shuichi Sekine for your co-work on the incubation of bile acids with PCLS. On a personal side you are like my brother, thank you for the advices in the professional career. I hope to visit your cute family sometime in Japan.

I would like to extend my thanks to Dr.Marieke Elferink and Dr.Willem Schoonen, who gave me the overview and insights of the work done at the start of this project. Marieke, thanks for arranging the bike trip in the countryside near your village.

I also would like to thank Emilia Gore and Christel Hoeve for being my paranymphs. I am glad to have you as my paranymphs.

Jan, thank you for being my guardian in the lab. I like your Dutch expression 'Tsjonge, jonge, jonge!', whenever I ran to you for the medical emergency kit. Thank you for the advices and sharing your knowledge about work and life. Gillian, sweet secretary, thanks for all the administrative work. I like your humor and it was great fun to listen to your stories.

I honestly feel that PhD is a process of learning also from students. I would like to thank students for working and teaching me by their own ways: Emilia, Sabine, Samiksha and Nashwa. I wish you good luck in your careers.

I would like to express my gratitude to the present and previous members in the PTT group (Pharmacokinetics, Toxicology and Targeting) for your help, care and support. Many thanks to Eduard, Catharina, Christa, Adriana, Henk, Bert, Marlies, Christina, Carian, Kaisa, Amirah, Adhy, Kenni, Roberta, Daphne, Laura, Amit, Fransien, Valentina, Natalia, Mackenzie, Na, Nia, Magdalena, Benoit, Xiaoyu, Brech and others for being great colleagues and friends. It was great to know you and I really enjoyed coffee and lunch breaks, borrel and lab outings. Thanks also to the visiting guests: Giulia, Emmanuel, Ivan, Andrea, Elizabeth, Sarah, Angelo, Sophie though you were in the PTT group for short period, the time we spent together became a treasure in my memory. Christa, it was great fun to talk to you and discuss on various aspects in and outside the lab. Andreia, Carian and Christina, good luck with your defense soon. Emma, Casper and Susana, I really had great time with you guys in our "the office". Amit, I was surprised to see that you speak Dutch as good as native speaker in just 4 years and I enjoyed our talks about work and life. Sara, Victoria, Andriea and Sylvia, thank you for being great roomates, friends and sisters. Ming, now Dr.Li, I really enjoyed working with you and surprised with your knowledge on everything. I also would like to extend my thanks to the members in the Peter's group (Dorenda, Bao Tung, Tobias, Raditya, Rick, Isabel, Jo, Nia, Emma, Emilia, Su). Jo, you are one of the very coolest persons I ever met. I really like saying hi to you in Thai style whenever I meet you. I wish you all success and happiness with your personal and professional life.

The cherishing memories of Winchoterdiep 46 international student house will be my great part of nostalgia. I miss you guys, especially Lucia, Irene, Abhi, Raquel, Boris, Kerem, Shirin, Mehran, Tamara, Maja, Roxana, Kethlin, Eva, Jelle, Sven, Priyvrat, Sylvia, Belen, Marina, Sean and others. Special thanks to people from different countries whom I met through Erasmus Student Network (ESN), Sander, Sandra, Maria, Luise, Natalia, Agnes, Alicia, Leonardo, Oriol, Alexia, Marcijn, Eleonore, Rosa-Lin, Daan, Nicolas, Alex, James, Andres, Anna, Mathew, Mida, Astrid, Anda, Simon, Maren Gue and others. Alexia, you are gifted with an amazing voice, best wishes for your singing career. Sander, my Hungarian brother, thanks for all the fun activities and travel we did together.

I would like to thank the HOST-IFES and Vineyard Groningen where I met amazing people. Hendrick, Bram, Neeraj, Danica, Angelika, Maurits, Martijn, Arend, Femke, Andres, Shiva and Nina and others. Hendrick and Bram, thank you for arranging the meetings and always liked the discussions we had together. Neeraj baba, our conversation on 6D is hilarious.

I would like to express my thanks to Indian community, which made my stay in Groningen more memorable and pleasant one. My special thanks go to Gopi-Saritha, Rajendra-Chaitali, Shodan-Chaitanya, Eswar-Monica, Tushar-Jasmine, Gaurav-Neha, Pramod-Meena, Ganesh-Subha, Akshay-Spoorthi, Rajender-Shilpa, Raja-Sai Sree, Kiran-Shruthi, Gaurav, Balaji, Vikram, Rama-Ashoka, Aditya, Kushi, Shivakumar, Sasanka, Venkatesh-Nisha, Vinod, Sunil-Smitha, Jai-Ruchi, Goutham, Pranov, Praneeth, Vineet, Kiran, Mallikarjun, Suresh babu and many others. Venkatesh and Nisha, I am very grateful to you for your care, guidance. I admire your knowledge on professional and social aspects. Shiva and Ananya, I felt like home being with you, thanks for everything. Shiva, I appreciate your care for friends and your humor brings uncontrollable laughs. Khayum, Mr.Positive, I admire your positive attitude on all aspects of life. Siddesh, it was great pleasure to discuss with you about the philosophical aspects. Martin, you always inspired me with your technical skills. Pramod, thanks for your hospitality during the initial days of stay in Groningen. Malli, you are one of the cool guy I ever met.

Thanks to Vinod uncle, Meena aunty and Joann-Hans for your care and homely atmosphere. Adrian, broer, You are very energetic and positive. I wish you all success and happiness with your personal and professional life.

Special thanks to Vamsee for being my mentor and for your guidance. Arun, you are one of the most hilarious person I ever met. I really enjoyed our time in GCP. Sandeep, thanks for your support and encouragement. Prakash Rati, you inspired me to think beyond boundaries.

I thank Alexandra, Babak, Bart, Mandy, Mick, Renata, Julia, Katja and others from the Springs sport school for the nice time. I really enjoyed the insane and other work out sessions and dinner nights with you guys.

I also would like to thank all my friends and teachers from primary school, high school, graduate studies (NPU, GCP, NIPER).

Ik wil ook graag mijn dank uitspreken aan mijn Nederlandse familie. Jan Willem, Gerda en de anderen: bedankt voor jullie zorg, gastvrijheid en voor de goede tijd. Christel, woorden schieten tekort, bedankt voor alles en voor je steun en motivatie.

Finally, to my family back home, in India. Amma and Nanna, I am grateful for your unwavering affection, care and support at each instance. Mavayya, you are instrumental in sowing the seed of education in our family. Many more thanks to all the family members who have celebrated each of my success and shared each of my difficulty, as if it were their own.

Anyone, whom I missed to thank in the lines above, was only due to over-sight. I beg your pardon and express my heartfelt gratitude for all the help.

- Suri